EPA-600/2-75-018

August 1975

Environmental Protection Technology Series

STUDY OF FLUX FORCE/ CONDENSATION SCRUBBING OF FINE PARTICLES

U.S. Environmental Protection Agency
Office of Research and Development
Washington, D. C. 20460

STUDY OF FLUX FORCE/ CONDENSATION SCRUBBING OF FINE PARTICLES

by

Seymour Calvert, Nikhil C. Jhaveri, and Timothy Huisking

A. P. T., Inc.
4901 Morena Boulevard, Suite 402
San Diego, California 92117

Contract No. 68-02-1082
ROAP No. 21ADL-005
Program Element No. 1AB012

EPA Project Officer: Leslie E. Sparks

Industrial Environmental Research Laboratory
Office of Energy, Minerals, and Industry
Research Triangle Park, North Carolina 27711

Prepared for

U. S. ENVIRONMENTAL PROTECTION AGENCY
Office of Research and Development
Washington, D. C. 20460

August 1975

EPA REVIEW NOTICE

This report has been reviewed by the National Environmental Research Center - Research Triangle Park, Office of Research and Development, EPA, and approved for publication. Approval does not signify that the contents necessarily reflect the views and policies of the Environmental Protection Agency, nor does mention of trade names or commercial products constitute endorsement or recommendation for use.

RESEARCH REPORTING SERIES

Research reports of the Office of Research and Development, U.S. Environmental Protection Agency, have been grouped into series. These broad categories were established to facilitate further development and application of environmental technology. Elimination of traditional grouping was consciously planned to foster technology transfer and maximum interface in related fields. These series are:

1. ENVIRONMENTAL HEALTH EFFECTS RESEARCH
2. ENVIRONMENTAL PROTECTION TECHNOLOGY
3. ECOLOGICAL RESEARCH
4. ENVIRONMENTAL MONITORING
5. SOCIOECONOMIC ENVIRONMENTAL STUDIES
6. SCIENTIFIC AND TECHNICAL ASSESSMENT REPORTS
9. MISCELLANEOUS

This report has been assigned to the ENVIRONMENTAL PROTECTION TECHNOLOGY series. This series describes research performed to develop and demonstrate instrumentation, equipment and methodology to repair or prevent environmental degradation from point and non-point sources of pollution. This work provides the new or improved technology required for the control and treatment of pollution sources to meet environmental quality standards.

This document is available to the public for sale through the National Technical Information Service, Springfield, Virginia 22161.

Publication No. EPA-600/2-75-018

ACKNOWLEDGEMENTS

Air Pollution Technology, Inc., wishes to express its appreciation to Dr. Leslie E. Sparks, E.P.A., Project Officer, and Mr. James Abbott, E.P.A. for excellent technical coordination and for very helpful assistance in support of our technical effort.

TABLE OF CONTENTS

LIST OF FIGURES

LIST OF TABLES

NOMENCLATURE

A = constant

B = constant

c_p = particle mass concentration, g/DNm^3 gas

C' = Cunningham correction factor, dimensionless

d = diameter, cm, μm or μmA≡ μm $(g/cm^3)^{1/2}$

d_{pg} = mass mean diameter, μm or μmA

E = efficiency, fraction or %

F = foam density, volume fraction liquid

G = gas rate, Kg/hr-m^2 column area

h_G = gas phase heat transfer coefficient, cal/sec-cm^2-°K

h_L = liquid phase heat transfer coefficient, cal/sec-cm^2-°K

k_G = gas phase mass transfer coefficient, gmole/cm^2-sec-atm

L = liquid rate, Kg/hr-m^2 column area

n = particle number concentration, no./cm^3

Pt = penetration, fraction or %

Pt_d = penetration for particle diameter "d_p", fraction or %

$\overline{Pt}$ = overall penetration, fraction or %

ΔP = pressure drop, cm W.C. or atm

q = vapor condensed per particle, g

q_m = vapor condensed per unit mass of inlet particles, mass fraction

q' = condensation ratio, g vapor condensed/g dry gas

R_n = particle concentration ratio defined in eq. (4-7), dimensionless

u = velocity, cm/sec

r = radius, cm, μm, or μmA

v = cumulative volume concentration, cm^3/cm^3

V_s = gas volume swept per volume of spray, m^3/l

σ_g = geometric standard deviation, dimensionless

ρ = density, Kg/m^3 or g/cm^3

Subscripts

a = aerodynamic
d = drop
i = inlet
o = outlet
p = particle
t = total

ABSTRACT

This report presents the results of a laboratory pilot scale evaluation of two Flux Force/Condensation (FF/C) scrubbers for the collection of fine particles. FF/C scrubbing includes the effects of diffusiophoresis, thermoporesis, Stefan flow and particle growth due to the condensation of water vapor. Fine particles are those smaller than 2 microns in diameter.

The two FF/C scrubbers tested were of multiple sieve plate and horizontal spray configurations. Effects of the scrubber configurations, liquid and gas flowrates, particle number concentration and the amount of vapor condensation were studied experimentally. Fractional particle penetrations were measured with cascade impactors and are presented in terms of particle penetration as a function of particle size. The experimental results are compared with predictions from mathematical models.

Optimum operational regions and the technical and economic feasibility of FF/C scrubbing are determined and demonstrated for a fine particle pollution source. It was confirmed that FF/C scrubbing is an attractive control method for fine particles when high efficiency is required or when the gas is hot enough to evaporate the necessary water vapor for condensation in the scrubber. A program to demonstrate FF/C scrubbing at pilot scale for the control of fine particulate emissions from industrial sources is described.

This report was submitted by Air Pollution Technology, Inc., in fulfillment of Contract No. 68-02-1082, under the sponsorship of the Environmental Protection Agency. Work was completed on December 14, 1974.

FOREWORD

This report, "Study of Flux Force/Condensation Scrubbing of Fine Particles", is the final report submitted to the Control Systems Laboratory for E.P.A. Contract No. 68-02-1082.

The principal objective of this program was to experimentally evaluate fine particle collection in two laboratory pilot scale flux force/condensation (FF/C) scrubbers and to determine the feasibility of application of FF/C scrubbing to industrial sources. The main activities under the scope of work were:

Based on the results of the previous theoretical and experimental study of FF/C scrubbing;

1. Design and fabricate two pilot scale FF/C scrubbers large enough for the exploration of scale-up problems.
2. Conduct a laboratory pilot experimental program to:
   - A. Determine feasibility for fine particle collection
   - B. Develop design equations and scale-up criteria
   - C. Determine optimum operating conditions for FF/C scrubbing
   - D. Investigate potential operational and maintenance problems
   - E. Determine effects of particle size distribution on the performance of FF/C scrubbers
3. Prepare revised engineering and cost analysis to incorporate results of the experimental study.
4. Recommend a detailed industrial pilot test program.

CHAPTER 1

INTRODUCTION

A major drawback of present day scrubbers is the large energy expenditure required to achieve high removal effi ciencies for fine particles in the size range of 0.1 to 2 microns in diameter. This is due to the decreased effectiveness of the inertial and diffusional collection mechanisms for particles in this size range. Flux force and water vapor condensation effects have the potential to improve fine particle collection in low energy scrubbers.

In this report, flux forces are defined as those caused by thermophoresis and diffusiophoresis (which includes the diffusiophoretic and Stefan flow forces); but not electrophoresis. Accordingly, we consider only those FF/C scrubbers where particle removal from the gas is aided by temperature or vapor concentration gradients and particle growth is due to vapor condensation. These effects can result from the cooling of a hot, humid gas by contact with cold liquid, the condensation of injected steam, or other means.

Several studies of scrubber operation where particle collection was enhanced by vapor condensation have been reported. Some investigations of the FF/C phenomena in particulate scrubbers have been made but the results have been either of qualitative nature or provided limited quantitative information applicable only to specific cases. Nothing adequate for the design of optimum industrial scale FF/C scrubbing system was found in the literature.

A systematic developmental study of FF/C scrubbing was started at Air Pollution Technology, Inc., under a previous contract, No. 68-02-0256, where the technical and economic feasibilities of applying FF/C scrubbing for fine particle collection were established. This study included

theoretical development of design equations for FF/C scrubbers. A limited bench scale experimental study was also performed to examine critical areas of application of these equations. The bench scale experimental study was extended further under Contract No. 68-02-0285 to evaluate multiple stage FF/C scrubbing, as reported in Calvert and Jhaveri (1974). It was concluded that multiple stage or continuous contact type scrubbers were most suitable for FF/C scrubbing application.

The purpose of the present study was to evaluate technical and economic feasibilities of FF/C scrubbing through an experimental study of two laboratory pilot scale FF/C scrubbers. Based on the available information, multiple sieve plate and horizontal spray FF/C scrubbers were selected. It was also important to evaluate the effects of scrubber operating parameters so that the region of optimum FF/C scrubber operation could be defined. To establish the economic feasi bility, the operating costs were compared with high energy scrubbers and a case study was made to compare the economics of FF/C scrubbing system with high energy alternatives designed to control gray iron cupola emissions.

CHAPTER 2

SUMMARY, CONCLUSIONS AND RECOMMENDATIONS

SUMMARY

Flux force and water vapor condensation effects have the potential to greatly improve the collection efficiencies of low energy scrubbers for fine particles. The object of the research reported here was to corroborate the limited experimental and theoretical evidence of the feasibility of FF/C scrubbing by conducting a detailed experimental study of two laboratory pilot scale (14 to 28 m^3/min or 500 to 1,000 CFM) FF/C scrubbers.

The economic feasibility of FF/C scrubbing was also evaluated during this study. The results define the range of emission properties for which FF/C scrubbing is determined to be economical. In general, FF/C scrubbing should be considered when high removal efficiencies are desired for fine particulate emissions; and the flue gas enthalpy is higher than 100 Kcal/Kg or spent steam is available in the plant. These conditions are common for industrial combustion processes, which include several major stationary pollution sources in the United States. The Midwest Research Institute Report (1971) ranks sources based on the total tonnage of particulates emitted annually.

Table 2-1 lists industrial sources of particulate pollutants ranked among the top fifteen in the nation in the M.R.I. Report (1971). Emission properties of these sources are favorably suited for the application of FF/C scrubbing. The annual emissions listed were determined by subtracting the amount of emissions removed in the existing control equipment from the total emissions. The "net control" listed is the product of the average efficiency of control devices and the application of the control devices for the industrial

Table 2-1. MAJOR INDUSTRIAL PARTICULATE SOURCES FOR WHICH FF/C SCRUBBING IS ATTRACTIVE

NOTE: The following information was taken from the Midwest Research Institute Report (1971). The source number (Roman numeral) refers to its rank in the U.S. as an industrial particulate pollution source.

SOURCE	ANNUAL PRODUCTION	NET CONTROL FRACTION	EMISSIONS MKg/yr
IV. IRON AND STEEL			
A. Sinter Plants (Sintering process)	46,300,000 MKg of Sinter	0.90	46,300
B. Coke Manufacture			
1. By-Product	81,600,000 MKg of Coal	0	81,600
2. Pushing & Quenching	82,800,000 MKg of Coal	---	19,000
C. Blast Furnace	80,600,000 MKg of Iron	.99	52,600
D. Steel Furnaces			
1. Open Hearth	59,700,000 MKg of Steel	.40	306,000
2. Basic Oxygen	43,500,000 MKg of Steel	.99	9,000
3. Electric Arc	15,200,000 MKg of Steel	.78	16,300
E. Scarfing	118,800,000 MKg of Steel	.68	57,200
VI. FOREST PRODUCTS			
A. Wigwam Burners	24,900,000 MKg of Waste	0	120,000
B. Pulp Mills			
1. Kraft Process	22,000,000 MKg of Pulp		
a. Recovery Furnace		.91	149,000
b. Lime Kilns		.94	29,900
c. Dissolving Tanks		.30	38,100
2. Sulfite Process	2,300,000 MKg of Pulp		
(Recovery Furnace)	756,000 MKg of Pulp	.91	9,000
3. NSSC Process	3,200,000 MKg of Pulp		
a. Recovery Furnace	1,100,000 MKg of Pulp	.91	900
b. Fluid-Bed Reactor	470,000 MKg of Pulp	.70	38,100
4. Bark Boilers	---	---	74,400

TABLE 2-1 (Continued)

SOURCE	ANNUAL PRODUCTION	NET CONTROL FRACTION	EMISSIONS MKg/yr
VII. LIME			
A. Rotary Kilns	14,700,000 MKg of Lime	0.81	267,000
B. Vertical Kilns	1,600,000 MKg of Lime	.39	3,600
VIII. PRIMARY NONFERROUS METALS			
A. Aluminum			
1. Calcining of Hydroxide	5,300,000 MKg of Aluminum	.90	52,600
2. Reduction Cells			
a. H. S. Soderberg	730,000 MKg of Aluminum	.40	31,700
b. V. S. Soderberg	640,000 MKg of Aluminum	.64	9,000
c. Prebake	1,600,000 MKg of Aluminum	.64	18,100
B. Copper			
1. Roasting	520,000 MKg of Copper	.85	6,000
2. Reverb. Furnace	1,300,000 MKg of Copper	.81	25,400
3. Converters	1,300,000 MKg of Copper	.81	29,900
C. Zinc			
1. Roasting			
a. Fluid-Bed	690,000 MKg of Zinc	.98	13,600
b. Ropp, multi-hearth	138,000 MKg of Zinc	.85	3,600
2. Sintering	560,000 MKg of Zinc	.95	2,700
3. Distillation	560,000 MKg of Zinc	---	13,600
D. Lead			
1. Sintering	420,000 MKg of Lead	.86	15,400
2. Blast Furnace	420,000 MKg of Lead	.83	9,000
3. Dross Reverb. Furnace	420,000 MKg of Lead	.50	1,800
XI. ASPHALT			
A. Paving Material	228,000,000 MKg of Material		
1. Dryers		.96	150,000
2. Secondary Sources		.96	36,300

TABLE 2-1 (Continued)

	SOURCE	ANNUAL PRODUCTION	NET CONTROL FRACTION	EMISSIONS MKg/yr
	B. Roofing Material	5,680,000 MKg of Asphalt		
	1. Blowing		0.50	2,700
	2. Saturator		---	12,700
XII.	FERROALLOYS			
	A. Blast Furnace	540,000 MKg of Ferroalloy	.99	900
	B. Electric Furnace	1,900,000 MKg of Ferroalloy	.40	140,000
XIII.	IRON FOUNDRY			
	A. Furnaces	16,000,000 MKg of Hot Metal	.27	95,300
XIV.	SECONDARY NONFERROUS METALS			
	A. Copper			
	1. Material Preparation			
	a. Wire Burning	270,000 MKg Insulated Wire	0	37,200
	b. Sweating Furnaces	58,000 MKg of Scrap	.19	--
	c. Blast Furnaces	260,000 MKg of Scrap	.68	1,800
	2. Smelting & Refining	1,100,000 MKg of Scrap	.57	15,400
	B. Aluminum			
	1. Sweating Furnaces	450,000 MKg of Scrap	.19	5,400
	2. Refining Furnaces	920,000 MKg of Scrap	.57	900
	3. Chlorine Fluxing	120,000 MKg of Cl Used	.25	46,300
	C. Lead			
	1. Pot Furnaces	48,000 MKg of Scrap	.90	--
	2. Blast Furnaces	108,000 MKg of Scrap	.90	900
	3. Reverb. Furnaces	500,000 MKg of Scrap	.90	2,700
	D. Zinc			
	1. Sweating Furnaces			
	a. Metallic Scrap	47,000 MKg of Scrap	.19	--
	b. Residual Scrap	190,000 MKg of Scrap	.19	2,700
	2. Distillation Furnace	210,000 MKg Zn Recovered	.57	1,800

category. The information and ranks were taken from the M.R.I. Report (1971). It is clear from Table 2-1 that FF/C scrubbing is a feasible and attractive particulate control method for several major industrial sources.

Experimental Program

Based on results from our previous studies, multiple plate and spray FF/C scrubbing configurations were selected for the experimental study. Test aerosols with fine iron oxide and titanium dioxide particles were generated in the laboratory by dry dispersing the respective pigment powders. Gas heating and steam were used to precondition the scrubber gas to the desired experimental conditions. A forced draft cooling tower was used to cool the recirculating scrubber water.

Effects of several operating parameters were studied during the experiment. In general, particle collection in the FF/C scrubbers was higher as the amount of vapor condensed per unit of gas scrubbed (condensation ratio) was increased or the inlet particle number concentration was decreased. Addition of a fifth plate to the multiple plate FF/C scrubber, considerably improved the performance for the same condensation ratio. But changing the liquid to gas flowrate ratio within the scrubber operative range showed no significant effect on scrubber performance. A more uniform distribution of vapor condensation over the stages or plates of the multiple plate scrubber was also found to result in better scrubber performance.

A mathematical model was used to predict the experimentally determined multiple plate FF/C scrubber performance. The model was based on the theoretical collection of particles in the bubbles on a sieve plate due to the FF/C phenomena. Inability to predict the plate hydrodynamics and the gas liquid contact area remains the critical area of uncertainty in the application of the model. However, the model can predict scrubber perfor-

mances that correlate well with experimental results. The model can now be used to scale-up the FF/C scrubber and design industrial FF/C scrubbing systems.

Spray Scrubber

Operating parameters besides the condensation ratio and inlet particle number concentrations which were studied for the spray FF/C scrubber are: the effect of the spray drop size, the effect of decreasing cooling water requirement, the mode of overall gas-liquid contact and the scrubber inlet liquid flowrate. The scrubber performance was better when the size of sprayed drops was smaller and when the amount of cold water sprayed in was higher for the same condensation ratio. The performance was also better when the scrubber inlet gas was exposed to the colder water spray first, resulting in the maximum temperature and vapor pressure gradients.

A mathematical model for the FF/C spray scrubber based on the unit mechanism approach gave only partial agreement with the experiment. Performance for cold gas without FF/C phenomena benefits was compared with a mathematical model based on accounting for collection by single drops as they decelerate after leaving the spray nozzle. The correlation was good for particles of about 1.0 μmA diameter. However, experimental efficiencies were higher for smaller particles, possibly because of particle collection on the back of drops. Experimental efficiencies were lower for the collection of larger particles, possibly indicating lower utilization of sprayed liquid, higher drop coalescence and gas channeling. Design equations were developed empirically to represent the experimental results, and be used for scale-up and design of industrial FF/C scrubbing systems with similar spray configuration.

Costs

Operating costs of a FF/C scrubber were compared to those of a high energy scrubber capable of equal performance. The costs of electrical power at $0.03 KWH, purchased steam at $6.40/MKg and recirculating cooling water at $0.9/MKg were used for this comparison. The results indicate that when high fine particle collection efficiencies are required or when the gas to be scrubbed is hot or humid, FF/C scrubbing is economically more attractive.

In an earlier report, Calvert et al. (1973) had evaluated the economic feasibility of FF/C scrubbing compared to other alternatives for two industrial sources. Based on the additional information on the performance of FF/C scrubbing obtained from this research, the economics of an FF/C system for a gray iron cupola were estimated. Good cost and performance data for a high energy (H.E.) scrubber on a cupola were available from another study and provided a basis for comparison. Capital investment requirements for the two systems are roughly the same but the H.E. scrubber costs about 70% more than the FF/C system for all annual operation expenses except labor, maintenance, liquid treatment, and solid waste disposal. Most of the cost advantage of FF/C scrubbing is due to a $63,500/yr higher power cost for H.E. scrubbing.

CONCLUSIONS

The following conclusions can be drawn from the results of this study:

1. The experimental study confirmed previous predictions of the technical feasibility of FF/C scrubbing. High collection efficiencies (>95%) for fine particles can be achieved with a condensation ratio of about 0.15 g vapor condensed/g dry gas, in a FF/C scrubber.
2. Performances of the multiple plate and horizontal spray FF/C scrubbers were roughly comparable for the higher condensation ratio range and for the same particle concentration. Thus, the horizontal spray FF/C scrubber is economically more attractive due to the lower capital cost and the lesser power requirement for scrubbing the same amount of gas. However, reasonably fine spray with the drop diameter of about 400 μm is needed to achieve the high efficiency. Thus, if a slurry is used to scrub the gas, and if the scrubber operation is not continuous, plugging of the spray nozzles may become a serious operational problem. The plate scrubber is more adaptable to changes in the flue gas conditions although the spray is superior for gas "turn down" (i.e., lower gas rate).
3. Of the several mechanisms involved in FF/C scrubbers, diffusiophoresis and inertial impaction enhancement by particle growth, which are practically independent of particle size, are the most important for fine particle collection. Thus, the condensation ratio and inlet particle number are significant operating parameters for FF/C scrubbing.

4. Effects of other operating parameters, such as the gas and liquid flowrates and contact scheme, on the performance of the two FF/C scrubbers have been experimentally studied. The results can be used to design the optimum FF/C scrubbing system depending on the specific properties of the industrial pollution sources.
5. Based on the experimental data, mathematical models and empirical design equations are described, which can be used to scale-up similar FF/C scrubbers for industrial applications.
6. Economic considerations define the most favorable area of application for FF/C scrubbing as those situations in which the enthalpy of vaporization is available from the gas to be cleaned, or when high collection efficiencies are required for fine particles, or when future capacity expansion is anticipated, or a combination of the three. The smaller the size of the particles to be scrubbed, the more economically attractive FF/C scrubbing will look. These conclusions are illustrated by a case study of an economic comparison of FF/C and high energy scrubbing systems for a gray iron cupola.

RECOMMENDATIONS

The laboratory pilot scale experimental study reported here has established the technical and economic feasibility of FF/C scrubbing. Engineering design equations for the two configurations studied are also described. The following research and developmental program is recommended:

1. Experimentally demonstrate the feasibility of FF/C scrubbing on selected industrial sources.

Pilot scale systems with capacities to scrub from 2.4 to 4.8 m^3/sec (5,000 to 10,000 CFM) should be used for demonstration. Problem industrial sources with fine particulate emissions and hot or humid flue gas should be selected for the demonstration. The FF/C scrubbing systems should be designed to operate at the optimum conditions with flexibility to account for process changes. These demonstration programs, for three industrial sources: a glass furnace, a secondary non-ferrous metal recovery furnace, and a foundry cupola, are detailed in the report.

2. Theoretical and experimental evaluation of other scrubbing configurations, such as a mobile bed (TCA) scrubber should be made to determine the best configuration applicable to FF/C scrubbing systems.
3. Evaporative cooling of scrubber liquid containing suspended and dissolved solids is critical for the economic feasibility of FF/C scrubbing. The cooling towers generally available use packings which are susceptible to scaling by the solids. A different configuration, such as using sprays instead of the packings, may be more applicable. Experimental development of the cooling towers on a laboratory and subsequently on an industrial pilot scale is clearly warranted.
4. Theoretical and experimental study of the speci fic details of plate hydrodynamics, spray utili zation, heat and mass transfer in gas-liquid systems, the nucleation of condensation and other matters which significantly influence FF/C mecha- nisms should be made in order to resolve the present areas of uncertainty.

CHAPTER 3

BACKGROUND

Flux force effects on particles have been known for many years and the background is reviewed and discussed in depth by authors such as Waldmann and Schmitt (1966), Goldsmith and May (1966), Hidy and Brock (1970) and Calvert et al. (1972). The studies reported by these authors include both theoretical and experimental work. The experimental systems were designed so as to be readily definable and were much simpler than a scrubber in terms of the number of phenomena and the unsteady conditions involved.

Several studies of scrubber operation have also been reported where particle collection was enhanced by vapor condensation, such as Schauer (1951) and Lapple and Kamack (1955). However, systematic studies of the effects of FF/C phenomena were attempted only recently. Rozen and Kostin (1967) studied the collection of fine oil mist in a perforated plate column under controlled conditions of vapor condensation. They found that their results could be represented by an empirical equation relating the particle penetration, "Pt", with the mass of steam condensed per gram of inlet particles, "q_m" as:

$$Pt = 12.5\ q_m^{-0.56} \qquad (3\text{-}1)$$

A study of steam injection into a laboratory scale scrubber was carried out by Lancaster and Strauss (1971). They measured an increase in particle collection efficiency which was in direct proportion to the amount of steam injected rather than the amount of vapor condensed. They concluded that the increase in collection efficiency was due to particle growth.

Calvert et al. (1973) present a detailed description of the previously reported studies on FF/C scrubbing. Technical feasibility of FF/C scrubbing was established in this report, based on theoretical development of FF/C scrubber performance models and limited bench scale experimental work. Further bench scale experimental work, reported by Calvert and Jhaveri (1974) led to the following conclusions:

1. Diffusiophoresis and inertial impaction enhanced by particle growth are the most significant particle collection mechanisms in FF/C scrubbers, while thermophoresis has a minor effect. All of these mechanisms are practically independent of the particle size.
2. Performance of an FF/C scrubber depends heavily on the amount of vapor available for condensation and the number concentration of particles.
3. Multiple stage or continuous contact type of scrubbers are most suitable for FF/C application. They can be readily adapted to provide different conditions and geometry along the gas path to accommodate changing flowrates and particle concentrations.
4. The most critical assumptions for the application of FF/C scrubber engineering design equations are the specific details of heat and mass transfer, mode of gas-liquid contact and nucleation of condensation on the particles. Better particle collection is obtained if the ratio of gas phase mass transfer coefficient to the liquid phase heat transfer coefficient is higher.

Based on the above information, multiple plate and spray scrubber configurations were selected for experimental study. The multiple plate FF/C scrubber configuration has the benefit of higher transfer coefficient ratio compared to the packed bed configuration. Also, due to the distinct separation of stages, it permits higher operational flexibil ity and allows for accurate measurement of stream conditions within the scrubber. The spray FF/C scrubber has the benefit of low energy requirement and low capital costs since high gas velocity is permissible, compared to the other low energy scrubbers considered.

The following parameters were determined to affect the particle collection mechanisms, diffusiophoresis and inertial impaction enhanced by particle growth, most significantly:

1. Multiple plate scrubber
    a. Condensation ratio
    b. Particle number concentration
    c. Number of stages or plates
    d. Ratio of the scrubber liquid to gas flowrates
    e. Distribution of vapor condensation over the stages or plates
2. Spray scrubber
    a. Condensation ratio
    b. Particle number concentration
    c. Spray drop diameter
    d. Cold liquid flowrate
    e. Overall gas-liquid contact mode
    f. L/G

Effects of these parameters on scrubber performances were experimentally evaluated in this study.

CHAPTER 4
EXPERIMENTAL PILOT PLANT

Based on the theoretical considerations described in the previous section, a multiple sieve plate scrubber and a horizontal spray scrubber were selected for the study of FF/C scrubbing on a pilot plant scale. During this study, fractional penetrations of fine particles through the scrubbers were experimentally determined for several scrubber operating conditions. In this section, the following information is described for both the FF/C scrubber systems:

1. Details of the pilot scale scrubber systems
2. Scrubber operating procedures
3. Particulate sampling procedures
4. Methods of data analyses and calculation
5. Accuracy of measurements
6. Operational conditions studied

THE MULTIPLE SIEVE PLATE FF/C SCRUBBER

Pilot Scale Scrubber System

The schematic process flow diagram of the pilot scale FF/C scrubber system is shown in Figure 4-1. Components of the scrubber system are listed in Table 4-1. The scrubber had a design capacity of 0.24 actual m^3/sec (500 ACFM) inlet gas flowrate. Since it was decided to test the horizontal spray scrubber, the second FF/C scrubber studied, at a gas flowrate of 0.47 actual m^3/sec (1,000 ACFM), the remaining components of the scrubber system were designed to handle this higher capacity. As an illustration, flowrates in the lines shown in Figure 4-1 are described in Table 4-2, when the inlet gas stream to the scrubber is at 77°C, saturated with water vapor. The FF/C scrubber and the particle generators are described below together with the instrumentation and calibration procedures.

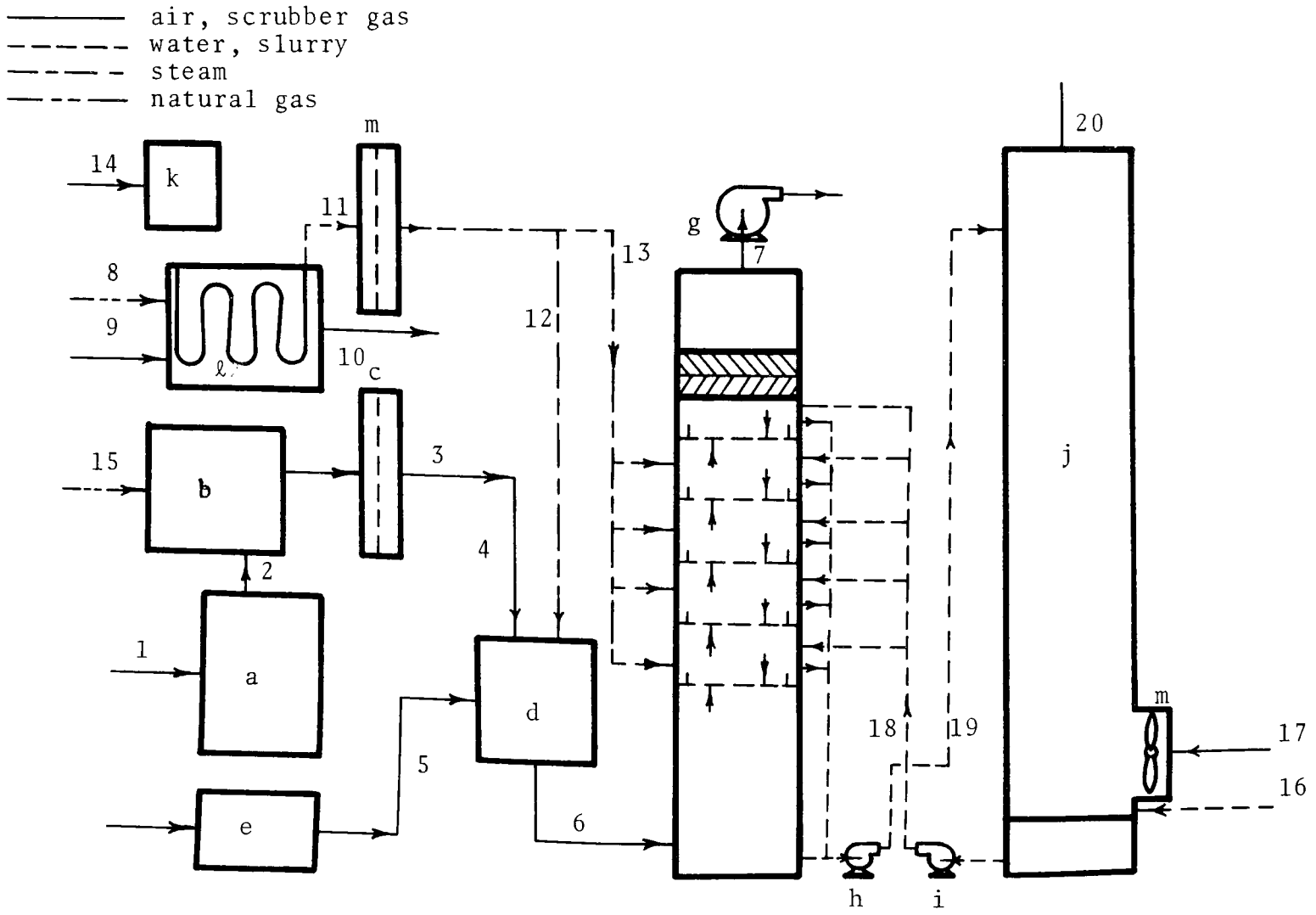

Figure 4-1 - The pilot scale multiple plate FF/C scrubbing system.

Table 4-1. EQUIPMENT SPECIFICATIONS

Equipment:

a. Prefilter
   Four automobile air filters with a capacity of 8.5 m^3/min air, each

b. Heat exhanger
   Gas-fired air heater to heat air from 24°C to 100°C

c. "Absolute" filter
   MSA "Ultra-air" filter with a capacity of 0.476 m^3/sec of gas

d. Particle and steam mixer
   Disc and donut type mixer 0.25 sec residence time.

e. Particle generator
   Up to 10% particles/cm^3 of scrubber gas inlet

f. FF/C scrubber
   Sieve plate scrubber

g. Scrubber exhaust fan
   Centrifugal fan with design capacity of 0.476 m^3/sec and ΔP of 50 cm W.C.

h. Pumps
   227 ℓ/min and 15 m head (60 gpm and 50 ft of head)

i. Pump
   227 ℓ/min and 15 m head, self priming

j. Water cooling tower
   A splash type cooling tower. Cooling range 47°C at 190 ℓ/min

k. Boiling water treatment
   11.3 ℓ/min ion exchanger

ℓ. Steam boiler
   760 Kg/hr steam at 2.0 atm

m. Cooling tower fan
   4.25 m^3/sec and 2.5 cm W.C.

Table 4-2. STREAM FLOW RATES OF THE MULTIPLE PLATE FF/C SCRUBBING SYSTEM

Stream No.	Compositions	Temp. °C	Vol. Flow		Mass Flow Kg/hr.	Enthalpy* Kcal/Kg	Press.
			m^3/sec	ℓ/sec			
1 & 2	0.0675 mole H_2O/mole, air mix.	29°	0.129	-	514	9.65	ΔP_{12}=0.5 cm W.G.
3 & 4	"	100°	0.153	-	514	42.5	15.7 cm W.G.
6	0.696 mole H_2O/mole, air mix.	77°	0.240	-	735	290	20.8 cm W.G.
7	0.475 mole H_2O/mole, air mix.	32°	0.132	-	530	26.8	46.2 cm W.G.
8	0.00675 mole H_2O/mole, air mix.	29°	0.056	-	221.4	9.65	-
9	Natural Gas	29°	0.0045	-	35.6	-	20 cm W.G.
10	0.154 mole H_2O mole, air mix.	232°	0.104	-	257	190	-
11	Steam	106°	-	-	221	644	1.33 Kg/cm^2
12	Steam	106°	-	-	221	644	1.33 Kg/cm^2

* air or water

Table 4-2. STREAM FLOW RATES OF THE MULTIPLE PLATE FF/C SCRUBBING SYSTEM (Continued)

Stream No.	Compositions	Temp. °C	Vol. Flow		Mass Flow Kg/hr.	Enthalpy* Kcal/ Kg	Press.
			m^3/sec	ℓ/sec			
13	Steam	106°	-	-	221	644	1.33 Kg/cm^2
14	City Water	24°	-	0.071	254.5	24	3.16 Kg/cm^2
15	Natural Gas	29°	-	-	0.0006	-	20 cm W.G.
16	City Water	24°	-	-	13.8	24	3.16 Kg/cm^2
17	0.00675 mole H_2O/mole, air mix.	29°	4.75	-	19,800	9.65	-
18	Process Water	32°	-	0.97	3,500	32.2	-
19	Process Water	74°	-	1.03	3,600	70.5	-

* air or water

FF/C Scrubber

Scrubber shell: 0.3m x 0.3m x 5.2m, fabricated from 14 ga cold rolled steel. It had a removable flange in the front, for access into the scrubber. The inside walls were coated with a high temperature polyester finishing resin for protection against corrosion and leaks.

Plate design: The scrubber could be operated with a maximum of five plates. All the plates were identical, 1.5 mm thick, with 3.2 mm round perforations, adding up to a free area of 9% per plate. The perforations were countersunk to avoid the formation of a vena contracta in the gas jet through a perforation. The plate active area was 9.3×10^{-2} m^2. Each plate had straight 5.1 cm x 30.5 cm inlet and outlet wiers, with three 2.5 cm downcomer pipes installed behind the outlet wier.

Liquid flow: The scrubber inlet liquid from the cooling tower holding tank was introduced on the top plate of the scrubber. It then cascaded down through the plate downcomers to a 0.3m x 0.4m x 1.1m enclosure provided at the bottom of the scrubber, from which it was drained into the 200 liter scrubber water holding tank.

Entrainment separator: A wire mesh entrainment separator was installed in the scrubber over the top plate. The 0.3m x 0.3m x 0.15m entrainment separator with 98.2% voidage was made from 0.28 mm stainless steel wire in a standard knit design.

Steam introduction: Steam introduction manifolds were installed under all the five plates. Up to 120 Kg/hr of dry saturated steam could be introduced through 20 round holes, 1 cm in diameter, from each manifold. The steam could thus be introduced as turbulent jets through the holes, which were located to promote steam mixing in the gas stream below the plates.

Plate pressure drop characteristics were studied for each of the five plates in the scrubber. These characteristics define the operating gas and liquid flowrates on the sieve plate and are also essential for scale-up of the sieve plate column. The operating regions of a sieve plate are well discussed by McAllister, et al. (1958).

The pressure drop characteristics are plotted as a function of gas and liquid mass flowrates on Figures 4-2 through 4-6 for the five plates. The dry plate pressure drops are also shown for reference. The plates are numbered successively from the bottom to the top plate. The pressure drop characteristics were similar to the characteristics for type III sieve plates, as discussed by McAllister, et al. (1958). These characteristics were obtained using ambient air and water. The "weep" points are indicated on each plot by arrows. During the scrubber performance study, the plates were operated at gas and liquid flowrates above the "weep" points and below the flooding conditions.

Particle Generators

Two aerosols were used during the study, generated by dry dispersing pigment powders. In each case, the powder, after drying, was sieved through a 16 mesh screen. The pure black iron oxide powder, purchased from Pfizer Incorporated, was then fed to the inlet of a high pressure blower through a screw feeder arrangement. The radial blades of the blower were drilled to increase recirculation and shear on the dispersed particles within the blower casing.

The second pigment used was "Unitane OR-600" titanium dioxide powder, purchased from the American Cyanamid Company.

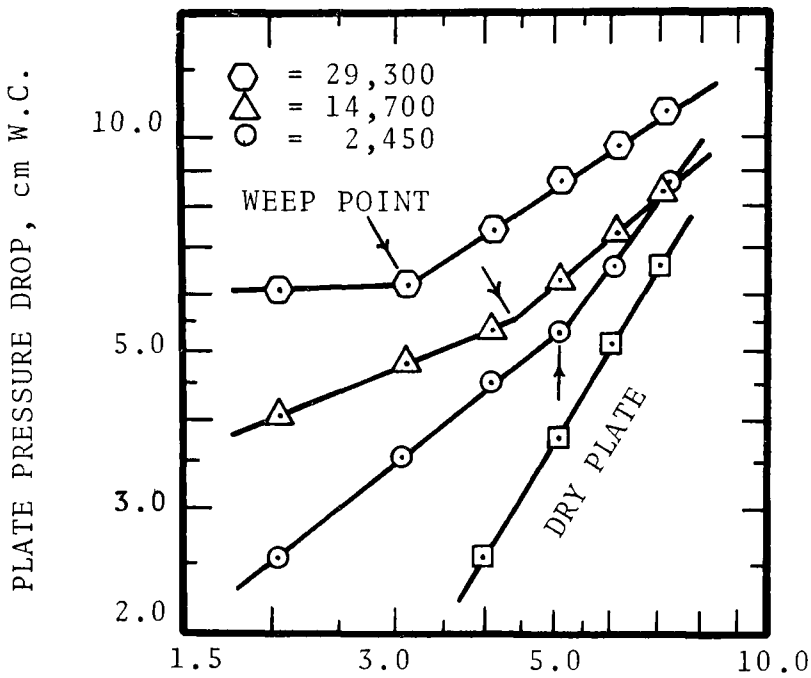

Figure 4-2 Pressure drop characteristics of the bottom plate (plate 1). L is in Kg/hr-m^2.

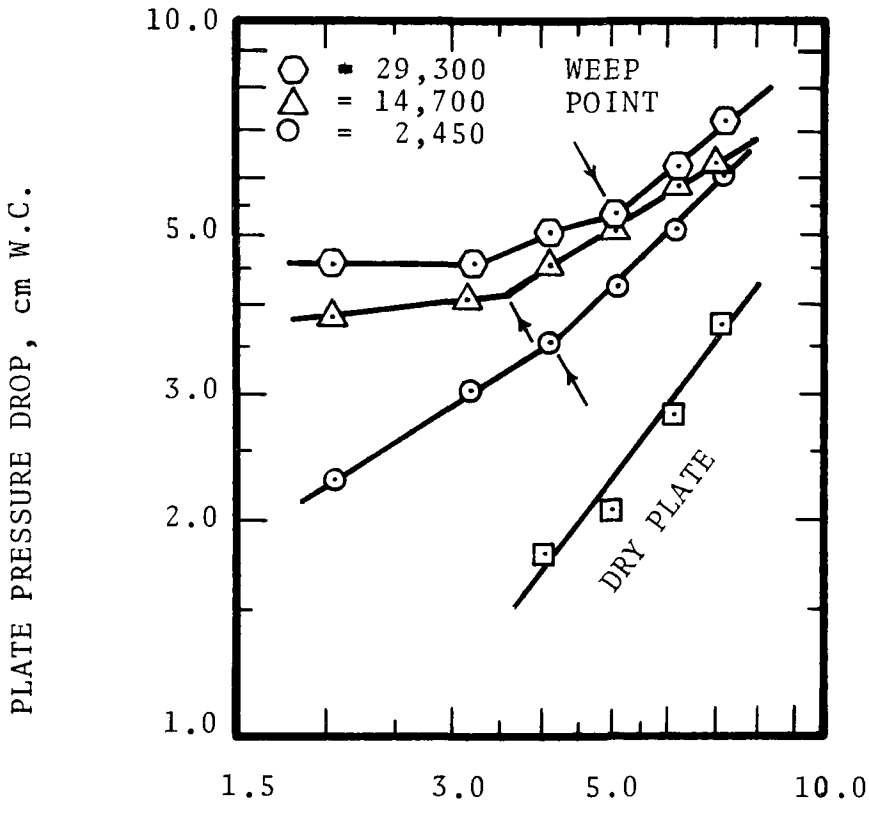

Figure 4-3 - Pressure drop characteristics of Plate 2. L is in Kg/hr-m^2.

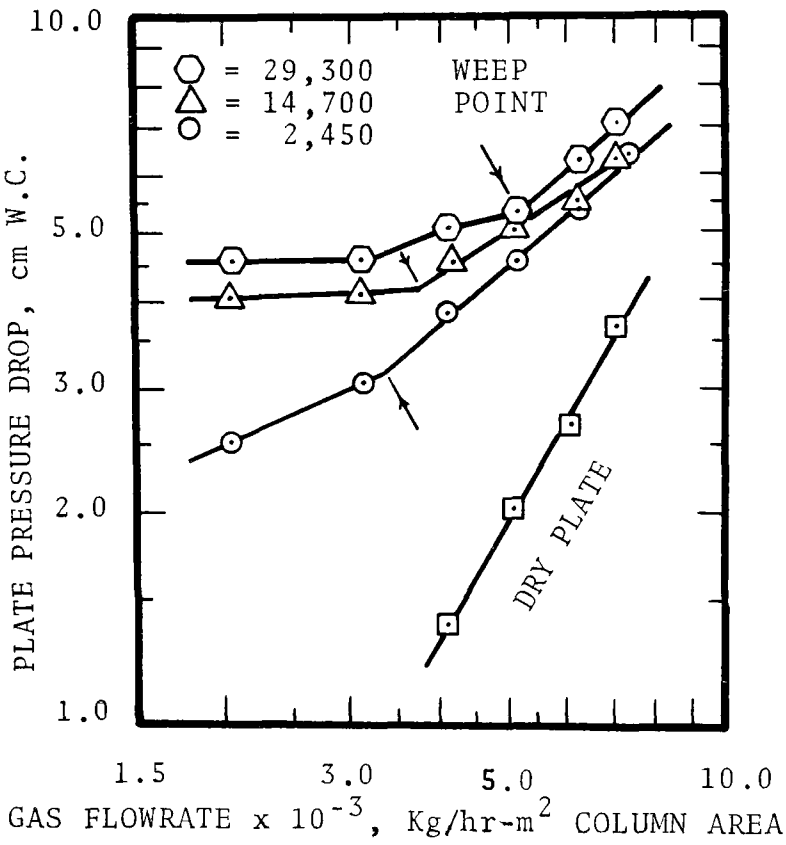

Figure 4-4 Pressure drop characteristics of Plate 3. L is in $Kg/hr\text{-}m^2$.

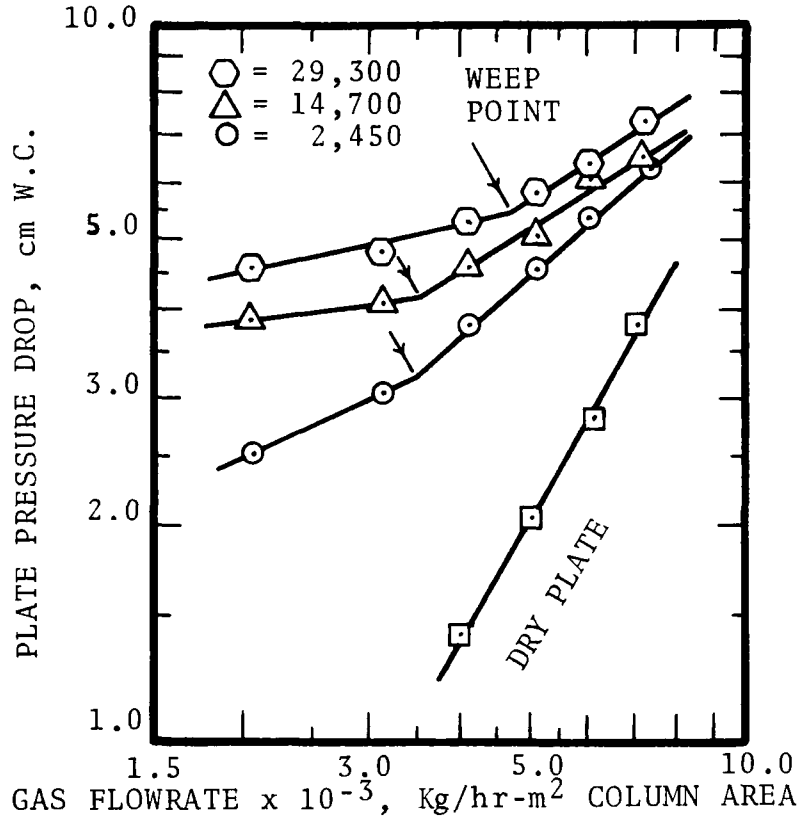

Figure 4-5 - Pressure drop characteristics of Plate 4. L is in Kg/hr-m^2.

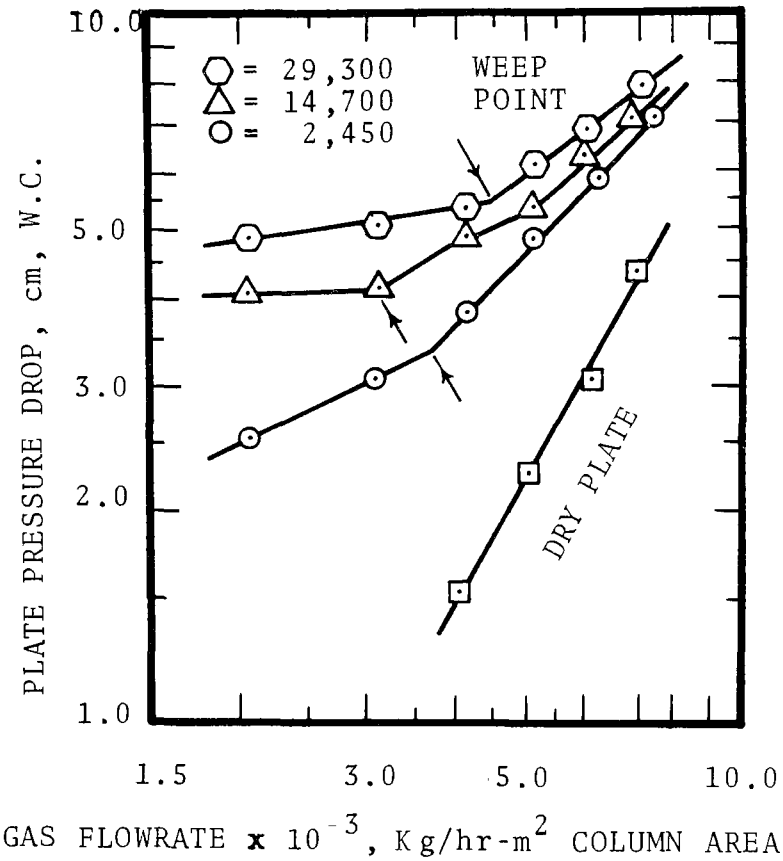

Figure 4-6 Pressure drop characteristics of Plate 5. L is in Kg/hr-m^2.

The powder was fed by a screw feeder arrangement into a compressed air ejector, immediately downstream of a 0.64 cm orifice. The compressed air pressure upstream of the orifice was maintained at 0.7 atm, gage.

The feed rates of the powders were controlled depending on the particle loading required. A cyclone and a multiple round jet impactor, both with cut diameters of 4 μmA, were used in series to remove coarse particles from the dispersed aerosols. Electrostatic charges on the dispersed particulates were then neutralized with nine "Staticmaster" ionizing units supplied by Nuclear Products Company, with 500 microcuries of Polonium 210 in each. These units were located in the aerosol duct upstream of the mixing section.

Instrumentation and Calibration

The inlet gas flowrate was measured with a venturi meter located in the 15.2 cm gas ducting. It was cali brated against flowrates measured by standard pitot tube traverses, in the range of 0.05 to 0.18 normal m^3/sec. Scrubber system liquor flowrates were also measured by venturimeters and rotameters installed in the 3.8 cm piping. They were calibrated by measuring the weight of water flowing through the pipes in a given time, in the range of 0.5 to 1 liter/sec. Error in the flowrate measurements was kept at less than ±0.2% of the flowrate by measuring at least 140 Kg of water for each calibration point.

Temperatures in the scrubber system were measured by copper-constantan (type T) thermocouples. The thermo-electric voltages were recorded on a strip chart recorder equipped with a potentiometric amplifier. The thermo-couples were calibrated against a standard mercury bulb

thermometer using constant temperature baths, and were found to correlate well with the standard E.M.F.-temperature relationships. Thus, the limits of error in measuring temperatures were ±0.8°C according to the manufacturer's specifications.

The scrubber gas line pressures were measured by U-tube, inclined and well-type manometers, and "Magnehelic" pressure gauges. Pressure drops across the liquor venturi meters were measured with two-fluid (water and mercury) well-type manometers.

Moisture content in the inlet gas stream to the scrubber was measured by wet and dry bulb thermometers. Gas stream downstream of the bottom sieve plate was considered to be saturated and the moisture contents were determined from the temperature of the gas.

PARTICULATE SAMPLING SYSTEM

Two identical particle sampling trains were used to measure the particulate loadings and size distributions in the scrubber gas inlet and outlet streams simultaneously. The particulate properties were measured with cascade impactors, followed by Gelman type A glass fiber filters. The cascade impactors used were six and eight stage, non-viable Andersen samplers and two University of Washington, Mark IIIF in-stack impactors. The samples were collected on aluminum substrates coated with high vacuum silicon grease to prevent particle bounce. The particulate loadings were rechecked by sampling with the glass fiber filters only, for each operating condition.

The samples were drawn through two 1.3 cm diameter sampling probes installed in the 3.7 cm sampling ports in the scrubber inlet and outlet gas ducts. The sampling

instruments, either the cascade impactors or the filter holders, were located close to the sample ports. 1.3 cm aluminum tubes were installed across the sampling instruments so that the sample flows could bypass the instruments in each train. The sample flowpaths were controlled with 3-way valves. Moisture from the sample gas was removed by three cold impingers and a silica gel dryer located downstream of the sampling instrument in each train.

The sampling probes, the sampling instruments and the aluminum tubing to the cold impingers were heated with insulated heating tapes controlled with variacs, to prevent water condensation in the lines. The dry gas sample flowrates were measured with a dry gas meter and a rotameter in each train. The sampling rates were controlled by valves on the high pressure and bypass lines of the oil less vacuum pumps. Prior to each run, the sampling instruments were heated to the stack gas temperatures. The sampling lines were also heated and flushed by drawing gas through the bypass lines.

EXPERIMENTAL PROCEDURE

The auxiliary equipment and the measurement instrumentation were checked and started up prior to the start-up of the scrubber. The liquor tanks were filled with city water and the boiler and cooling tower operation were started. The scrubber was started up by first starting the water flowrate and adjusting it to the experimental condition and then starting the scrubber blower to draw filtered ambient air through the scrubber. After a steady state was reached, the gas heater was fired and the air was heated up to the desired temperature. Then steam was introduced to attain the experimental moisture content in the gas stream. Again, after a steady state was reached

the particles were introduced to attain the experimental operating condition. It normally took 60 to 90 minutes to attain the experimental condition.

The flowrates, temperatures, pressures, moisture contents and scrubber pressure drops were measured every time a steady state was attained during the above procedure. These parameters were also measured just before the start-up of particulate sampling, at least once during the sampling or every thirty minutes, and just after the sampling was completed. Sampling time in the scrubber inlet duct varied from 15 minutes to 60 minutes depending on the particulate loading, and the sampling rate ranged from 0.68 to 1.0 m^3/hr at the probe. The outlet sampling time was from 2 to 3 times the inlet and the sampling rate was about twice the inlet sampling rate to allow for the lower outlet particle loadings.

When the total sampling time exceeded 30 minutes, the sampling was interrupted and the coarse particles caught in the cyclone and the impactor on the particle generator were cleaned out. This was necessary to maintain a steady performance of the particle generator. As the inlet and outlet ducts were sampled simultaneously, small variances in the particle generator performance did not significantly affect the results. Also, since at least 90% of the particles were smaller than 2 μm, the sampling rates were not adjusted to get isokinetic velocities at the probes.

The experimental conditions were found to stay very stable once a steady state was reached. For all the experimental runs reported, the temperature conditions for the experiment varied within ±1.5°C during the experimental period.

THE SPRAY FF/C SCRUBBER

Pilot Scale Scrubber System

The schematic process flow diagram of the FF/C scrubber system is shown in Figure 4-7. Components of the scrubber system are listed in Table 4-3. The scrubber had a design capacity of 0.47 actual m^3/sec (1,000 ACFM) inlet gas flowrate. As an illustration, flowrates in the lines shown in Figure 4-7 are described in Table 4-4 when the inlet gas stream to the scrubber is at 77°C, saturated with water vapor. The FF/C scrubber and the particle generator are described below.

FF/C Scrubber

Scrubber shell: 76.2 cm diameter x 3.8 m long made from "Techite" fiber glass reinforced plastic sewer pipe, with removable end flanges.

Spray arrangement: The scrubber consisted of three sections, with a spray nozzle manifold in each section. Each manifold had a capacity to spray 1.3 liters/sec of liquid with a sauter mean drop diameter of 400 μm. The nozzles were located in a grid pattern on the manifolds to obtain a uniform distribution of spray in the scrubber cross-section. The liquid was sprayed co-current in the direction of gas flow. Thirty-two size 1/4B3 "Whirljet" nozzles supplied by Spraying Systems Company, were used on each manifold.

Liquid flow system: The system was specially designed so that the cold scrubber liquid from the cooling tower could be sprayed either through all of the three manifolds in the scrubber, or through either the first or the last manifold in the scrubber. In the later cases, the scrubber was operated as a three-stage scrubber by spraying the outlet liquid

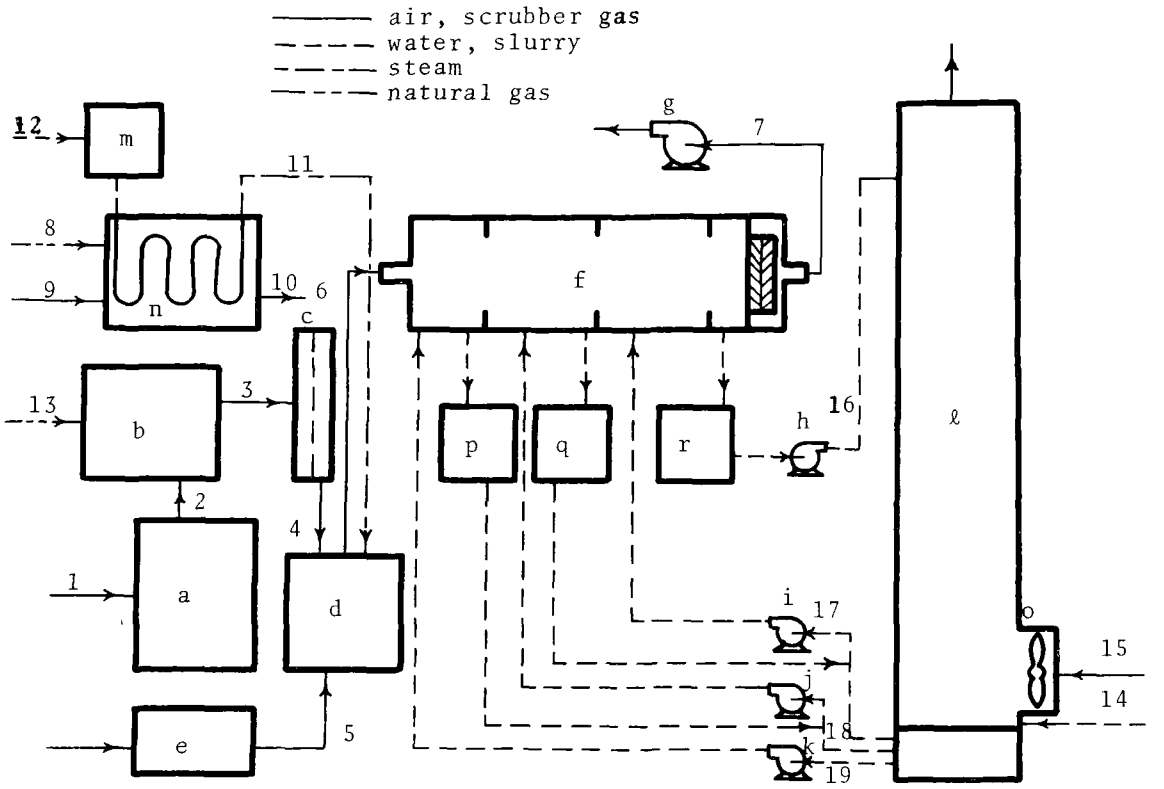

Figure 4-7 - Process flow sheet for the FF/C spray scrubbing system.

Table 4-3. EQUIPMENT SPECIFICATIONS

Equipment:

a. Air prefilter
   Four automobile air filters with a capacity of 8.5 m^3/min air each

b. Air heater
   Gas-fired air heater to heat air from 24°C to 100°C.

c. "Absolute" air filter
   MSA "Ultra-Air" filter with a capacity of 0.476 m^3/sec of air.

d. Air, particulates and steam mixer
   Disc and donut type mixer, 0.25 sec residence time.

e. Particle generator
   To generate dry dispersed solid particulates with a mass mean diameter less than 2 μmA, up to 10^9 particles/cm^3 of scrubber inlet air.

f. FF/C scrubber
   Horizontal spray scrubber with a mesh type mist eliminator.

g. Scrubber exhaust fan
   Centrifugal fan with design capacity of 0.476 m^3/sec and ΔP of 50 cm W.C.

h. Pump
   227 ℓ/min and 15 m head (80 gpm and 50 ft head)

i, j, k. Pumps
   114 ℓ/min and 3.4 atm head, each. (30 gpm and 50 psi head).

l. Water cooling tower
   A splash type, forced draft cooling tower. Cooling range 47°C at 190 ℓ/min

m. Boiler water treatment
   11.3 ℓ/min ion exchanger.

n. Steam boiler
   760 Kg/hr steam at 2.0 atm.

o. Cooling tower fan
   4.25 m^3/sec and 2.5 cm W.C. head

TABLE 4-3 (continued)

p, q. Inter-stage liquor holding tanks.
200 liters capacity, each.

r. Scrubber liquor holding tank
450 liters capacity.

Scrubber liquor circuit
3.8 cm nominal diameter pipes, fittings, connections and valves.

Steam circuit
5 cm, 3.8 cm and 2.5 cm diameter pipes, connectors, valves, steam traps, 15.2 cm mist eliminator; all insulated.

Scrubber gas ducting
15 cm diameter inlet duct with connectors, insulated.
15 cm diameter outlet duct with connectors, insulated from scrubber outlet to sampling ports.

Table 4-4 - STREAM FLOW RATES OF THE SPRAY SCRUBBING SYSTEM

Stream No.	Compositions	Temp. °C	Vol. Flow		Mass Flow Kg/hr	Enthalpy* Kcal/Kg
			m^3/sec	ℓ/sec		
1 & 2	0.024 mole H_2O/mole dry air, air mixture	29	0.258	-	1,028	9.65
3 & 4	" "	100	0.306	-	1,028	42.5
6	0.696 mole H_2O/mole dry air, air mixture	77	0.480	-	1,450	206
7	0.0483 mole H_2O/mole dry air, air mixture	32	0.264	-	1,060	26.8
8	0.00675 mole H_2O/mole dry air, air mixture	29	0.112	-	442.8	9.65
9	Natural gas	29	0.009	-	71.2	-
10	0.154 mole H_2O/mole dry air, air mixture	232	0.208	-	514	190
11	Steam	106	-	-	442	644
12	City water	24	-	0.142	509	24
13	Natural gas	29	-	-	9.6	-
14	City water	24	-	-	26.8	24
15	0.00675 mole H_2O/mole dry air, air mixture	29	4.75	-	19,800	9.65
16	Process water	51	-	3.95	13,975	51
17	" "	20	-	1.20	4,525	20
18	" "	20	-	1.20	4,525	20
19	" "	20	-	1.20	4,525	20

* air or water.

collected in one section of the scrubber, into the next section, and then into the third section in series. Thus, the cold liquid requirement was reduced to one-third of the amount when cold liquid was sprayed in all of the three sections. When the cold liquid was sprayed into the first section, the gas-liquid contact was co-current through the three sections and when it was sprayed in the last section, the contact was counter-current. Separation of sprayed liquid from one section to another was effected by sets of baffles, storage tanks and pumps, as shown in Figure 4-7.

Entrainment separator: A wire mesh entrainment separator, 38.1 cm diameter, 15.2 cm long, made from 0.28 mm stainless steel wire in a standard knit design with 98.2% voidage, was installed downstream of the third spray section.

Particle Generator

The second particle generator described earlier, to dry disperse titanium dioxide powder, was used for this study. Due to the higher particle loading required, the compressed air pressure upstream of the orifice was increased to 1.0 atm, gage.

Instrumentation and Calibration

The inlet gas flowrate was measured with a standard pitot tube located downstream of the air prefilter. The scrubber system liquor flowrates, temperatures, line pressures and moisture contents were measured with the same instruments as described earlier for the multiple plate scrubber. The measuring instruments were periodically calibrated, as described earlier.

PARTICULATE SAMPLING SYSTEM

Two identical particulate sampling trains, described earlier, were used to measure the particulate loadings and size distributions in the scrubber gas inlet and outlet streams, simultaneously. Two University of Washington Mark IIIF in-stack cascade impactors and Gelman type A glass fiber filters were used to measure the particulate characteristics.

The sampling procedure was also the same as described earlier, except that the sampling elements were installed in the respective stacks to minimize losses in the sampling probes. The elements were also heated with electrical heating tapes prior to sampling, to prevent condensation in the sampling train lines.

EXPERIMENTAL PROCEDURE

The experimental start-up and shutdown procedures were the same as reported earlier for the multiple plate scrubber. The scrubber system flowrates, temperatures, pressures and moisture contents were measured every time a steady state was attained during the above procedure. These parameters were also measured just before the start-up of particulate sampling, at least once during the sampling or every thirty minutes, and just after the sampling was completed. The sampling times and rates were the same as described earlier. The experimental conditions were found to stay very stable, once a steady state was reached. For all the experimental runs reported, the temperature conditions for the experiment varied within $\pm 1.5^{\circ}C$ during the experimental period.

The methods of data analysis and calculation, and thus the accuracy of measurements, were the same as described earlier for the multiple plate scrubber.

EXPERIMENTAL CONDITIONS STUDIED

During the experimental study, the scrubber performance was studied for five scrubber operational modes. The experimental runs for one of the operational modes, with cold water sprayed in all of the three sections of the scrubber, were repeated to check the reproducibility of results. The operating modes are described in Table 4-5. During each mode, scrubber performance was studied for a range of "q'", varying from the cold runs to q' = 0.2.

METHODS OF ANALYSIS AND CALCULATION

As mentioned earlier, the particle characteristics and the scrubber performance were measured by sampling with absolute glass fiber filters and cascade impactors. Information on total particulate loadings and thus the overall scrubber penetrations, $\overline{Pt}$, were obtained from both of the above sampling apparatus. Sampling with the cascade impactors provided additional information on the particle size distributions, fractional loadings and thus the fractional penetrations, and the inlet particle number concentrations.

Particle Loadings and Overall Penetrations

The total particle loadings in the inlet and outlet ducts were calculated in the following manner:

1. The sample flowrate was converted to the standard conditions of 0°C and 76 cm of mercury pressure.
2. Total weight gain on the sampling elements was measured with an analytical balance, Sartorius Model 2443; ±0.05 mg precision.

Table 4-5. SPRAY SCRUBBER OPERATION MODES

Dust used: Titanium dioxide, -16 mesh
$n_i \simeq 10^6/cm^3$

No.	Operating Mode	Inlet Liquid Flowrate per Section(ℓ/sec)	Drop Size	Notes
1	One Stage	~1.0	Small (Mass mean dia~350μm)	a. No.2 was a repetition of No.1.
2	One Stage	~1.0	Small	b. Liq. flow-rate for No.3 was reduced by reducing the no. of spray noz-zles.
3	One Stage	~0.76	Small	
4	One Stage	~0.76	Large (Mass mean dia~450μm)	
5	Three Stages Co-current	~1.0	Small	c. Liq. flow-rate for No.4 was reduced by reducing the spray pressure.
6	Three Stages Counter-current	~1.0	Small	

3. The particle mass loading, c_p(g/DNm^3), was calculated from:

$$c_p = \frac{\text{(total weight gain, g)}}{\text{(Sampling rate, DNm}^3\text{/min) x (Sampling time, min)}} \quad (4\text{-}1)$$

4. The overall penetration was calculated from:

$$\overline{Pt} = \frac{c_{po}}{c_{pi}} \quad (4\text{-}2)$$

where "c_{po}" and "c_{pi}" were the outlet and inlet particle loadings measured simultaneously for the run.

Particle Size Distribution

The particle size distributions were measured gravi metrically using the cascade impactor data. The particles were assumed to have a log normal distribution. Cumulative mass of particles collected on a stage and all the stages below, including the absolute filter, were calculated as a percentage of the total weight gain. The cut diameters for the impactor stages were calculated from the sampling rate, based on the manufacturer's specifications. The geometric mass mean aerodynamic diameter, "d_{pg}", and the geometric standard deviation, "σ_g", were then determined from a plot of the aerodynamic cut diameters against the percent cumulative loading smaller than the cut diameters, on a log probability paper.

Particle Number Concentration

Particle size distribution as measured by cascade im-pactors was in terms of mass and it was necessary to con vert this into a number distribution. For log-normal size distributions it is simple to determine number mean diameter

from mass mean diameter but this does not provide information as to the number concentration. A method was developed for computing the number concentration by multiplying a hypothetical number concentration based on "d_{pg}" by a correction factor which is dependent on "σ_g". The derivation of this relationship is given below.

The total number concentration of particles, "n_t", can be computed from:

$$\int_0^{V_t} \frac{dn}{dv}\, dv = n_t, \text{ no/cm}^3 \qquad (4\text{-}3)$$

and,

$$\frac{dn}{dv} = \frac{3}{4\,\pi r_p^3}, \frac{\text{no. of particles}}{\text{cm}^3 \text{ of particles}} \qquad (4\text{-}4)$$

where n = cumulative particle number concentration, smaller than "r_p", no/cm^3

v_p = cumulative particle volume concentration, cm^3/cm^3

v_t = total particle volume concentration

r_p = particle radius, cm

We define $V \equiv \frac{v}{v_t}$ = cumulative volume fraction, dimensionless. And,

$$\int_0^{V_t} \frac{dn}{dv}\, dv = v_t \int_0^1 \frac{dn}{dv}\, dV \qquad (4\text{-}5)$$

The influence of particle radius can be related to the mass mean radius by:

$$R_{ni} \equiv \left(\frac{dn}{dv}\right)_i \Big/ \left(\frac{dn}{dv}\right)_m = \left(\frac{r_{pg}}{r_{pi}}\right)^3 \qquad (4\text{-}6)$$

where R_{ni} = ratio of actual no. concentration for particle radius "r_{pi}" to hypothetical no. concentration based on "r_{pg}", dimensionless

Subscript i is for radius "r_{pi}"

Subscript m is for mass mean radius, "r_{pg}"

Thus, "R_n", total number concentration ratio, is:

$$\int_0^1 R_{ni}dV = R_n = \frac{\text{actual no. concentration}}{\text{no. conc. based on } r_{pg}} \qquad (4\text{-}7)$$

This equation was integrated numerically for different values of "σ_g". Note that for a log-normal distribution the probability of the ratio of size to mean size is normally distributed. Therefore, "R_n" is defined by "σ_g" only. A plot of "R_n" versus "σ_g" was thus obtained. From the total particulate loading and "d_{pg}" at scrubber inlet, the hypothetical number concentration was calculated for each run. Particle density of the iron oxide aerosol was assumed to be 2.5 g/cm^3 from Kotrappa and Wilkinson (1972), and 3.0 g/cm^3 for the titanium dioxide aerosol. Then, using the experimental "σ_g", "n_i", the particle number concentration at the scrubber inlet, was determined from the plot.

These values of "n_i" were checked periodically by using the Gardner and Pollack Condensation Nuclei Counters. The values were found to agree within a factor of 3.

Fractional Penetrations

The computation of penetration as a function of particle aerodynamic diameter, or the fractional penetration through the scrubber was done by a stepwise graphical procedure. The procedure is based on the following equations:

Overall penetration can be defined as:

$$\overline{Pt} = \frac{1}{c_{pt}} \int_{o}^{c_p} Pt_{d_{pa}} \, dc_p \qquad (4\text{-}8)$$

where "c_{pt}" is the total particle loading and "$Pt_{d_{pa}}$" is the penetration for particle diameter, "d_{pa}", and it is given by:

$$Pt_{d_{pa}} = \frac{f(d_{pa})_o}{f(d_{pa})_i} = \frac{\left[\frac{dc_p}{d(d_{pa})}\right]_o}{\left[\frac{dc_p}{d(d_{pa})}\right]_i} \qquad (4\text{-}9)$$

where $\left[\frac{dc_p}{d(d_{pa})}\right]$ is the slope of cumulative mass loading less than "d_{pa}" versus the aerodynamic particle diameter curve, at "d_{pa}", and equals "$f(d_{pa})$".

Thus, to determine the fractional penetration, the following procedure was followed:

1. Cumulative mass loading for all the stages and the filter, below the stage with a cut diameter of "d_{pa}", were plotted against "d_{pa}" from the inlet and outlet cascade impactor samples.
2. Slopes of the inlet and outlet plots above were determined for several "d_{pa}" values in the range of 0.4 to 5 μmA. The fractional penetrations were then determined and plotted from the ratio of the slopes, as described above.

ACCURACY OF MEASUREMENT

Accuracy in measuring the particle size distributions, fractional penetrations, overall penetrations and the

inlet particle number concentrations from the cascade impactor data depended on several factors. The precision of the balance, impactor handling procedures, and measurement of sampling rate influence the subsequent determination of cut diameters. Subjective judgements of the persons analyzing the data are involved when reading the graphs and determining slopes. It is beyond the scope of this study to determine the accuracy statistically. Best possible care was taken in the laboratory, sampling and analytical procedures to obtain accurate data and results. At least two runs were made at every operating condition to duplicate the data.

During the determination of overall penetrations using "absolute" glass fiber filters, as least 5 mg of sample was collected on each filter. Precision of the analytical balance was ±0.05 mg. Thus, the maximum error due to the weighing accuracy in determining $\overline{Pt}$ was:

$$\overline{Pt} = \frac{c_{p_o}}{c_{p_i}}$$

$$\text{Thus,} \quad \frac{d\overline{Pt}}{\overline{Pt}} = \frac{dc_{p_o}}{c_{p_o}} - \frac{dc_{p_i}}{c_{p_i}} \qquad (4\text{-}10)$$

As the absolute values of the error were small compared to the actual weights and as the error terms are additive,

$$\text{Maximum error, } \overline{Pt} = \frac{\Delta c_{p_o}}{c_{p_o}} + \frac{\Delta c_{p_i}}{c_{p_i}} \qquad (4\text{-}11)$$

$$\text{Thus, maximum error, } \overline{Pt} = \pm \frac{0.2}{5} = \pm 4\%.$$

EXPERIMENTAL CONDITIONS STUDIED

During the experimental study, the scrubber performance was studied for six scrubber operational modes. For each operational mode, the scrubber performance was studied for a range of the amount of water vapor condensed in the scrubber per unit of dry air flow, "q'", varying from the cold runs when particles were scrubbed from ambient air to $q' \simeq 0.2$. The operating modes are described in Table 4-6.

Table 4-6 MULTIPLE PLATE SCRUBBER OPERATIONAL MODES

No.	No. of Plates	Inlet Liq. Flowrate (ℓ/sec)	Particle Material	n_i (no./cm^3)	Notes
1	5	0.64	Iron Oxide	low, ~10^5	During No. 6, steam introduction was distributed under two plates.
2	4	0.64	Iron Oxide	low, ~10^5	
3	4	0.64	Titanium Dioxide	high, ~10^8	
4	4	0.38	Titanium Dioxide	high, ~10^8	
5	5	0.38	Titanium Dioxide	high, ~10^6	
6	5	0.38	Titanium Dioxide	high, ~10^6	

CHAPTER 5
EXPERIMENTAL RESULTS AND DISCUSSIONS

Experimental and sampling procedures, and the methods of data analyses and calculation of results are described in the preceding chapter. During the experimental study, scrubber performances were determined as fractional penetration of particles (with respect to the aerodynamic particle diameter) and the overall particle penetration through the scrubbers. Since the scrubber inlet particle characteristics (size distribution and number concentration) were different for each run, the fractional penetrations provide a common base for comparing scrubber performances for different operating conditions. The scrubber operating conditions and performance are tabulated, with the fractional penetration plots for cascade impactor runs, in Appendix 5.A for the multiple plate scrubber and Appendix 5.B for the spray scrubber experiments.

THE MULTIPLE SIEVE PLATE FF/C SCRUBBER

Results

The multiple plate scrubber was evaluated at six operating modes as listed in Table 4-6. For each operating mode, the scrubber performance was measured for a range of "q'" values. Effects of the following variables were also determined:

1. Addition of a fifth plate.
2. Changing the L/G ratio by changing the inlet liquid flowrate.
3. Distribution of vapor condensation on the plates by distributing steam introduction under two plates.
4. The effect of inlet particle number concentration, "n_i".

As discussed in Chapter 3, particle growth and diffusiophoresis are expected to contribute the most to the enhancement of particle capture in the scrubber during vapor condensation. Thus, the amount of vapor condensed in the scrubber per unit of dry gas, "q'", and the scrubber inlet particle number concentration, "n_i", are the significant parameters to determine the enhancement of particle capture in the FF/C scrubber.

Penetrations, "Pt", for 1.0 μmA and 0.6 μmA particles are plotted against "q'" in Figures 5-1 through 5-5 for the scrubber operating modes studied. Data points on these plots were read from the fractional penetration plots in Appendix 5.A. These data points were found to be scattered on "Pt versus q'" plots, possibly indicating the effects of other parameters, such as "n_i", the inlet liquid temperatures and scrubber pressure drops.

DISCUSSION

Calvert and Jhaveri (1974) have summarized the high points of the previously available data on FF/C scrubbing on a plot of penetration versus the condensation or injection ratio. On Figure 5-6, the plate scrubber performance is similarly compared with the results of Rozen and Kostin (1967), for 1.0 μmA particles. The following is indicated by the plot:

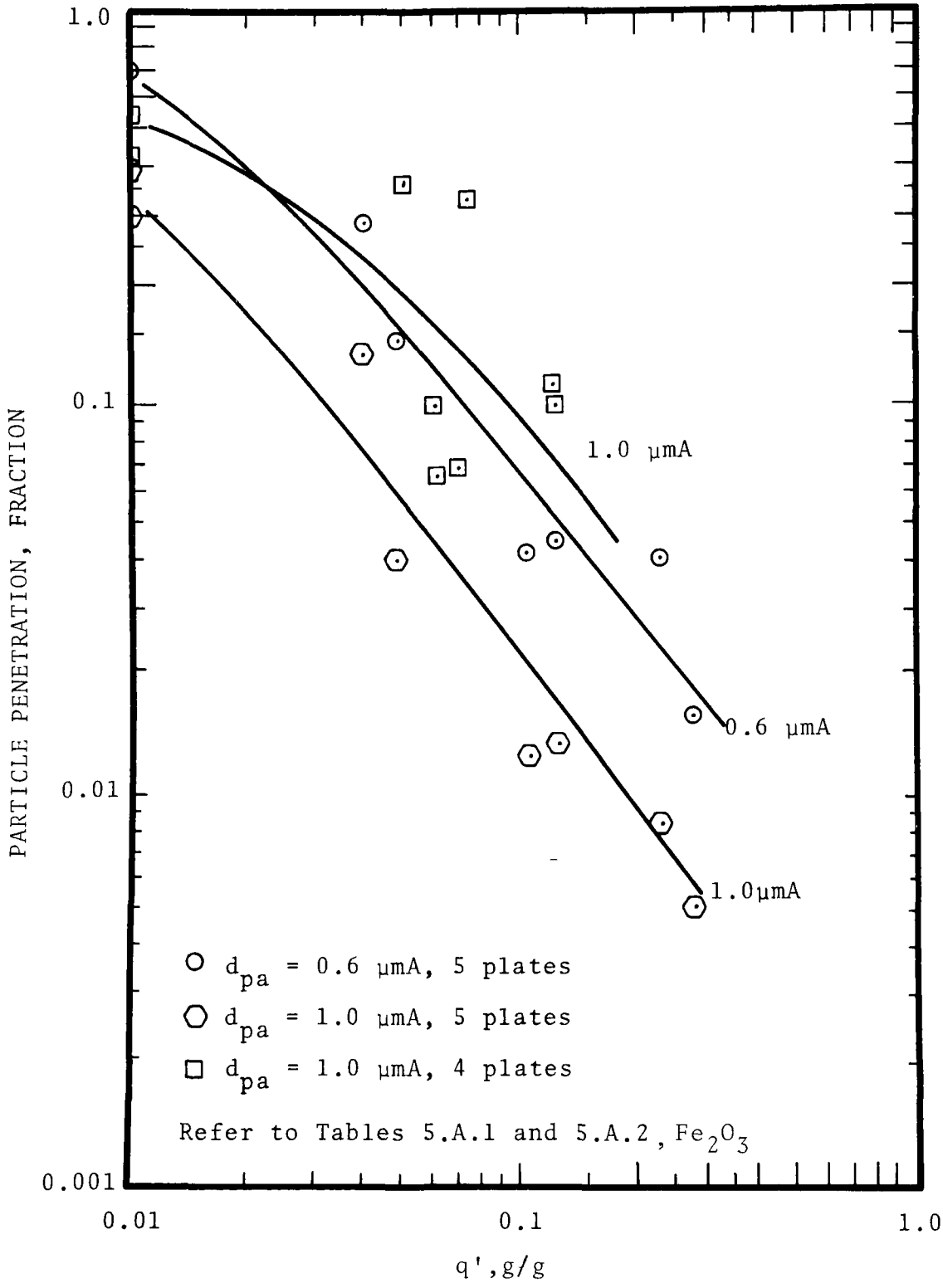

Figure 5-1 - Penetration versus condensation ratio, four and five plates.

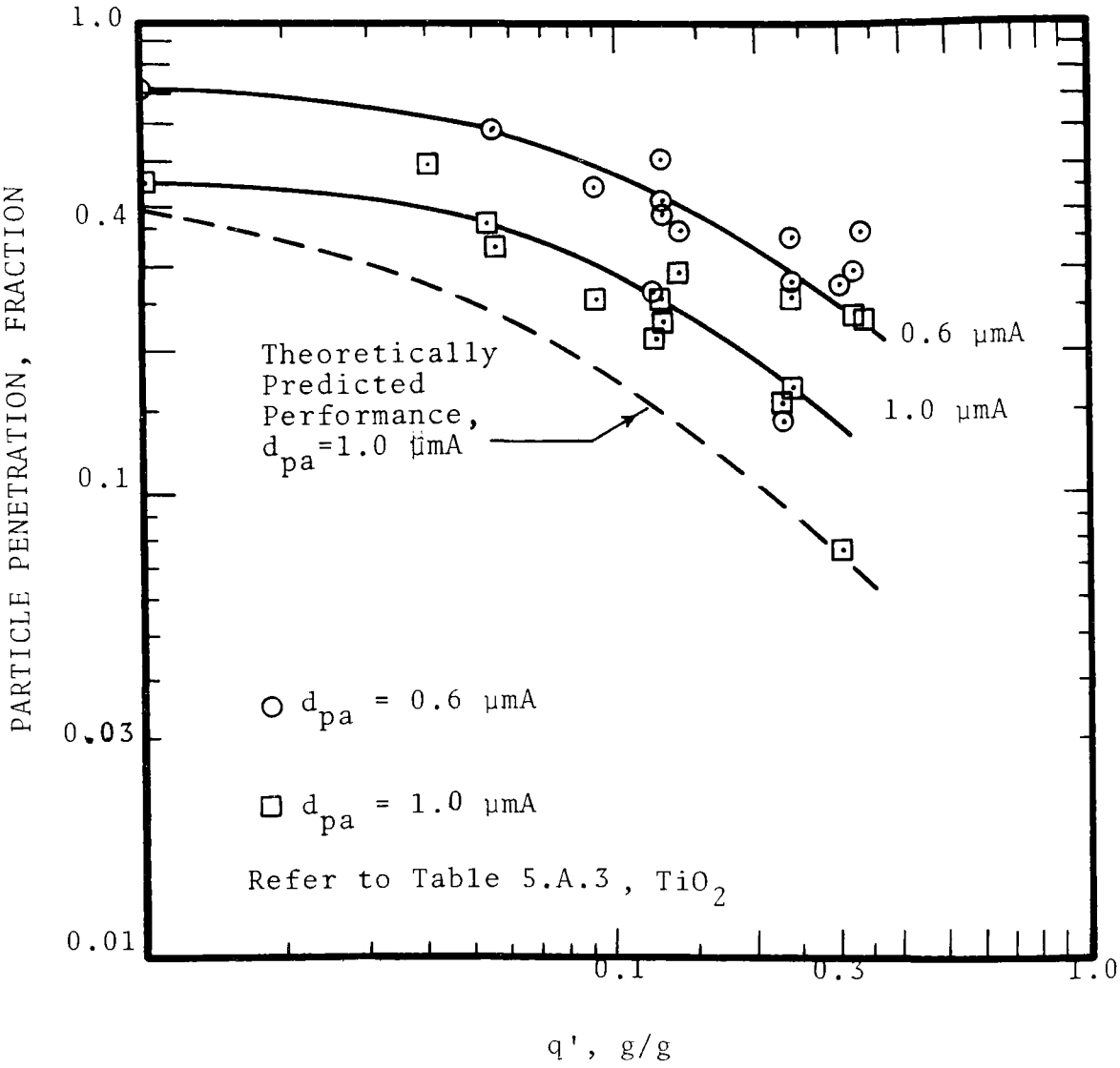

Figure 5.2 - Penetration versus condensation ratio, four plates

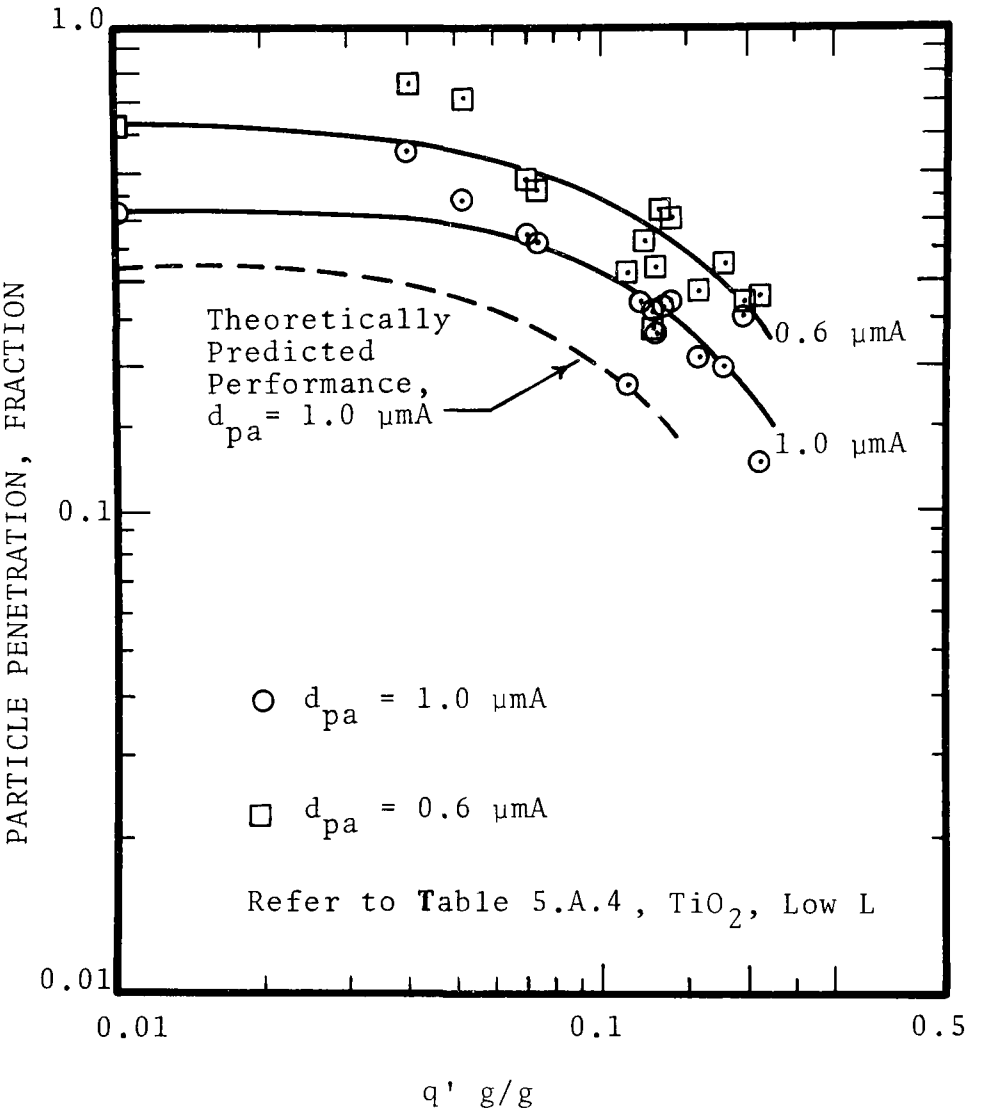

Figure 5.3 Penetration versus condensation ratio, four plates.

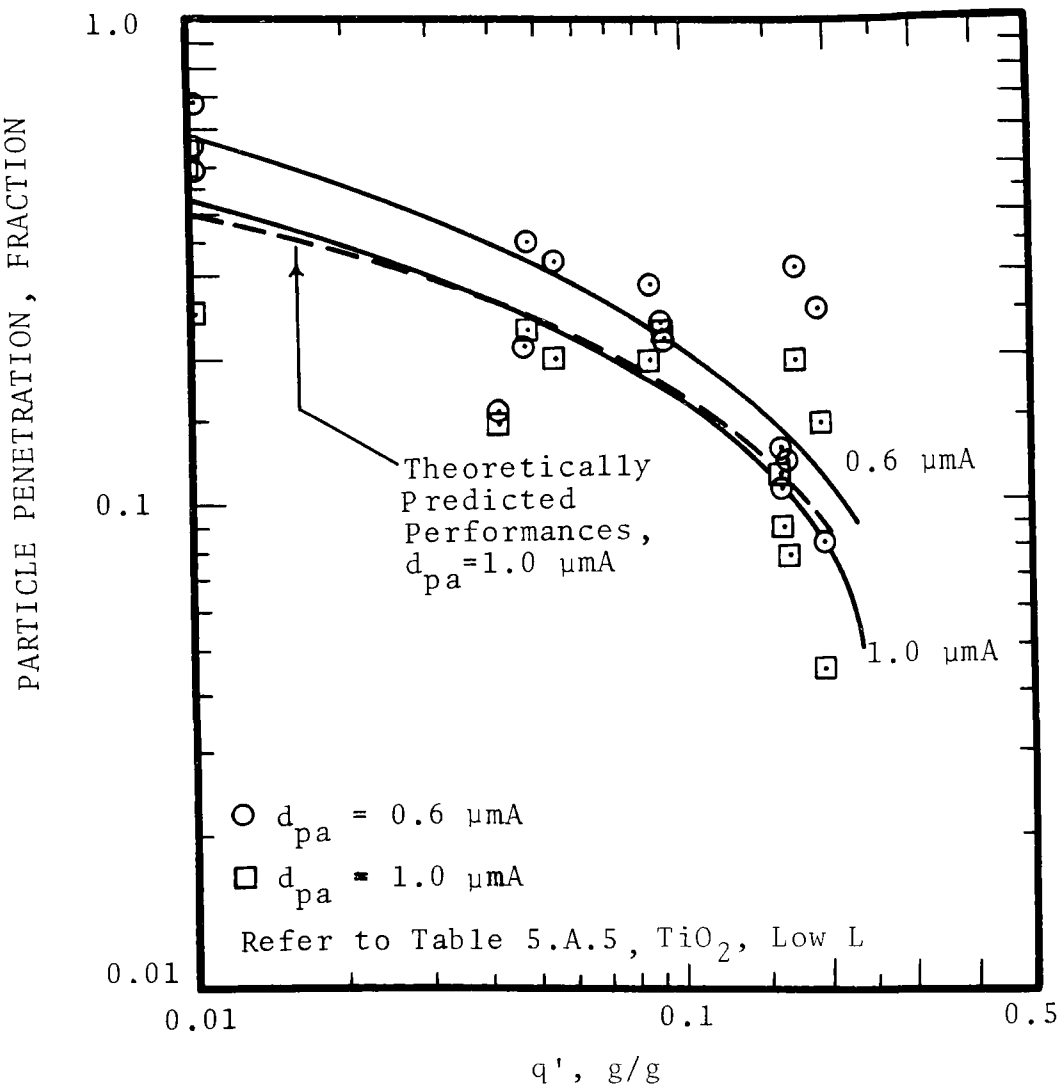

Figure 5.4 Penetration versus condensation ratio, five plates

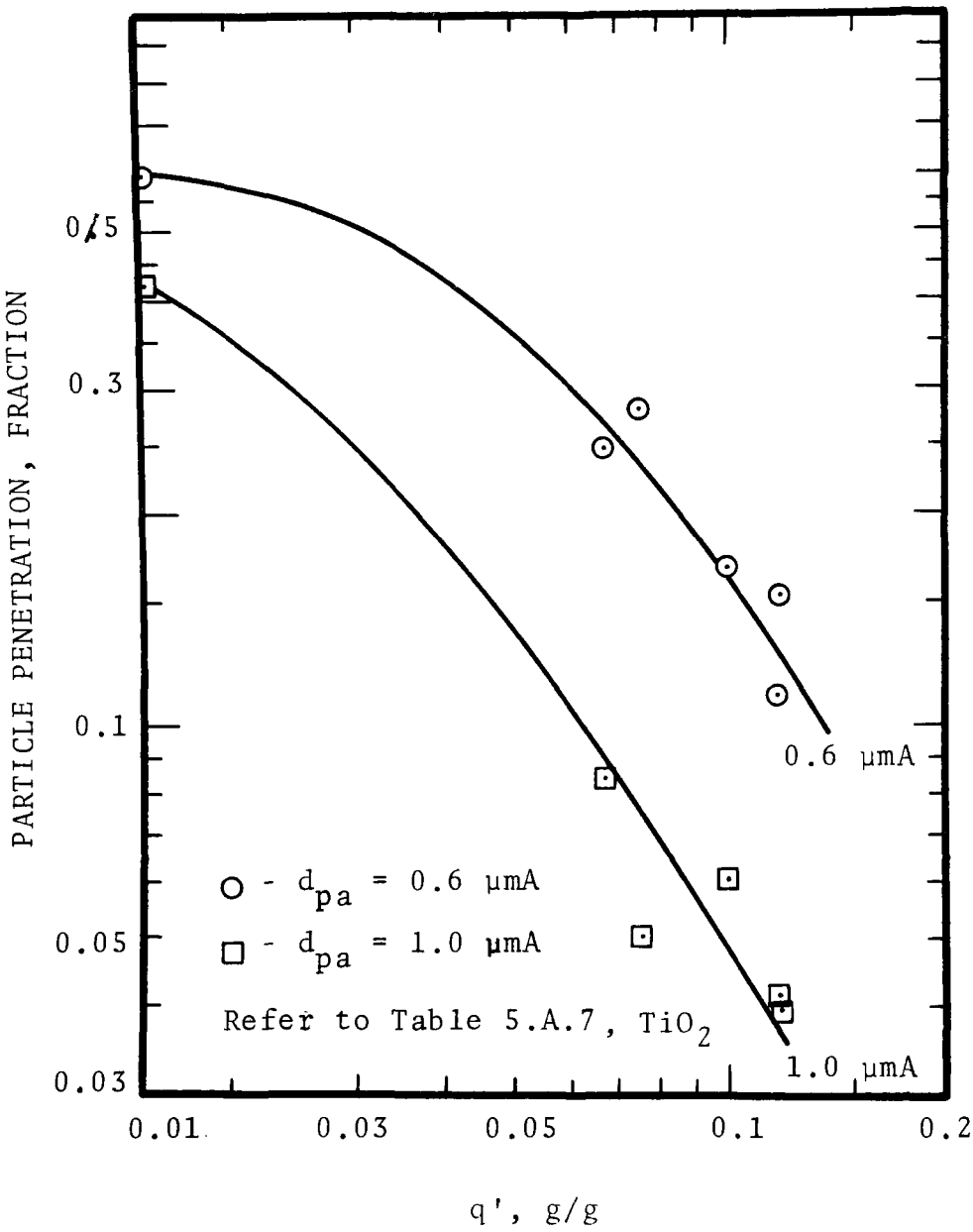

Figure 5.5 Penetration versus condensation ratio, five plates, distributed steam inlet.

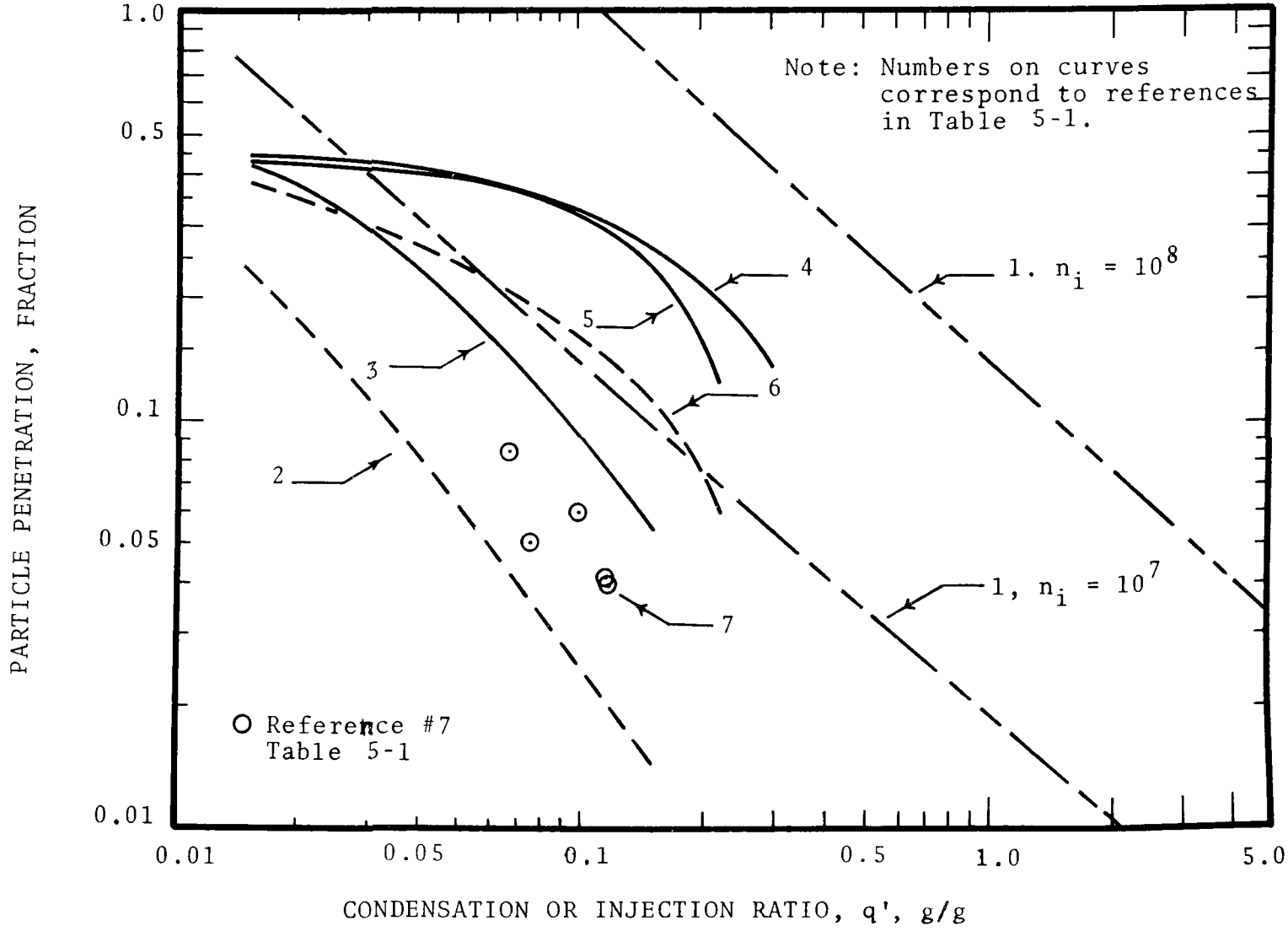

Figure 5-6 -FF/C scrubber performance comparison

Table 5-1. FF/C scrubber performance comparison

Ref.	Experimental Studies	Scrubber Type	d_{pg} (μm)	Particle Material	n_i (no./cm^3)
1	Rozen and Kostin (1967)	Alternate hot and cold sieve plates	0.3	Oil	10^5 10^8
2	present investigation	Five sieve plates L = 0.64 ℓ/sec	0.55	Black Iron Oxide	~3 x 10^5
3	present investigation	Four sieve plates L = 0.64 ℓ/sec	0.55	Black Iron Oxide	~3.6 x 10^5
4	present investigation	Four sieve plates L = 0.64 ℓ/sec	0.5	Titanium Dioxide	3 x 10^6 -7.2 x 10^9 most~10^8
5	present investigation	Four sieve plates L = 0.38 ℓ/sec	0.5	Titanium Dioxide	2.4 x 10^7 -8.8 x 10^8 most~10^8
6	present investigation	Five sieve plates L = 0.38 ℓ/sec	0.5	Titanium Dioxide	5 x 10^5 -1.7 x 10^7 most~10^6
7	present investigation	Five sieve plates L = 0.38 ℓ/sec Steam introduction distributed under two plates	0.5	Titanium Dioxide	3 x 10^5 -3.4 x 10^6 most~10^6

1. Particle penetration depends heavily on the condensation ratio, "q'". Calvert et al. (1973) have shown that "q'" is sufficient to define particle deposition rate, without regard to "n_i", if there is no condensation on the particles.
2. A comparison of curve 5 with 6 and curve 2 with 3, indicates that for the same "q'" and comparable operating conditions, addition of a fifth plate significantly improved the performance of the multiple plate scrubber. During runs for curves 5 and 6, the gas flowrate at the scrubber inlet was maintained approximately constant but the particle concentration was higher for curve 5. During runs for curves 2 and 3, the overall scrubber pressure drop was maintained approximately constant by decreasing the gas flowrate for the five plate scrubber so plate hydrodynamics may have changed. The improvement by the addition of a fifth plate is expected to be mainly due to particle growth, although particle concentration and hydrodynamic effects may also be involved.
3. A comparison of curves 4 with 5 indicates that for the same "q'" and comparable operating conditions, a decrease in the L/G ratio did not significantly affect the performance of the scrubber. The L/G ratio was changed from 3.8 ℓ/m^3 (29 gal/MCF) to 2.28 ℓ/m^3 (17 gal/MCF), by reducing the liquid flowrate. Both of the L/G ratios were within the operating range on the plates as shown in Figures 4-2 through 4-6. This observation was consistent with the observations of other investigators as reported by Semrau and Witham (1975) for orifice type scrubbers. It should be noted, however, that the scrubber performances are compared at the same "q'". Thus a lower L/G ratio with re-

circulated liquid would require a larger cooling range in the liquid cooling system.

4. A comparison of data when steam was injected at two points in the scrubber (reference #7), with curve 6, shows that for the same "q'" and comparable operating conditions, the scrubber performance improved significantly when the vapor condensation was distributed over two sections of the multiple plate scrubber. Calvert et al. (1973) and Calvert & Jhaveri (1974) have reported theoretical studies of the effect of distributing vapor condensation in multiple sections of multi stage FF/C scrubbers. An experimental study of this effect was reported by Rozen and Kostin (1967). These studies indicated that irrespective of the particle collection mechanisms effective in a scrubber, distribution of vapor condensation along the scrubber results in higher particle collection efficiency. As the particles used in this study were wettable, the higher collection efficiency is expected to be due to the decrease in "n_i" (due to particle collection on the bottom three plates), before steam was injected under plate 4. Thus, the amount of vapor available for condensation per particle, "q", is higher for plates 4 and 5, resulting in better collection efficiency.

5. A comparison of curves 2 and 6 and curves 3 and 4 shows that for the same "q'" and comparable operating conditions the scrubber particle collection efficiency was higher for lower "n_i". This effect can be shown theoretically to accompany condensation on particles and their growth at the expense of the water vapor concentration in

the gas. A higher particle number concentration requires higher amounts of condensed vapor to grow, effectively reducing the diffusiophoretic sweep velocity to deposit them. Also, the fewer the particles which share a given quantity of condensation, the larger they will grow and the easier they are to collect.

Comparison with Theoretical Predictions

A mathematical model of an FF/C sieve plate scrubber, developed and experimentally verified by Calvert et al. (1973) was extended to predict the performances of the multiple plate scrubber. For the purpose of comparison with the experimental results, the inlet particle diameter was assumed to be 1.0 μmA. The model is described in detail in Chapter 6. A spray scrubber model is also described in Chapter 6.

THE SPRAY FF/C SCRUBBER

Results

The spray scrubber was evaluated at five operating modes, as listed in Table 4-5. For each operating mode, the scrubber performance was measured for a range of "q'" values. Effects of the following variables were also determined:

1. The amount of cold water sprayed in the scrubber was varied. Effect of reducing the cold water spray in a 3:1 ratio was studied by operating the scrubber in a three-stage mode.
2. The L/G ratio was controlled by changing the inlet flowrate.
3. Liquid drop size distribution was changed at the same L/G ratio.
4. Overall gas-liquid contact mode was altered by operating the three stage scrubber in the co-current or counter-current mode.

As particle growth and diffusiophoresis are expected to contribute the most to the enhancement of particle capture in the scrubber, the effects of "q'" and "n_i" on "Pt" were determined. "Pt" for 1.0 μmA and 0.6 μmA particles are plotted against "q'" in Figures 5-7 through 5-12 for the operating modes studied. Data points on these plots were read from the fractional penetration plots in Appendix 5.B. Again, the data points were found to be scattered, possibly indicating the effects of other parameters, such as "n_i" and the inlet liquid temperatures.

DISCUSSION

The spray scrubber performance is compared with the results of Lancaster and Strauss (1971) and with some plate scrubber data on Figure 5-13, a plot of particle penetration

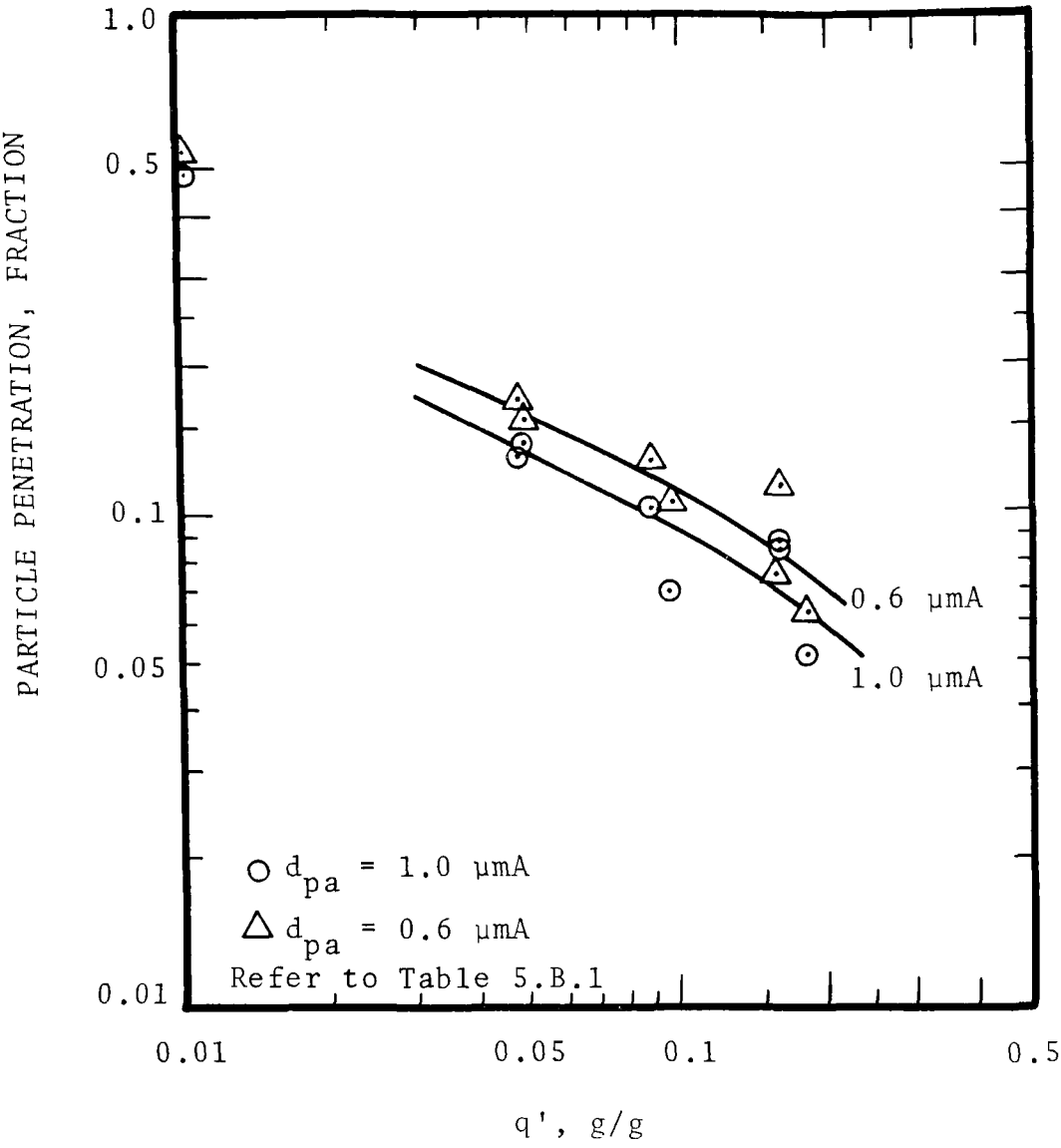

Figure 5-7 Penetration versus condensation ratio one stage spray.

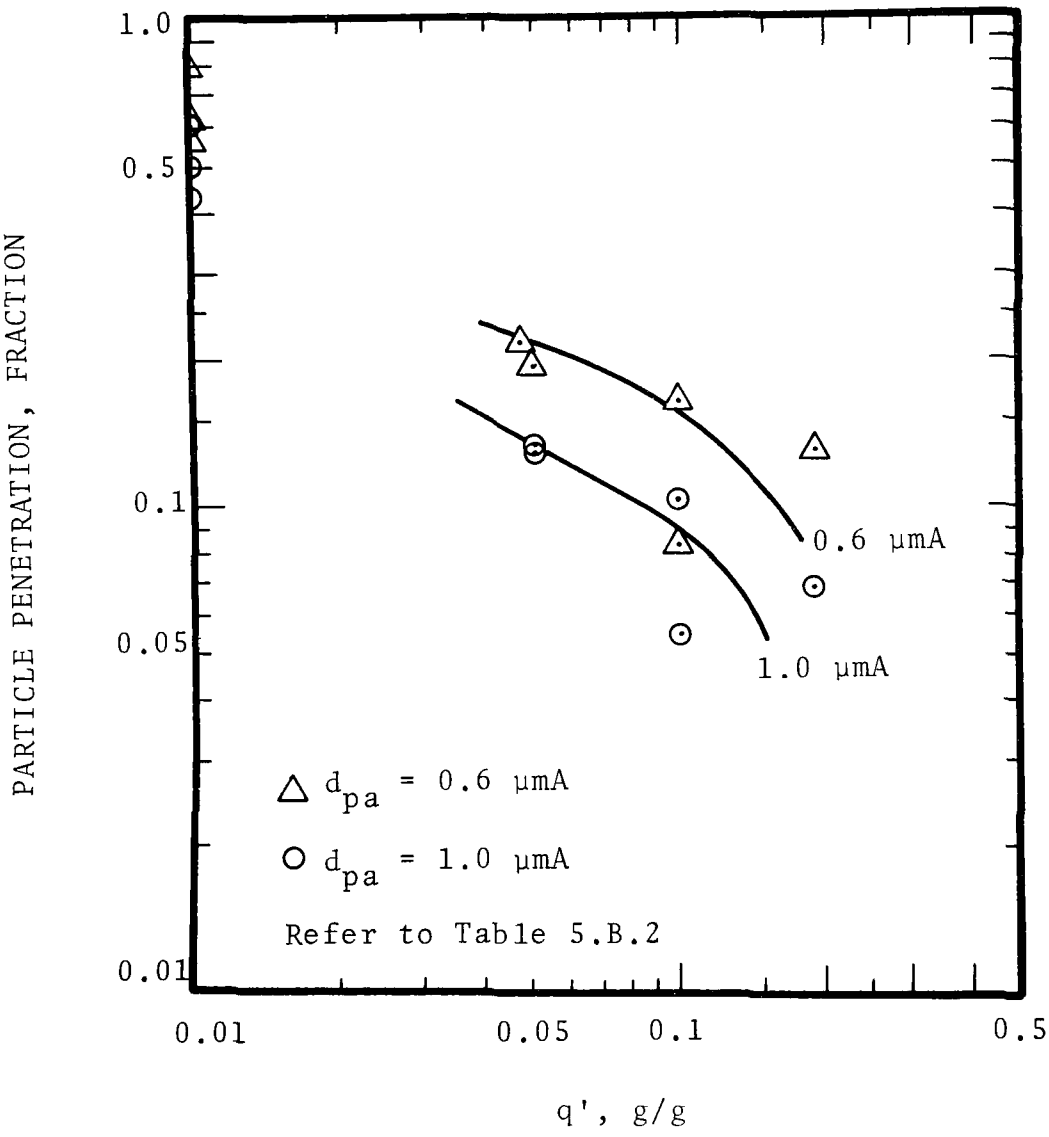

Figure 5-8 Penetration versus condensation ratio, one stage spray.

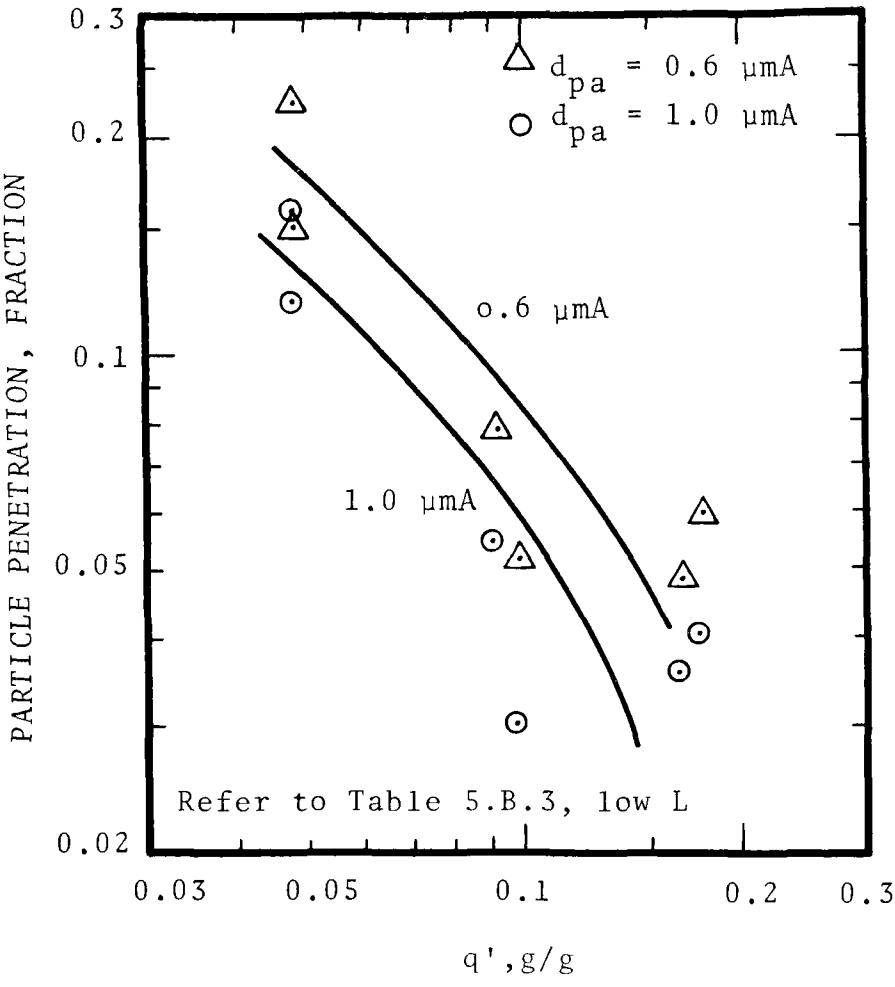

Figure 5-9: Penetration versus condensation ratio, one stage spray.

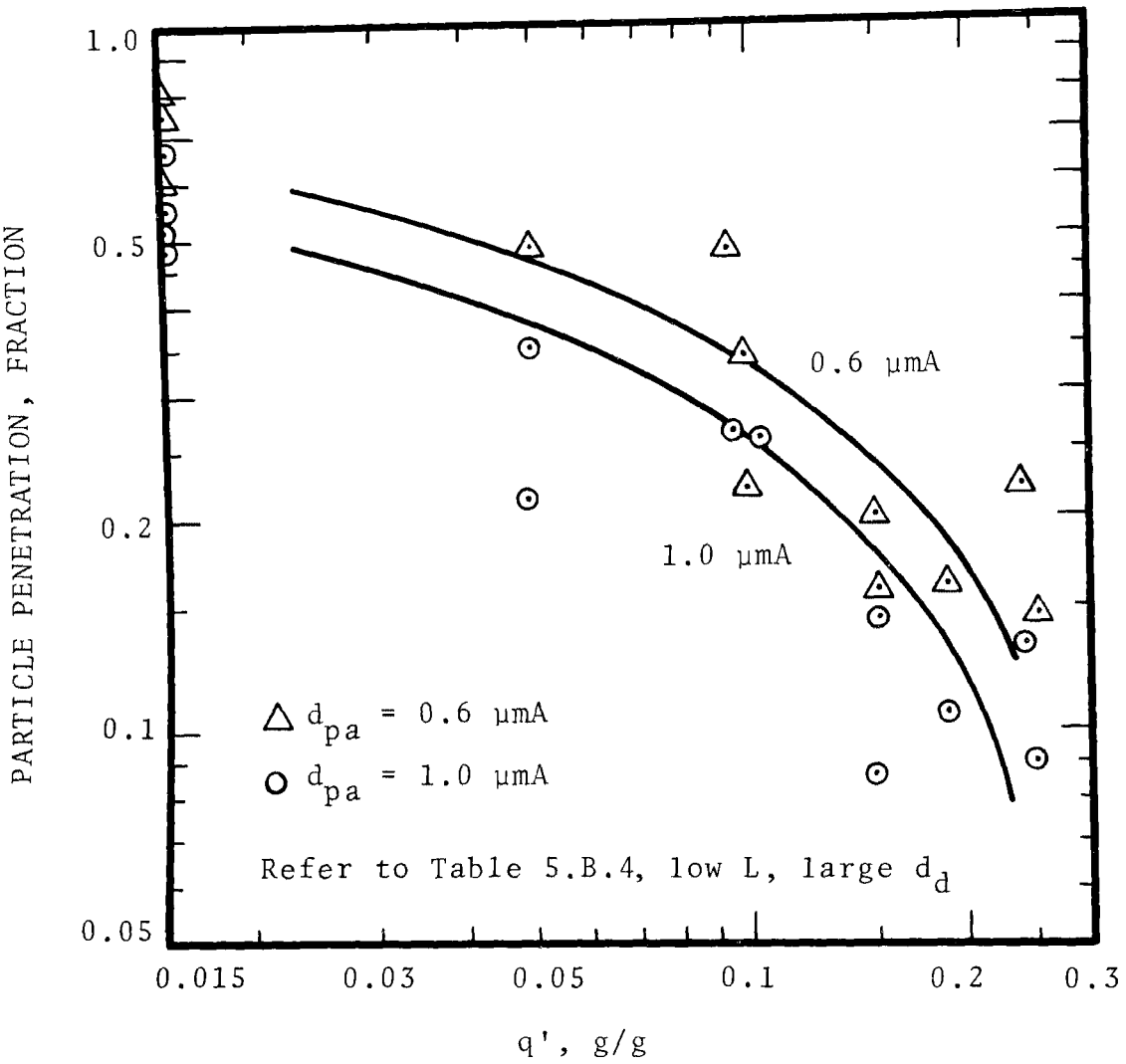

Figure 5-10 Penetration versus condensation ratio, one stage spray.

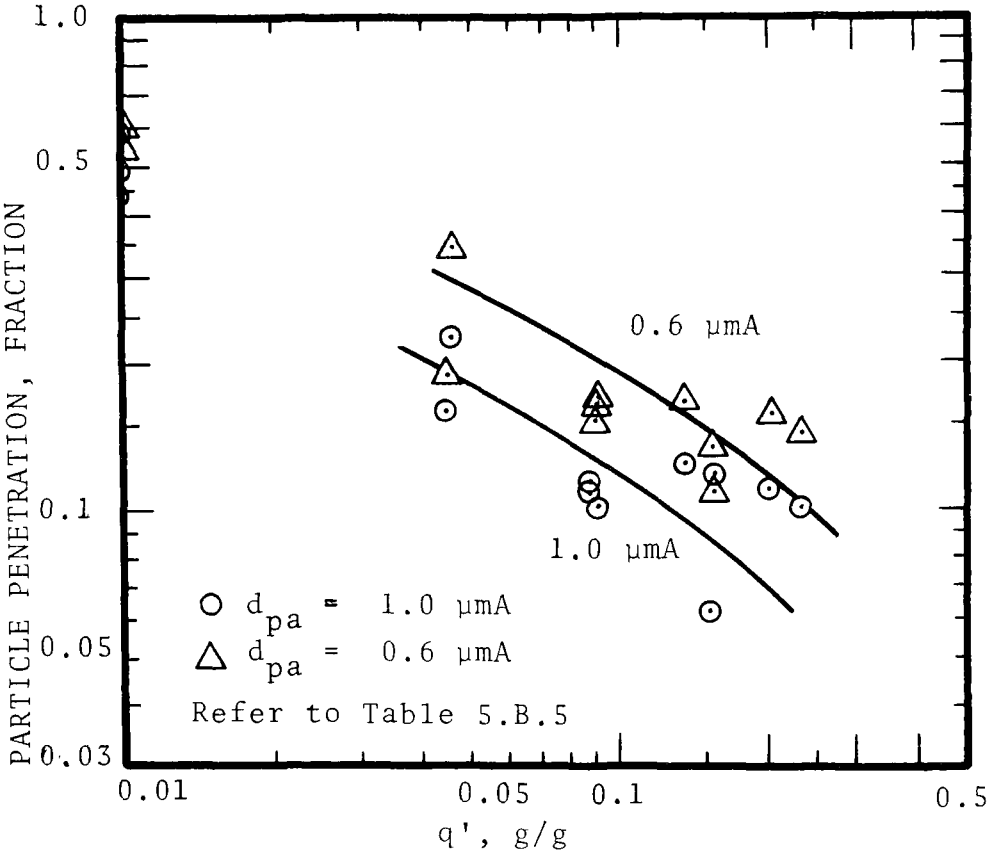

Figure 5-11 Penetration versus condensation ratio, three stage co-current spray.

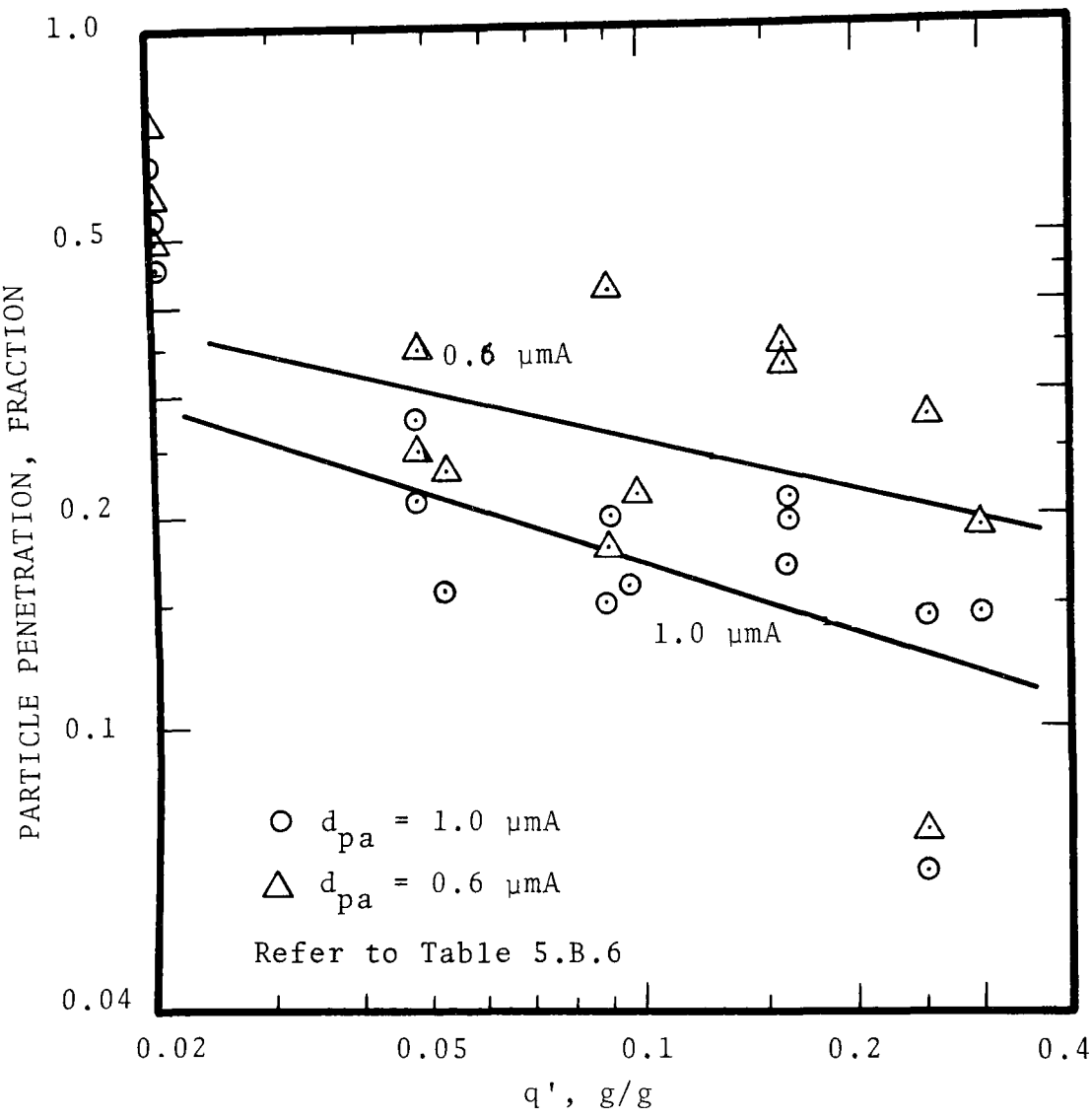

Figure 5-12 - Penetration versus condensation ratio, three stage counter-current spray.

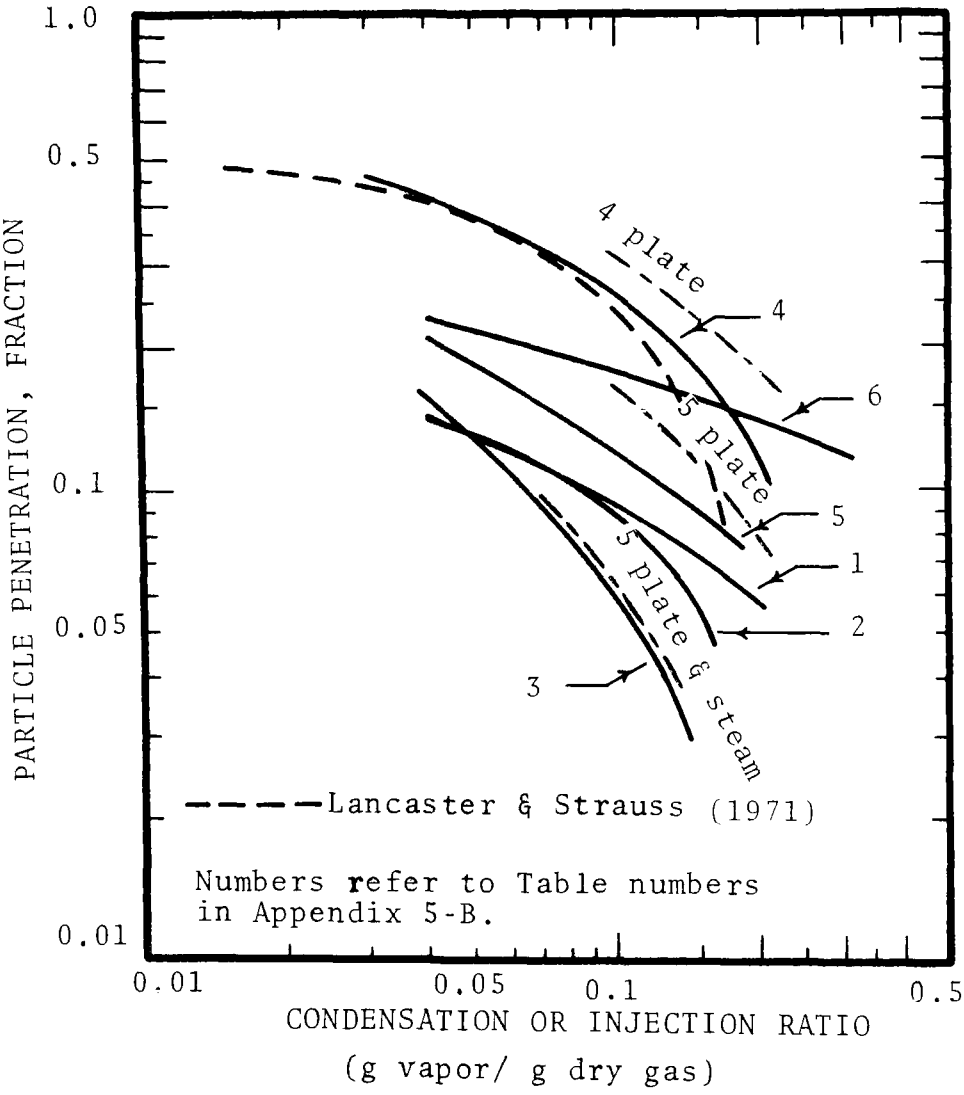

Figure 5-13 Comparison of FF/C plate and spray scrubber results for 1 μmA particles

versus condensation or injection ratio, for 1.0 μmA particles. The following is surmised from the plot:

1. Particle penetration depends heavily on the condensation ratio, "q'". Calvert et al. (1973) have shown that "q'" is sufficient to define particle deposition rate, without regard to "n_i", if there is no condensation on the particles.
2. A comparison of curves 1 and 2 shows that the scrubber performance could be reproduced, if operated at nearly the same conditions, thus reinforcing the validity of experimental data and techniques.
3. A comparison of curves 1 or 2 and 3 indicates an apparent anomaly. The amount of water sprayed into the scrubber during runs indicated by curve 3 was about 25% less than that sprayed for the runs indicated by curves 1 and 2. Thus, curve 3 may be expected to have higher penetrations. This effect may be due to better liquid utilization when the water sprayed in was less, resulting in a higher collection efficiency of large particles by impaction. (Note that particle growth is higher at higher "q'" values.) Spray drop diameters during all the runs were the same. The better liquid utilization may be due to less drop coalescence and lesser wall losses when the liquid flowrate was less. This effect bears further experimental investigation.
4. A comparison of curves 3 and 4 illustrates the effect of spray drop diameter. Although the liquid and gas flowrates were identical for these runs, the spray drop volume mean dia-

meter for curve 4 was about 1 5 times the dia meter for curve 3. Thus, the particle collection by impaction and the spray drop space density (number of drops in a unit scrubber volume) are lower for curve 4, resulting in the high penetrations.

5. A comparison of curves 1 or 2 (1 stage) with 5 (co-current), shows that the particle penetrations are higher when the amount of cold liquid sprayed is reduced by about 67% although the total liquid spray rate is the same. In both the operating modes cold liquid was sprayed in the section where the gas enthalpy and vapor content were highest. Thus, the highest possible temperature and vapor concentration gradients were imposed in this section. The slightly higher penetrations for curve 5 indi cate that although most of the particle growth occurred in the first section of the scrubber, FF/C mechanisms were also effective in the second and third sections.
6. A comparison of curves 5 with 6 (counter-current) indicates the importance of causing particle growth quickly in a FF/C scrubber. The only difference in scrubber operation was that for curve 5, the coldest water was sprayed into the gas with the highest enthalpy and water vapor content; while for curve 6, the hottest water was sprayed into this gas in the first section, thus providing a more uniform distribution of gradients along the length of the scrubber. Curve 5 penetrations are lower, probably due to more particle growth for co-current contacting

CHAPTER 6
FF/C SCRUBBER PERFORMANCE PREDICTION METHODS

The prediction of particle collection performance for FF/C scrubbers in advance of experiments can be done by means of theoretically based mathematical models. The approach used is to derive particle collection equations which account for all of the applicable unit mechanisms, which could be active in the scrubber. Such models are then used to predict particle collection in the two FF/C scrubbers descri bed earlier. The predicted performances are compared to the experimental results.

Experimental results for the multiple plate FF/C scrubber compared well with the predicted values. The predicted performances of the horizontal spray FF/C scrubber, however, compared well with the experimental results only in a small range of particle size. Thus, a set of empirical design equations was developed for the spray scrubber by fitting curves through the experimental results. Limitations on the use of these models for predicting performance of the FF/C scrubbers are discussed.

THE MULTIPLE SIEVE PLATE FF/C SCRUBBER

A mathematical model of an FF/C sieve plate scrubber, developed and experimentally verified by Calvert et al. (1973) was extended to predict the performances of the multiple plate scrubber. Particle collection on a sieve plate was represented by the unit mechanism of transfer from bubbles. The model incorporates the following phenomena:

1. Heat transfer between bubbles and liquid.
2. Heat and mass transfer between bubbles and particles.

3. Particle deposition by:
   A. Impaction during bubble formation
   B. Diffusiophoresis
   C. Thermophoresis
   D. Centrifugation during bubble rise

The following general assumptions were made:

1. Gas bubbles are spherical, of constant diameter (d_b = 0.4 cm), and perfectly mixed internally (except for the interfaces).
2. Gas properties are as for air and water vapor.
3. Foam density is constant throughout the foam layer on the plate.
4. Liquid bulk temperature is constant throughout the foam although the liquid-bubble interface temperature can vary. The bulk temperature is the average of inlet and outlet liquid temperatures.
5. Particles are wettable, insoluble spheres.
6. Condensation on particles can occur whenever the saturation ratio is 1.0 or larger.
7. All the particles are subjected to condensation and growth.

Several transfer phenomena contribute toward the deposition of particles from the gas stream on a sieve plate. To determine the overall particle collection, equations were developed for each of the significant transfer phenomena and then combined for the sieve plate. Since these phenomena are dependent on the magnitudes of the liquid and gas phase conditions at each point along the sieve plate column, these conditions then need to be determined for use in the design equations. Detailed derivations of the equations listed below are described by Calvert et al. (1973) and are omitted here for brevity.

Particle Deposition

Inertial Impaction During Bubble Formation

During the formation of bubbles on a sieve plate, contact between gas and liquid phases is due to the jets of gas emerging from the perforations and impacting on the liquid. Particles are thus deposited on the liquid surface by inertial impaction. Particle collection can be determined from:

$$Pt_d = \exp\left(\frac{40\ F^2 d_p^2 \rho_p C' u_h}{9\ \mu_G d_h}\right) \qquad (6\text{-}1)$$

where F = foam density, volume fraction liquid
d_p = particle diameter, cm
ρ_p = particle density, g/cm^3
C' = Cunningham slip correction factor
u_h = gas velocity in the perforation, cm/sec
μ_G = gas viscosity, poise
d_h = diameter of perforation, cm
Pt_d = penetration of particles of diameter d_p, for collection during bubble formation

Equation 6-1 was experimentally verified by Taheri and Calvert (1968) for hydrophilic particles and for $0.38 \leq F \leq 0.65$. In the normal operating range of the sieve plate, 50% of particles with the diameter of approximately 2.5 μmA would be deposited due to this phenomenon. However, the particle deposition drops sharply as the diameter decreases. For hydrophobic particles, experimental results reported by Taheri and Calvert (1968) can be used, although a generalized design equation was not developed by them.

B. Particle Collection on the Sieve Plate

The total particle flux from the gas to the liquid is defined as the sum of fluxes due to diffusiophoresis,

thermophoresis and centrifugation. Particle deposition by Brownian diffusion was neglected as it is not very effective for particles > 0.1 μm diameter. Thus,

$$N_S = N_D + N_T + N_C \left(\frac{\text{no. particles}}{\text{cm}^2\text{-sec}}\right) \qquad (6\text{-}2)$$

and, $N_S = u_{ps} n_p$

where u_{ps} = overall deposition, velocity cm/sec

n_p = particle concentration, $\frac{\text{no. particles}}{\text{cm}^3}$

For a spherical bubble of radius "r_b", the rate of change of particle concentration is:

$$\frac{dn_p}{dt} = \left(\frac{3}{r_b}\right) N_S = \left(\frac{3n_p}{r_b}\right) u_{ps} \qquad (6\text{-}3)$$

where $u_{ps} = u_{pD} + u_{pT} + u_{pC}$ = sum of deposition velocities (6-4)

Thus, the penetration for a period = Δt is:

$$Pt\ (d_p) = \exp\left[- \frac{3}{r_b} \left(u_{ps}\right) \Delta t \right] \qquad (6\text{-}5)$$

Diffusiophoretic deposition velocity for air and water system can be expressed as:

$$u_{pD} = \frac{0.85\ RT_G k'_G\ (p_G - p_{Li})}{(1-p_G)}\ (\text{cm/sec}) \qquad (6\text{-}6)$$

where p_G = partial pressure of the diffusing component, water vapor in the gas phase, atm

p_{Li} = partial pressure of water vapor at the gas-liquid interface, atm

T_G = gas phase temperature, °K

R = gas constant

k'_G = mass transfer coefficient, gas to liquid, $\frac{\text{g-mole}}{\text{cm}^2\text{-sec-atm}}$

Thermophoretic deposition velocity for air and water system can be expressed as:

$$u_{pT} \approx 6.14 \times 10^{-3}\ C'\ h_G\ T_G\ (T_G - T_{Li}) \qquad (6\text{-}7)$$

where T_{Li} = temperature at the gas-liquid interface, °K

Centrifugal deposition velocity in the foam can be expressed as:

$$u_{pC} = \frac{d_p^2 \rho_p C' u_t^2}{18\ \mu_G r_b} \qquad (6\text{-}8)$$

and for bubble radius, r_b=0.2 cm, tangential velocity, u_t=bubble rise velocity=20 cm/sec;

$$u_{pC} = 1.85 \times 10^8\ \frac{d_p^2 \rho_p C'}{T_G}\ \text{(cm/sec)} \qquad (6\text{-}9)$$

To determine particle deposition from the above equations, the particulate, gas and liquid conditions at each point along the rise of the bubble in the foam need to be determined. In the model discussed here, the tangential velocity of the bubble is assumed to be equal to the velocity of rise. Thus, the bubble completes one rotation per rise of one bubble diameter. For computational purposes, the rise of one bubble diameter is used for a differential increment in distance and time on the sieve plate. The gas and liquid conditions along the foam height are determined from heat and mass transfer in bubbles. Particle growth is computed from a similar treatment for the particulate-gas system in the bubbles.

Heat and Mass Transfer in Bubbles

The vapor-liquid equilibrium relationship for water can be approximated within a few percent by:

$$p_{eq} = \exp\left(13.64 - \frac{5.1 \times 10^3}{T}\right) \text{ atm} \qquad (6\text{-}10)$$

where p_{eq} = water vapor partial pressure in equilibrium at T°K

Temperature and vapor pressure at the bubble interface are determined by using Equation 6-10 in conjunction with the equation for the overall energy balance at the bubble interface:

$$k'_G L_M (p_G - p_{Li}) \quad h_L (T_{Li} - T_L) \quad h_G (T_{Li} - T_G) = 0 \qquad (6\text{-}11)$$

where L_M = latent heat of vaporization for water, cal/g-mole

h_L = liquid phase heat transfer coefficient, cal/sec-cm^2-°K

T_L = temperature of liquid bulk, °K

h_G = gas phase heat transfer coefficient, cal/sec-cm^2-°K

The gas temperature, composition and flowrate, and the liquid temperature change along the foam height due to vapor condensation and sensible heat transfer. The vapor condensation can be expressed as:

$$M_T = M_p + M_b \quad \frac{\text{g/mol } H_2O \text{ vapor}}{\text{cm}^2 \text{ of plate area}} \qquad (6\text{-}12)$$

where M_T = total vapor condensed

M_p and M_b = vapor condensed on the particles and liquid respectively

The overall transfer rate can then be expressed in the form of a difference equation for an increment as:

$$\frac{\Delta M_T}{\Delta t} = \frac{4\pi}{54} (r_2^3 - r_1^3)\, n_p V_b \Delta Z + k'_G a_b\, (p_G - p_{Li}) \Delta Z \quad \frac{\text{g-mol}}{\text{cm}^2\text{-sec}} \qquad (6\text{-}13)$$

where a_b = bubble surface area per volume of foam

$$= V_b \left(\frac{6}{d_b}\right) \frac{\text{cm}^2}{\text{cm}^3}$$

r_2, r_1 = the final and initial particle radii in the increment, respectively, cm

n_p = number concentration of particles in gas, no /cm^3

V_b = volume fraction bubbles in froth, cm^3/cm^3

ΔZ = height of bubble rise, cm, in time "Δt", sec

d_b = bubble diameter, cm

The change of gas temperature can be expressed as:

$$GC_{pM}\Delta T_G = h_G a_b (T_{Li} - T_G)\Delta Z + \Delta M_p L_M \quad \frac{\text{cal}}{\text{cm}^2\text{-sec}} \qquad (6\text{-}14)$$

where C_{pM} = molal heat capacity of gas, cal/mol-°K

G = molal gas flowrate per unit area of plate, g-mol/cm^2-sec

Particle Growth

The rate of change of particle radius can be expressed as:

$$\frac{dr_p}{dt} = \frac{k'_{pG}\, (p_G - p_{pi})}{\rho_M} \quad \frac{\text{cm}}{\text{sec}} \qquad (6\text{-}15)$$

where $k'_{pG} = \frac{2D_G P}{RT_G d_p p_{BM}}$ $\frac{\text{g-mol}}{\text{cm}^2\text{-sec-atm}}$ = mass transfer coefficient, gas to particle

D_G = diffusivity, cm^2/sec

P = total pressure, atm

p_{BM} = mean partial pressure of non-transferring gas, atm

p_{pi} = vapor partial pressure at the particle interface, atm

ρ_M = molal density of water, $\frac{\text{g-mol}}{\text{cm}^3}$

Thus, particle growth over a finite period can be expressed as:

$$r_2^2 - r_1^2 = \frac{2D_G P(p_G - p_{pi})\Delta t}{RT_G \rho_M p_{BM}} \text{ cm}^2 \qquad (6\text{-}16)$$

"p_{pi}" can be determined from Equation (6-10) if "T_{pi}" is known. For air-water system and small increments in temperatures:

$$T_{pi} - T_G \approx 0.925\ (T^* \quad T_G) \qquad (6\ 17)$$

where T^* = saturation (equilibrium) temperature corresponding to the partial pressure of water in the bulk gas, "p_G".

A computer program was developed to solve the mathematical model comprised of Equation 6-2 through 6-17 listed above, for predicting particle collection in a sieve plate. Particle collection during bubble formation was not included in the program as it depends only on the initial conditions. The computer program is listed in Appendix 6.A. Input parameters are entered in two sets in the

program to provide flexibility. The first set of parameters include:

TIN - the inlet gas temperature

PIN - water vapor partial pressure in the inlet gas

TLB - average liquid bulk temperature on the sieve plate

RP - particle radius in the inlet gas

CNP - inlet particle number concentration, no /cm^3

The second set of inlet parameters include:

GM - total gmoles inlet gas/sec-cm^2 plate area

RK - $2\ k'_G\ pBM/P$, at inlet conditions

RH - $h_G\ (T_G)^{1/2}$, at inlet conditions

RKL - $2\ (RK) \times 10^4/h_L$

RHL - $(RH)/h_L$

DB - diameter of the bubble, cm

VELB- velocity of bubble rise, cm/sec

VB - volume fraction bubbles in froth

DZ incremental distance for difference calculations

THT incremental time corresponding to DZ

NI - number of increments in the calculation = foam height/DZ

Values for the second set of inlet parameters are listed in Appendix 6.A as examples only. Results from the program are listed in two formats, as actual end values and in a graphical form, illustrating results at each computational step. End values of the gas temperature, vapor partial pressure, particle radius and the overall penetration are printed out. The graphical print-out denotes values of the following four parameters at each increment in THT:

$S' = \frac{S}{2}$ = one half of the saturation ratio in the gas phase

$T' = \frac{T_G - T_L}{T_{Go} - T_L} = \frac{\text{present } \Delta T}{\text{inlet } \Delta T}$

$$Pt = n_{p/n_{po}} = \frac{\text{present particle concentration}}{\text{inlet particle concentration}}$$

$$r'_p = r_{po/r_p} = \frac{\text{inlet particle radius}}{\text{present particle radius}}$$

By definition, the above four dimensionless parameters range in value from 0.0 to 1.0 and are plotted on the "Y" axis. Normalization of the parameters in this manner simplifies the "scaling" required for machine plotting. The "X" axis denotes time in increment of THT.

Comparison with Experimental Results

To validate the above model, experimental conditions for three modes of multiple-plate FF/C scrubber operations reported in Chapter 5 were used to predict collection of 1.0 μmA particles. These compared well with the experi mental results. Based on the experimental results of Calvert et al. (1973), the following values were assumed:

$$k'_G = \frac{2.09 \times 10^{-4} P}{\rho_{BM}} \text{ gmole/cm}^2\text{-sec-atm}$$

$$h_G = 2.48 \times 10^{-2} T_G^{-0.5} \text{cal/sec-cm}^2\text{-°K}$$

$$h_L = 0.01 \text{ cal/sec-cm}^2\text{-°K}$$

$$F = 0.4$$

If there were no heat loss from the column, the gas and liquid temperatures predicted by the model using the above values would agree with the experimental data. However, since there were heat losses from the column, the above assumptions should be refined with careful experimental studies of plate hydrodynamics and transfer properties.

Predictions of the particle collection in the multiple plate column were made by a plate-by-plate procedure start ing with the bottom plate. Using experimental data, per- formances were predicted for the following operating modes

of the scrubber:

1. Five plates, high n_i, low L/G
2. Four plates, high n_i, low L/G
3. Four plates, high n_i, high L/G

These modes were selected because the "n_i" values corresponded to the practical emissions reported for industrial pollution sources.

The predicted performances are plotted as penetration versus condensation ratio, on Figures 5-2, 5-3 and 5-4. Comparison of the predicted performance with the experimental results for d_{pa} = 1.0 μmA particles indicate that both the curves follow the same trend, or have comparable slopes on the log-log paper. This suggests that the particle collection mechanisms were predicted correctly, although they differed in magnitude. Predicted performance of the five plate scrubber correlated well with the experimental results. However, predictions for the four plate scrubber operations were biased towards lower penetrations.

In its present form, the computerized model has two main limitations. The equations as used were derived for air-water system at the total pressure of 1 atm. As the pressure drop across a FF/C scrubber is low, assuming atmospheric pressure does not introduce any significant error. However, if the gas and liquid properties are significantly different from the air-water system, the program must be changed accordingly, starting from the generalized equation described in the text. The second limitation is that only one particle size can be input in the program. Thus, if a relationship between "Pt" as a function of "d_p" is desired, the program has to be manually run for the desired number of particle diameters. However, with a minor program modification and additional input for particle size distribution, the program can be used to develop the "Pt" versus "d_p" relationship automatically.

THE HORIZONTAL SPRAY FF/C SCRUBBER

Particle collection in the FF/C spray scrubber is affected by inertial impaction, diffusiophoresis, and thermophoresis. During this study our approach was to develop equations for particle collection by inertial impaction, and use them in conjunction with the mathematical models for particle growth and collection by flux forces as described by Calvert et al. (1973).

Particle collection efficiency by inertial impaction in a spray scrubber can be predicted by means of methods described in the "Scrubber Handbook" (Calvert et al. 1972), for cases where the drop velocity is constant, or may be considered so. When the spray is generated by high pressure nozzles, the drop velocity is initially very high compared to the terminal settling velocity. Therefore the collection efficiency of the drop decreases greatly as the drop slows down and the overall collection by the drop is the integrated effect of efficiency over the drop trajectory.

Walton and Woolcock (1960) studied this problem in connection with the use of pressure sprays to control coal mine dust. They computed the relationship between collection efficiency and the distance traveled by a drop for several particle sizes and drop diameters. Figure 6-1 is taken from their paper and shows these relationships as predicted for coal dust (density = 1.37 g/cm^3). Drop velocity is also plotted so that one can find efficiency as the drop accelerates from a given initial velocity.

The relationships given in Figure 6-1 can be used to predict the collection efficiency of a spray scrubber making the following assumptions which we used in our model:

1. Assume that the particle concentration is uniform as the aerosol enters a spray stage, that it decreases exponentially as it passes through the stage, and that it is completely mixed (i.e. uniform concentration) before entering the next stage.
2. Assume that collection is by inertial impaction on the front of the drop only. This is the same as Walton and Woolcock assumed.
3. Assume that the percent of the gas area covered by the sprays (co-current) varies as shown in Figure 6-2, which is based on the arrangement of nozzles used in our pilot plant spray scrubber.
4. Assume that the drop diameter is uniform.

Based on the above assumptions, the equations describing the multi-stage, co-current spray scrubber are as follows:

Volume of gas which is swept clean of particles per unit of liquid volume is:

$$V_s = \left(\frac{3}{4r_d}\right) R_d E \times 10^{-3}, (m^3/\ell)$$

where

V_s = Gas volume swept clean per liter of drops, m^3/ℓ
r_d = Drop radius, cm
R_d = Drop range (i.e., distance traveled), cm
E = Average particle collection efficiency over range "R_d", fraction

If the collection of particles is a first order process,

$$Pt_\Delta = \exp - \left(V_s \frac{L}{G}\right)$$

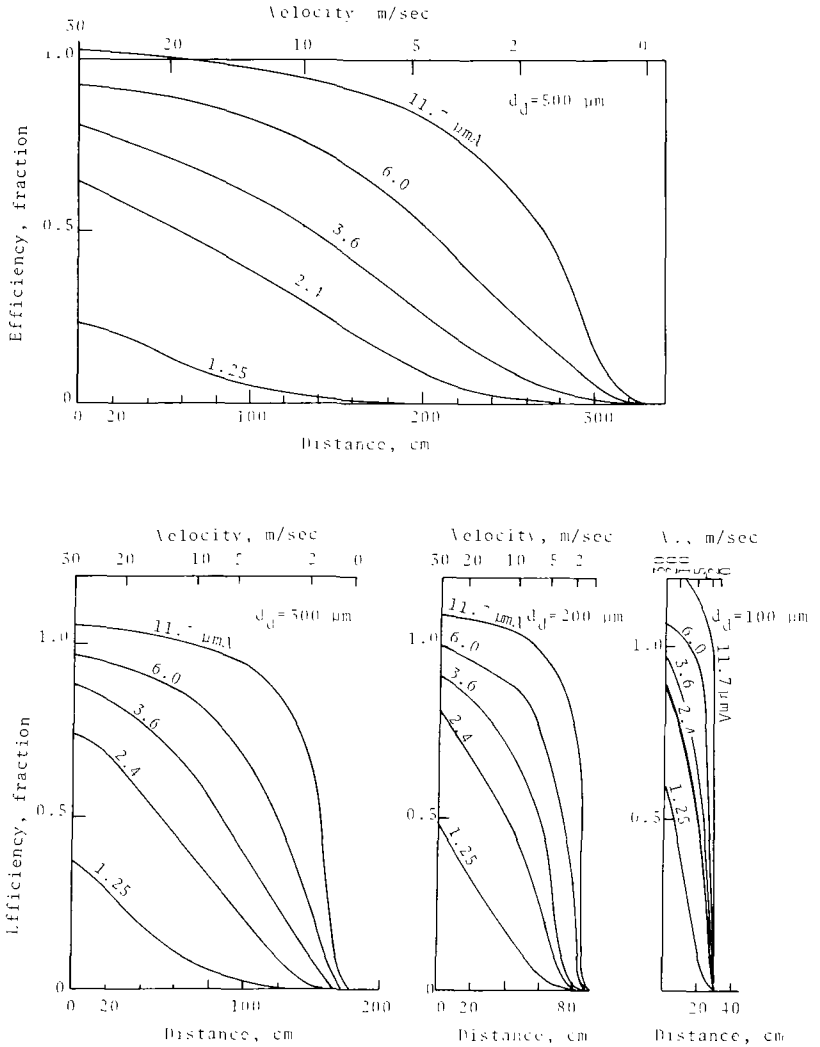

Figure 6-1 Predicted particle collection efficiency for sprays by inertial impaction and interception

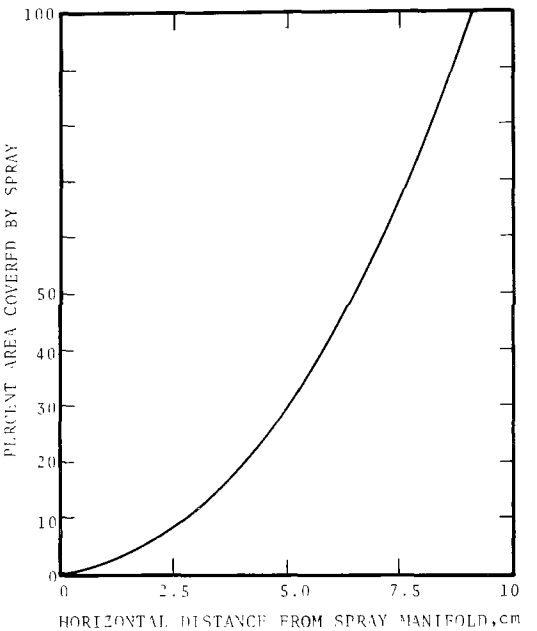

Figure 6-2 - Scrubber area covered by sprays.

where L/G = Liquid to gas flow ratio, (ℓ H_2O/m^3 gas)

Pt_Δ = Penetration per stage for a given particle diameter, fraction

The penetration for "N" stages is:

$$Pt_N = (Pt_\Delta)^N$$

The average efficiency was computed by plotting the product of efficiency times fraction of gas flow covered by sprays, versus the drop range (distance traveled) and then doing a graphical integration. These plots were made for several particle sizes and for an initial velocity of 20 m/sec and drop diameters of 0.05 cm and 0.03 cm. These conditions correspond to our pilot plant runs at 2.7 atm (40 psig) spray nozzle pressure. We also assumed that the maximum drop range is 100 cm, based on scrubber size.

The results of the computations for a liquid to gas ratio of 2.35 ℓ/m^3 (18 gal/MCF), corresponding to the flow rate per stage in our pilot plant runs, and for three stages are shown in Figure 6-3 for 0.05 cm drops and Figure 6-4 for 0.03 cm drops. Because of the difference in slope between the predictions and the experimental data we explored the influence of decreasing the amount of effective spray, assuming that there is agglomeration. The results are shown in Figures 6-3 and 6-4.

As can be seen, the predictions are fairly close to the data at the cut diameter (0.5 Pt) but not for other particle diameter. We have not yet been able to devise a model that will account for this discrepancy. It is quite possible that lower penetration for particles smaller than 1.0 μmA is due to their collection on the backs of the drops. However, we do not yet have a predictive cor-

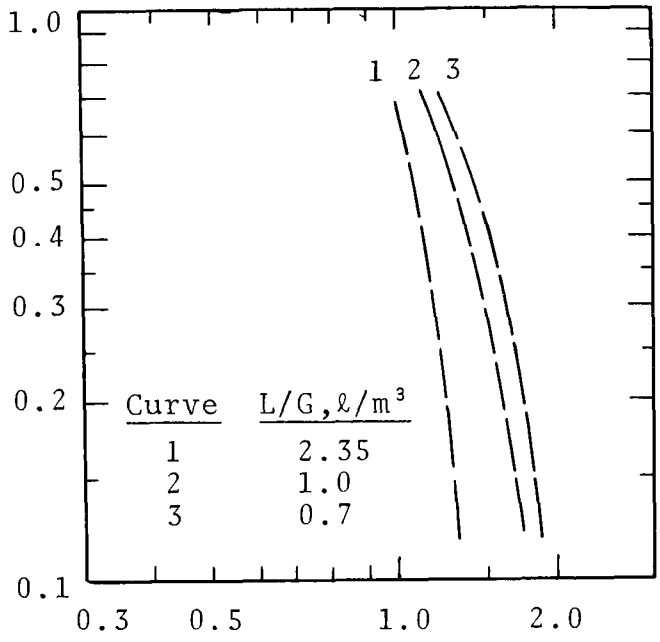

Figure 6-3. Spray scrubber penetration predictions for 500 μm drop diameter.

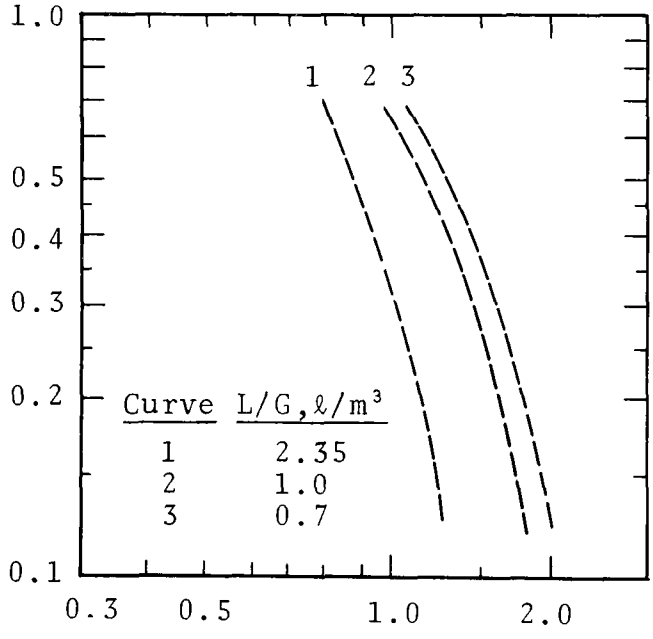

Figure 6-4. Spray scrubber penetration predictions for 300 μm drop diameter.

relation to account for this effect. Since a design equation for particle collection by inertial impaction could not be validated by our data, a model for FF/C spray scrubber was not developed.

In order to obtain design equations for scale-up purposes of FF/C spray scrubbers similar to the scrubber tested in this study, a curve fitting technique was used. Scrubber performance data for 1.0 μmA particles are plotted in Figures 6-5 through 6-7 , as particle penetration versus the amount of vapor condensed per particle, "q". This value was used instead of "q'"as it normalizes the effect of particle number concentration, "n_i". Again, scatter in the data was observed, possibly due to the effects of inlet liquid temperatures and the actual amount of vapor condensed on the particles. The range of scatter around the least square fit was within ±50%.

Curve fitting procedures were employed on each hori zontal spray FF/C scrubber data set to obtain the functional relationship between "Pt" and "q". The initial step is the assumption that the relationship between "Pt" and "q" can be represented as a power function:

$$Pt = Aq^B$$

or synonymously as the straight line equation:

$$\ln Pt = \ln A + B \ln q$$

The method of least squares was utilized to obtain the best straight line curve fit through the experimental set of paired variables, "ln Pt" and "ln q", where "ln q" was regarded as an ordinary variable measured without appreciable error, and "ln Pt" as the random variable.

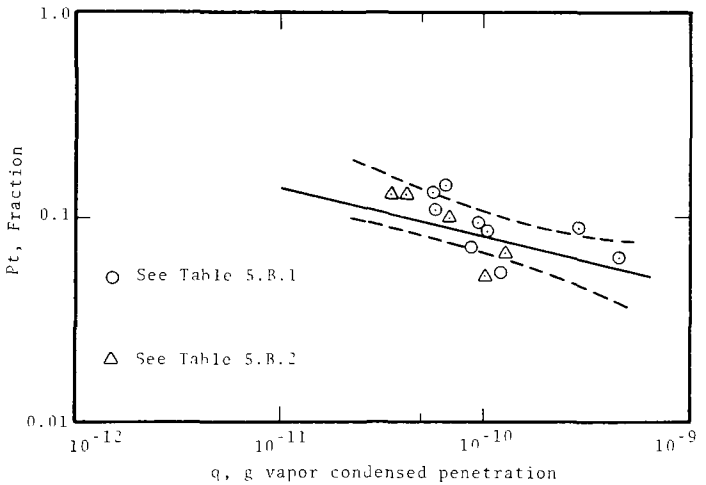

Figure 6-5. Experimental 1.0 μmA particle penetration for spray scrubber.

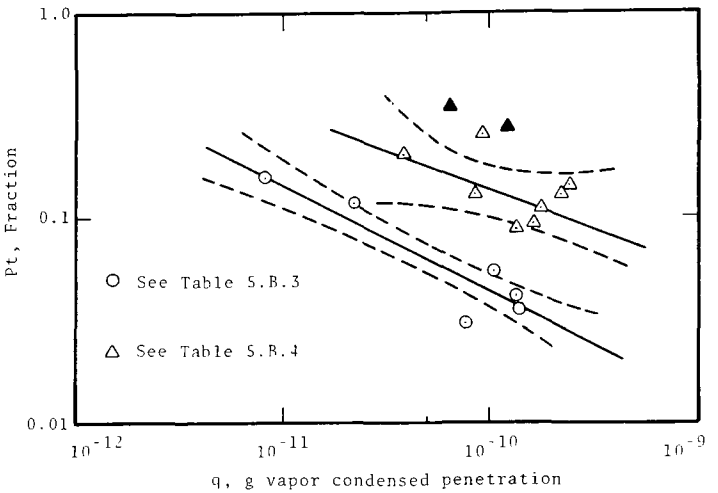

Figure 6-6. Experimental 1.0 μmA particle penetration for spray scrubber.

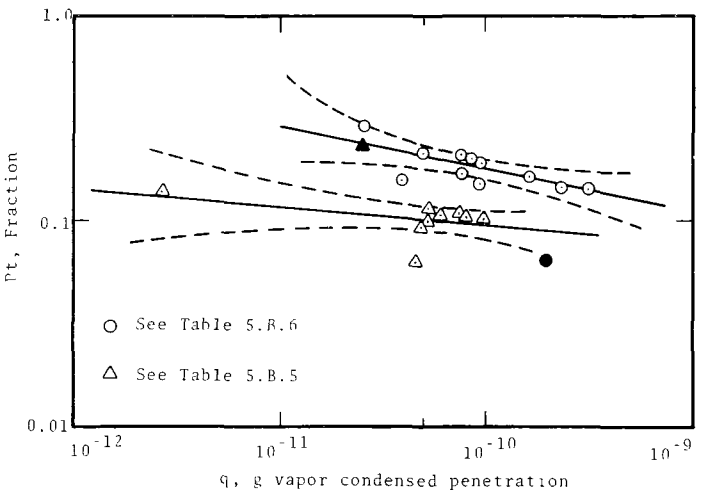

Figure 6-7. Experimental 1.0 μmA particle penetration for spray scrubber.

After the determination of the constants "A" and "B" for the straight line equation, the percent error for each data point was calculated. Those that indicated appreciable error (25% or greater) were eliminated (these points are shaded on the plots) and the least square straight lines were redetermined for the remaining number of data points. As shown in Table 6-1, four data points were thus not included in the determination of the least square straight lines out of a total of fifty-two points. This resulted in narrower bands for confidence limits and thus precluded the accounting of atypical scrubber performance.

The 90% confidence intervals for the mean values, "Pt", of the regression curve:

$$\ln Pt = A + B \ln q$$

were established utilizing the t-distribution table, 90% confidence level, and n-2 degrees of freedom where "n" was the number of data points. The equations are presented in Table 6-1 and by straight lines on Figures 6-5 through 6-7. The 90% confidence intervals are also represented by broken lines on these figures.

In lieu of a rigorous mathematical model, the equations developed above can be used for predicting particle collection in FF/C spray scrubbers. For particles smaller than 2 μmA in diameter, the collection is mainly dependent on particle growth and flux forces. Thus the penetration was expressed as a function of "q" in the equations. The equations can be used to predict the amount of vapor condensation required in the scrubber for the designed penetration of fine particles. Application of the above equations is limited to the design of FF/C spray scrubbers with the configuration and operating parameters similar to the pilot

Table 6-1. FF/C SPRAY SCRUBBER DESIGN EQUATIONS

SET * NO.	DESIGN EQUATIONS	DATA POINTS (n)
5.B.1+ 5.B.2	$Pt = -9.5q^{-0.31}$	14
5.B.3	$Pt = -15.4q^{-0.53}$	6
5.B.4	$Pt = -10.3q^{-0.36}$	8
5.B.5	$Pt = -4.2q^{-0.08}$	9
5.B.6	$Pt = -6.4q^{-0.2}$	11

* The set numbers refer to Table numbers in Appendix 5.B.

scrubber evaluated in this study. It is noted however that the pilot scrubber was operated at near optimum conditions for maximizing particle collection and thus covers the practical design range for the horizontal FF/C spray scrubbers.

CHAPTER 7
ECONOMIC FEASIBILITY

Experimental results discussed in the previous sections, together with the theoretical and experimental studies reported by previous investigators, clearly show that fine particles can be collected with high efficiency in FF/C scrubbers. The economic feasibility of FF/C scrubbing is discussed in the following section. Since there has been no published study of an industrial FF/C scrubber, actual data on the economics of such a system are not available. Thus, the discussion is limited to preliminary predictions of costs based on the available information on FF/C scrubbing.

Some general economic features of FF/C scrubbing are discussed below. Experimental results plotted on Figures 5-6 and 5-13 indicate that it should require from 0.1 to about 0.25 g water vapor condensed/g dry gas in a FF/C scrubber to attain high collection efficiency for fine particles. Such a condensation ratio generally requires preconditioning of the scrubber inlet gas to increase its moisture content.

Gas preconditioning could be done either by direct introduction of spent steam if the gas is dry and has low enthalpy, or by the evaporation of sprayed water when enough enthalpy is available in the gas. Direct injection of steam is beneficial because it can increase the local saturation ratio above 1.0, which is necessary for the growth of hydrophobic particles.

Cooling water is needed to condense the desired amount of vapor in the scrubber. In an industrial system the water is cooled in an evaporative cooling tower using ambient air, and then recirculated to the FF/C scrubber. In cooling towers of conventional design, the water temperature range is kept below about 17°C (30°F). A

larger water temperature range can be achieved in cooling towers of special design but the costs will be higher than usual, and there may be undesirable features such as fog formation. If the water temperature rise in the scrubber is 17°C (30°F), about 32 g of cooling water will be required to condense 1 g of water vapor.

COST COMPARISON

It is likely that one would have to make a choice between using high pressure drop or FF/C conditions in a scrubber system for fine particle collection. If equipment costs for the two types of system are roughly the same, most of the difference in operating costs will be due to power, water, and steam requirements. In order to compare the two approaches, operating costs have been estimated for an FF/C system and a high energy (Venturi) scrubber and the results are described below.

As an example case we have taken flow rate of 1,700 Kg/min of dry gas (D.G.) with molecular weight of 29.0 and an initial humidity of 0.01 g H_2O/gD.G. Various inlet gas temperatures are considered and it is assumed that the gas will reach its adiabatic saturation temperature in the high energy (H.E.) scrubber and 49°C in the FF/C scrubber outlet. A 10°C lower outlet temperature from an FF/C scrubber could generally be attained without great difficulty so that 49°C assumption is conservative. The saturated gas is assumed to travel from the scrubber to an induced draft fan and then to discharge. Thus the fan power requirement will depend on the humidity, temperature, and pressure of the scrubbed gas.

Costs were estimated for several operating modes of an FF/C scrubber and for some combinations of inlet gas temperature and pressure drop for an H.E. scrubber. Some

illustrative results are shown in Figure 7-1, a plot of hourly operating costs against condensation ratio with parameters of scrubber type and operating conditions.

Assumptions and cost bases for Figure 7-1 are as follows:

1. Inlet dry gas flow rate is 1,700 Kg/min, pressure is 1.0 atm. abs., humidity is 0.01 g H_2O/g D.G., molecular weight is 29.0, and temperature is as shown.

2. Cooling water could cost from 0.26¢/MKg (1¢/Mgal) to 4.0¢/MKg. Recirculated cooling tower water might be available for about 0.9¢/MKg, based on quoted costs and on cooling tower depreciation plus pumping costs, and is used in this example.

3. A water temperature range of 17°C is taken to represent the combined effects of temperature range and water costs. Thus, while the temperature range for scrubber water entering at 40°C and leaving at 70°C after contacting gas saturated at 75°C would be 30°C (corresponding to 18 g water required per g of vapor condensed) the cost of cooling would be higher than for a 17°C range. By assuming that both water requirement and cost are constant with "q'", it is implied that water cooling cost is proportional to cooling temperature range, which is conservative.

4. Electric power cost is 3¢/KWH and purchased steam cost is \$6.40/MKg (\$2.90/1,000 lb) based on fuel at \$10.32/Kcal (\$2.60/10^6BTU) and 85% generating efficiency.

5. Fan power cost is based on an overall fan and motor efficiency of 50%.

6. An FF/C scrubber can be designed for an overall power requirement equivalent to a 15 to 25 cm W.C. fan; whether spray, plate, or packed type. Fan power costs for the FF/C scrubber are based on the higher pressure drop; 25 cm W.C.

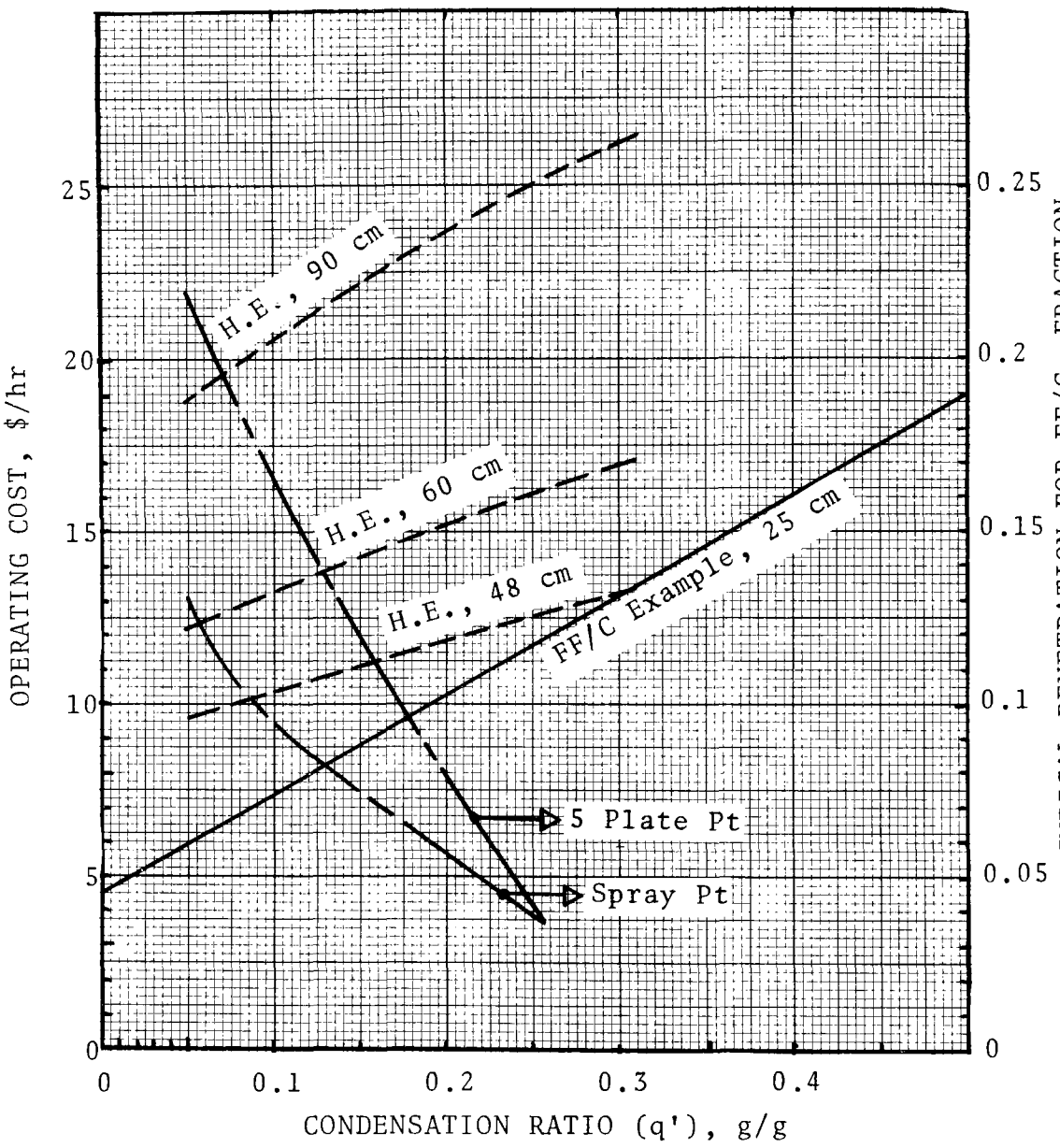

Figure 7-1, Operating cost comparison of FF/C and H.E. scrubbers.

7. Particle penetrations for H.E. scrubbers are predicted as a function of pressure drop by means of the method developed by Calvert (1974). The penetrations predicted for wettable particles of 1 μmA diameter are 0.1 (i.e., 10%) at 48 cm W.C., 0.05 at 60 cm, and 0.02 at 90 cm.

Results of Comparison

In addition to Figure 7-1, the results of this comparison are presented in Table 7-1, showing some combinations of gas conditions and operating costs. Figure 7-1 contains plots of typical values of experimental particle penetration as a function of condensation ratio for plate and spray type FF/C scrubbers so that the cost data can be readily interpreted.

The three dashed lines are for the fan power costs associated with H.E. scrubbers operating at 48, 60, and 90 cm W.C. pressure drop (as indicated on the plot) and at actual volumetric flow rates corresponding to a given condensation ratio. To illustrate the meaning of these lines, gas at 600°C and humidity of 0.01 g/g would reach an adiabatic saturation temperature of 66°C and humidity of 0.22 g/g in a H.E. scrubber. The volumetric flow rate due to 1,700 Kg/min of dry gas and 374 Kg/min of water vapor would be about 2.2×10^3 m^3/min at 66°C and 1.0 atm absolute pressure. The volumetric flow rate will be higher at lower absolute pressures corresponding to negative inlet fan pressures equivalent to the pressure drop across the scrubber system.

The cost of fan power is computed from the actual volumetric flow rate and pressure drop by the use of the relevant assumptions and costs given above. In order to compare the cost for H.E. scrubbing to that for FF/C scrubbing, they have been plotted against the condensation ratio which could have resulted if gas at the inlet

Table 7-1. GAS CONDITIONS AND FAN POWER COSTS

Inlet Gas		Ad. Sat. Gas		Fan Power Cost for 1,700 Kg D.G./min, ($/hr)				
Temp. (°C)	Humidity (g/gD.G.)	Temp. (°C)	Humidity (g/gD.G.)	Pressure Drop, cm W.C.				
				15cm	25cm	48cm	60cm	90cm
260	0.01	49	0.08	$2.67	$4.47	$ 9.06	$11.50	$17.70
400	0.01	58	0.14	--	--	9.80	12.40	19.30
500	0.01	66	0.22	--	--	11.20	14.00	21.80
800	0.01	71	0.3	--	--	12.40	15.60	24.20
1,000	0.01	75	0.39	--	--	13.50	17.00	26.00

conditions had been treated in an FF/C system. For the 600°C inlet temperature the condensation ratio would be the difference between the adiabatic saturation humidity and the assumed FF/C outlet humidity; that is, q'= 0.22-0.08=0.14g/g

At q'=0.14, Figure 7-1 shows the following:

Scrubber	Pt @ 1 μmA	Cost, $/hr
FF/C Plate	0.125	8.80
FF/C Spray	0.08	8.80
H.E. 48 cm W.C.	0.1	11.00
H.E. 60 cm	0.05	13.70
H.E. 90 cm	0.02	21.50
H.E. 42 cm*	0.125	9.50

Note: *Computed for comparison at same Pt as FF/C plate.

It can be seen from the above data that FF/C scrubbing would require lower operating costs than H.E. The cost advantage of FF/C scrubbing increases as the inlet gas enthalpy increases and the penetration requirement decreases. If low penetration is not required a low pressure drop H.E. scrubber may give satisfactory performance at lower cost than FF/C. The point where H.E. and FF/C scrubbing will have the same operating cost for the same efficiency, depending on FF/C scrubber type, is a gas temperature of about 400°C. The condensation ratio would be about 0.06 g/g and the predictions from Figure 7-1 and some additional computations for H.E. scrubbers are as follows:

Scrubber	Pt @ 1 μmA	Cost, $/hr
FF/C Plate	0.21	6.30
FF/C Spray	0.12	6.30
H.E. 30 cm W.C.	0.21	6.30
H.E. 44 cm W.C.	0.12	9.00

The preformed spray scrubber of the design studied in this program had higher efficiency than the sieve plate column for a given value of condensation ratio as the ratio decreases. In the "cold" operation mode (i.e., $q' \approx 0$) the spray gave better efficiency for a given power input than the sieve plate and other types of H.E. scrubbers, such as gas atomized sprays. For operation at about 2.4 ℓ/m^3 in each of three stages, as in the pilot scale spray scrubber, the liquid pumping power would be equivalent to about 17 cm W.C. pressure drop in terms of fan power. Thus it is to be expected that the pre-formed spray scrubber will be economically superior to H.E. scrubbers over the whole range of condensation ratio.

Steam Introduction

While the performance of an FF/C scrubber at a given condensation ratio is better if part or all of the water vapor is introduced as steam (i.e., 100% H_2O), the cost of purchased steam will generally be prohibitively high. However, under the right circumstances the use of some steam introduction could be economical.

The steam required for injection could be low pressure, < 2 atm. gage, (< 30 psig) spent steam. It may be obtained from the feed line to the boiler condenser in a process plant or generated in a low pressure waste boiler in a metallurgical operation. In this case, the steam cost would be significantly lower and will depend on the specific manufacturing process. In general, if such steam is avail

able for less than $1.88/MKg, the operating costs for a FF/C scrubber would be lower than a venturi scrubber.

Figures 5-6 and 5-13 indicate that the "q'" requirement levels out around q'=0.15, so that proportionately lesser condensation is required to obtain penetrations lower than 5% in a FF/C scrubber. Thus, in this region, a FF/C scrubber using some purchased steam would have lower operating costs compared to a venturi scrubber. Also, as the most important factors in FF/C scrubbing, diffusiophoresis and particle growth by condensation are practically insensitive to particle size. FF/C scrubbing would become economically more attractive as the size of the particles to be controlled gets smaller, in the range of 0.01 μm to 10 μm.

Industrial Application Costs

Calvert et. al. (1973) have evaluated the economic feasibility of FF/C scrubbing systems designed for two industrial sources: A Basic Oxygen Furnace and a Kraft Recovery Furnace. The gas cleaning devices in these systems were a FF/C spray scrubber for the Basic Oxygen Furnace and a combination of a venturi evaporator-scrubber followed by a FF/C condenser vessel with a spray scrubber for the Kraft Recovery Furnace.

The economic feasibility of FF/C scrubbing for a gray iron cupola is evaluated below. Due to the different designs and operating practices for cupolas, it is not possible to generalize emission characteristics so a specific cupola was selected for the case study. Emissions from this cupola are now controlled with a high energy scrubber whose performance was measured by A.P.T. (Calvert et al. 1974). Information on emissions, system behavior and costs were obtained from the cupola operators. The FF/C scrubber system was designed for the same particle control as the existing system and the equipment and operating costs are compared.

CUPOLA EMISSION CONTROL

Gray iron foundries use cupola, electric-arc, electric-induction and reverberatory air furnaces to obtain molten metal for production of castings. The iron melting process is the principal source of emissions in the foundry industry. Cupola furnaces are most commonly used for the melting operations. In the foundry industry, cupola emissions are dominant, totaling over 105,000 tons/yr as reported by M.R.I. (1971).

The cupola emissions are presently controlled by high energy scrubbers, fabric filters (bag-houses) and electrostatic precipitators. FF/C scrubbers are uniquely suited for cupola emission control, due to the combination of high stack gas temperatures (over 900°C), fine particle sizes (d_{pg}~1.5 μmA), moderately high dust loadings (over 3 g/DNm^3) and the presence of contaminant gases.

The FF/C system described below was designed for a 2 m (80") diameter cupola. Presently the cupola emissions are controlled with a high energy scrubber system. Details on the performance of this system together with the cost data have been reported by Calvert et. al. (1974). The cupola operation is briefly described below:

Size: 2 m (80") I.D., 9.8 m (32') high from tuyers to afterburners and 7.6 m (25') additional height to the top. The shell is water cooled to a height of 6 m (20') and then refractory lined to the top. The fuel gas flow to the two afterburners is controlled to maintain the offtake gas temperature between 870°C and 930°C.

Charge: Each charge consists of about 2,700 Kg of metal (mostly cast iron), between 270 Kg to 320 Kg of coke and fluxes as required. On an average there are 12 charges per hour.

The cupola emissions were reported to be as follows:

Flue gas rate = 3,400 Am^3/min (119,500 ACFM) @ 900°C.

Flue gas humidity = 0.01 $\frac{g\ vapor}{g\ dry\ gas}$, from humidity of the ambient air.

Particulate characteristics: 3.5 g/DNm^3 (8 gr/DSCF), log normally distributed with mass mean diameter, d_{pg}=1.15 μmA and σ_g=1.7.

The present high energy scrubber system has an overall particulate removal efficiency of 97% at the scrubber pressure drop of 275 cm W.C.

The FF/C Scrubber System

The FF/C scrubber system was designed to yield 97% particulate collection efficiency, identical to the performance of the high energy scrubber. A spray configuration was selected for the FF/C scrubber due to the low pressure drop requirement. Based on the FF/C spray scrubber tested in this study, q'=0.18 is considered sufficient to achieve the desired particulate removal, with the overall liquid sprayed to gas flowrate ratio of 4.5 ℓ/m^3(34 gal/MCF).

A process diagram of the FF/C scrubber system is shown in Figure 7-2. As described earlier, stack gas from cupola offtake is maintained at about 900°C by adjusting the afterburners. Immediately downstream of the refractory-lined offtake, 150 ℓpm of water is sprayed in as fine mist, cooling the gas to 427°C. This serves the purpose of reducing heat losses from the 90 m long duct to the scrubber system, as well as permitting the use of smaller diameter mild steel duct. Gas temperature at the quencher inlet is determined to be 280°C after accounting for the heat losses.

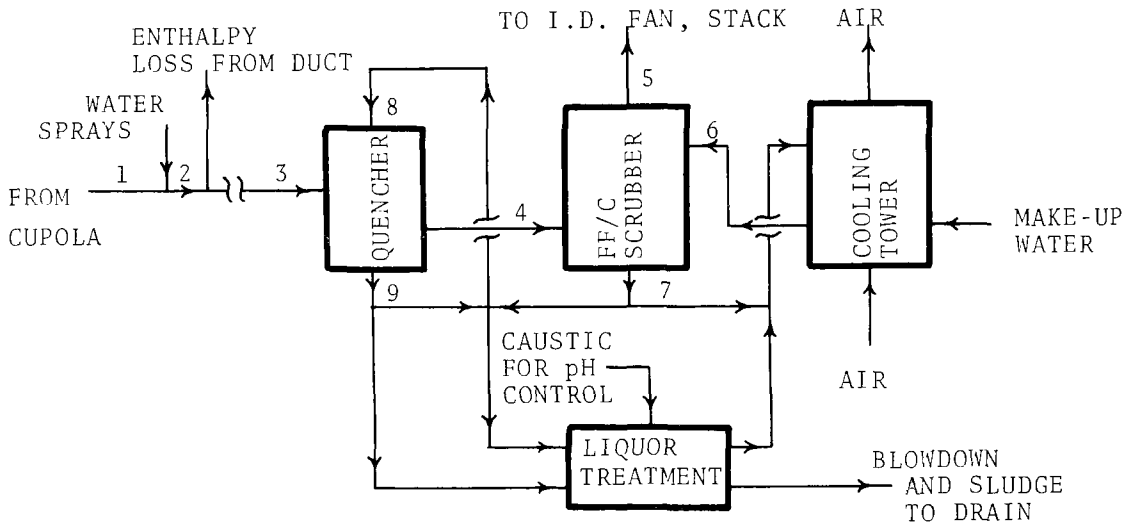

	STREAM NO.	TEMP °C	VOLUME FLOWRATE Am^3/min or ℓ/min	GAS HUMIDITY g vapor / g D.G.	PRESS cm W.C.	LOADING g/DNm^3
GAS	1	900	3,400	0.01	-2	3.5
	2	427	2,480	0.16	-7	3.5
	3	280	1,850	0.16	-15	3.5
	4	69	1,300	0.26	-20	3.5
	5	49	970	0.08	35	0.105
LIQUID	6	27	5,870			
	7	46	6,040			
	8	64	400			
	9	69	300			

FIGURE 7-2 Process diagram for cupola gas cleaning

The gas is then further cooled and humidified by recirculating water sprays in the quencher. As the size distribution of particles in the stack gas is fine, with over 99% by mass of particles smaller than 5 μmA, water sprays in the quencher are not expected to remove any significant amount of particles. The desired particulate removal is achieved in the FF/C spray scrubber. The scrubbed gas is cooled down to 49°C in the scrubber, condensing out 0.18 g vapor/g d.gas on the liquor sprays. The overall pressure drop across the system is determined to be 35 cm W.C.

The liquor system includes a cooling tower and provisions for clarification and pH control of the recirculated liquid. The uniformly packed cooling tower uses ambient air for evaporative cooling of the liquid sprayed in the scrubber. Clarification of the recirculated liquid is attained by settling out the suspended solids in tanks, with a total retention time of about 45 minutes. The settling process is enhanced by the addition of coagulants. Caustic soda solution is added in the tanks to maintain the pH between 6 and 7. A constant blowdown from the tanks controls the concentration of dissolved solids in the liquid stream. A water wash is provided in the cooling tower to periodically clean out scale formed on the packing surface. City water is added into the cooling tower to make up for the blowdown, entrainment, evaporative and other losses from the recirculated liquid system.

Cost Comparison

Equipment for the system shown schematically in Figure 7-2 was selected and sized for the purpose of cost estimation. Capital cost information was obtained from the following sources: A.P.T. Scrubber Handbook (1972), Cost Engineering in the Process Industries (1960), Modern Cost Engineering Techniques (1970), and Chemical Engineers' Handbook, Fifth ed., (1973). The method was based on

calculating the F.O.B. equipment cost and then multiplying by various factors for the costs of internals, piping, instrumentation, etc. The capital costs were then adjusted to a common time base, 1974, using the Marshall & Stevens Equipment Cost Index.

Installation costs for the scrubber system, to include modifications in existing process, site preparation, foundation, start-up, etc. were not determined, as they are expected to be comparable to the costs for the high energy scrubber system. Similarly, the operating costs for labor, liquid treatment, and solid disposal, together with the maintenance costs for labor and materials, are expected to be comparable for the two scrubber systems. Thus, the only operating costs compared are the electrical power requirements and annualized capital charged and depreciation taken as 20% of the capital costs. Table 7-2 shows the cost comparisons.

The FF/C scrubber system requires additional equipment such as the quencher and the cooling tower. Due to the higher flow requirements of recirculated liquid, the liquid system costs are also higher for the FF/C system compared to the high energy (H.E.) scrubber. However, these costs are more than offset by the higher cost for fans for the H.E. scrubber system. Three fans are required for the H.E. system, adding up to 1,080 KW (1,450 HP) as compared to one 127 KW (170 HP) fan required for the FF/C system. Note that costs for piping and ducting for both the systems are expected to be the same, although they are significantly different. The FF/C system has a higher piping requirement and requires the 90 m duct to be lightly insulated. These costs are expected to approximately offset the cost of addi tional ducting used in the H.E. system to jacket the 90 m duct.

A comparison of costs for the two systems indicates that the total equipment costs are approximately the same. The H.E. system, however, costs about $63,500 more per year to operate, as the annual cost for electrical power is more than 2.6 times that for the FF/C system. Electrical power cost of $0.03/KW-HR was used for the above calculations. Power costs have increased steadily in recent years and there are no immediate indications for a change in this trend. As the cost of electrical power increases and energy conservation becomes more important, the FF/C scrubbing system will prove to be more attractive, compared to a high energy scrubbing system.

Table 7-2. COST COMPARISON OF CUPOLA EMISSION CONTROL SYSTEMS

COST ITEMS	High Energy Scrubber System ($)(1)	FF/C Scrubber System ($)
A. Capital Costs		
1. F.O.B. quencher with internals, flange to flange	-- (4)	12,140
2. F.O.B. scrubber with internals, flange to flange including entrainment separator	18,600	32,460
3. F.O.B. cooling tower	--	34,950
4. Fans, motors and motor starter	156,370	35,000
5. Liquid treatment and solid handling equipment, including pumps.	50,030	80,000
6. Piping and ducting (2)	102,570	102,570
7. Instrumentation and electrical material (3)	22,900	15,640
TOTAL EQUIPMENT COST	350,470	312,760
B. Annual Operating Costs		
1. Electrical power for fans and pumps.	102,560	38,900
2. Annualized capital charges and depreciation (20% of capital costs)	70,100	62,550
TOTAL	$172,660	$101,450

Notes:

1. Actual costs obtained from the user, converted to 1974.
2. Due to equivalent complexity, the costs were assumed same for both systems.
3. Taken as 5% of equipment costs for the FF/C system.
4. Quench spray costs for both the systems are included in the ducting costs.

CHAPTER 8
FUTURE RESEARCH RECOMMENDATIONS

The preliminary objective of examining the technical and economical feasibilities of FF/C scrubbing for the collection of fine particles, through experimental evaluation of two FF/C scrubbers, has been achieved in this study. It has been clearly shown that FF/C scrubbing is capable of high efficiency fine particulate removal. Areas of economic application of FF/C scrubbing at industrial sources have been identified. These include some of the major stationary air pollution sources in the U.S.A. as listed in the Midwest Research Institute report (1971). Mathematical design models have been developed also for the two FF/C scrubbers studied. To continue this development work so that the advantages of FF/C scrubbing could be derived for industrial application, we recommend future research work in the following areas:

1. Demonstration of the feasibility of FF/C scrubbing on selected industrial sources.
2. Theoretical and experimental evaluation of other low energy scrubber configurations to determine the best configuration applicable to FF/C scrubbing systems.
3. Development of evaporative cooling devices suited for the cooling of scrubber liquid containing suspended and dissolved solids.
4. Theoretical and experimental determination of the specific details of heat and mass transfer in gas-liquid systems, the nucleation of condensation and other matters which critically affect the applicability of FF/C scrubber design equations.

DEMONSTRATION OF FF/C SCRUBBING

A detailed test program to demonstrate FF/C scrubbers at pilot scale for the control of fine particulate emissions from three industrial sources is described below. The fol lowing criteria were used for selecting the industrial sources:

I. The national importance of the industrial parti culate emission sources as major pollutants.
II. Applicability of FF/C scrubbing in terms of its technical and economic feasibility.
III. Sources which are either difficult or expensive to control with presently available particulate control devices.

Three sources were selected which would enable demonstration of the operational reliability of all the components of an FF/C scrubbing system. These sources are described below:

Secondary Nonferrous Metals Recovery Furnace

The secondary nonferrous smelting and refining industry generally uses gas-fired furnaces to recover copper, aluminum, lead and zinc from scrap and dross. The nature of furnace operations is such that emissions vary widely during the cycle from charging the scrap to pouring a melt. Peak emission surges occur in nearly all the furnace operations. The principal emissions from these furnaces are particulates in the form of smoke, dust, and metallic fumes. However, during copper wire reclamation, considerable amounts of acidic and corrosive gases comprised of fluorine and chlorine compounds are also present, depending on the composition of the wire insulation. With emission rates of about 127,000 ton/year, this industry was ranked among the top fifteen national source pollutants in a survey by Midwest Research Institute (1971).

Due to the cyclic nature of the emission, high flue gas temperatures (∿500°C to 900°C), presence of corrosive gases and high efficiencies required for fine particulates, the recovery furnace emissions have been difficult and expensive to control. Generally, afterburners are used following the furnace to burn out hydrocarbons in the flue gas. High energy scrubbers, electrostatic precipitators and fabric filters have then been applied to remove the particulates. None of these have proven reliable for maintenance free operation. No control device is presently available to control emissions from copper wire recovering operations, although over 300,000 ton of insulated wire is recycled annually resulting in emissions exceeding 41,000 ton/year.

We recommend that FF/C scrubbing should be demonstrated on a recovery furnace, especially one operated for copper wire reclamation. A pilot scale system with a capacity of 140 to 280m^3/min is recommended. A small furnace with a process load of about 450 Kg/hr, with 20-minute cycles, would be ideally suited for the demonstration. The total flue gas emission of such a furnace would be in the range of the pilot scale FF/C scrubber capacity so that the effect of the cyclic nature of emission could be best evaluated. This would permit also a study of the FF/C system performance for the simul taneous removal of fine particulates and corrosive gases, using alkaline scrubber liquor.

Glass Furnace

The glass manufacturing industry, and especially the container glass industry, is faced with a nation-wide need for the application of particulate control systems on the glass furnaces. Glass furnace emissions have been difficult and expensive to control due to a high fraction of fine particulates,

high stack gas temperatures and the presence of gaseous contaminants. However, these emission properties are favorably suited for economic application of FF/C scrubbing.

A typical furnace produces from 80 to 140 metric tons of glass per day on a 24 hrs/day schedule. Typical flue gas properties for a furnace producing amber glass are as follows:

Gas Conditions:
- Flowrate: 300 m^3/min @ 20°C
- Temperature: 450°C

Particulates:
- Loading: 0.2 g/m^3 @ 20°C
- Emissions: 4 Kg/hr.
- Composition: ∿90% Na_2SO_4
  ∿10% $CaSO_4$
  trace amounts of other constituents

The particles are ∿1.0 μmA, with geometric standard deviation less than 3.

Gaseous contaminants:
- SO_x: 80 ppm
- NO_x: 1,500 ppm

In addition to the removal of gaseous contaminants, over 80% removal of particulates is required and the opacity limited to less than 20%. An FF/C scrubber has the additional advantage of particle growth, as ∿90% particulates are soluble in water and would grow at a saturation ratio of less than one. This would be one of the major aspects of the demonstration. Again, a pilot scale system with a capacity of 140 to 280m^3/min is recommended.

Gray Iron Foundry Cupola

Gray iron foundries use several types of furnaces to melt and recover iron from scrap for the production of castings. Cupola furnaces are most prominently used for the melting operations. The iron foundry industry was ranked among the top 15 national stationary-source pollutants in the Midwest Research Institute (1971) survey. In the foundry industry, cupola particulate emissions are dominant, totaling over 105,000 ton/year. Physical processes, chemical reactions, and the quality of scrap affect the emissions of dust and fumes from cupola, thus no typical flue gas condition can be defined. For example, emissions from a 86 cm (34") cold blast cupola with a production rate of 45 Kg (100 lb) molten iron per minute are listed below:

Flue gas rate = 520 A m^3/min (18,350 ACFM) @ 980°C

Flue gas rate = 115 N m^3/min (4,000 SCFM)

NOTE: The flue gas rate and temperature are maintained constant by adjusting gas flowrate to an afterburner located above the charge door.

Average flue gas composition, before afterburn, vol %:

CO_2: 12%

CO : 14.9%

N_2 : 73.1%

Particulate loading: 1.0 g/DN m^3 (2.3 gr/DSCF)

The particulate size distribution data reported in the literature for cupola emissions were found to vary considerably from source to source. Due to the carbon particles present in the emission, the particles are considered to be non-wettable.

Cupola emissions have been difficult and expensive to control due to the high emission rates of fine particulates, high gas temperatures and significant changes in the emission characteristics during the operation cycle. At present,

electrostatic precipitators, high energy scrubbers and fabric filters (bag houses) are used to control these emissions. The high gas temperatures and fine particulate loadings prompt the economic use of FF/C scrubbers. Again, a 140 to 280m^3/min pilot scale FF/C system is recommended.

A detailed demonstration test program, including the cost and time estimates, is described below. Although the details of FF/C scrubbing system design will be different for each source, the overall process design, illustrated in Figure 8-1, will be the same. Since the test matrices for the demonstrations would also be of comparable complexities, we expect that the cost and period of performance for each demonstration will be the same. Any variations in these estimates can be easily accommodated when more details on the installation and operation of the industrial source in question are available.

In outline, the objectives consist of the following tasks:

1. Select a company which operates a suitable plant involving one of the above operations for the demonstration of FF/C scrubbing and obtain required clearances from the local air pollution control agency.
2. Design the demonstration scrubber system on the basis of:
   A. Pertinent data concerning the source obtained through source testing.
   B. Evaluations of alternative FF/C scrubber system designs.
3. Prepare a detailed test plan describing:
   A. The measurement techniques to be used.
   B. Error analysis of the measurement techniques.
   C. The proposed test matrix.
   D. The data handling procedures.

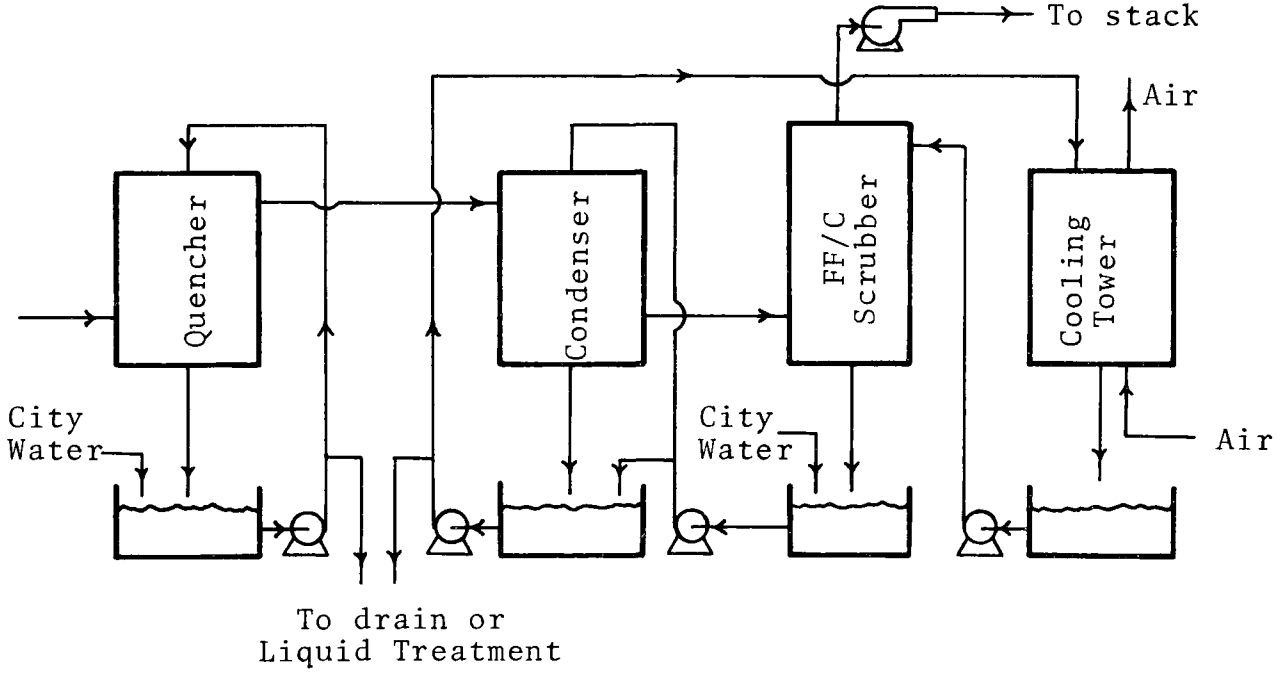

Figure 8-1 - Typical process design of a FF/C scrubber system

4. Fabricate, install and start up the FF/C scrubber system as developed in 2 above.
5. Conduct the test program as developed in 3 above.
6. Remove the pilot FF/C scrubbing system and restore the site to its normal condition less fair wear and tear.
7. Conduct an engineering and cost analysis of the FF/C scrubber system to evaluate:
   A. Scrubber operating and capital cost.
   B. Scrubber operation and maintenance problems.
   C. Scrubber reliability.
   D. Scrubber performance.
8. Based on the above analysis and the additional information available on scrubber design, design and estimate the cost of an optimum FF/C scrubber system for the industrial source.
9. Define the areas of FF/C scrubbing in which addi tional information is needed to improve the via bility of the FF/C scrubber application.
10. Survey emission conditions for similar sources to determine a group of industrial operations where the optimum FF/C scrubbing system developed above is economically applicable with minor modifications.
11. Recommend a test program to demonstrate a full scale FF/C scrubbing system on a simliar industrial source.

For the purpose of estimating the cost and time requirements, the following task breakdown was used:

Task 1 - Select company

a. Survey the industry and contact companies
b. Preliminary screening
c. Contact screened candidates to obtain additional information and perform sampling, where needed.

d. Refine calculations of conceptual designs based on "c" above.
e. Consult the contracting agency.
f. Select the company for the demonstration.
g. Consult the local air pollution control agency.
h. Finalize the arrangements.

Task 2 - Design the demonstration pilot plant

a. Obtain more data on the source
    1. Sample the source
    2. Conduct small-scale (10-20 CFM) tests on the source to test out concepts for scrubbing, liquor cooling, monitoring, etc.
b. Evaluate alternatives by means of:
    1. Preliminary designs
    2. Laboratory bench scale tests
    3. Laboratory pilot scale tests
    4. Additional small-scale tests at source
    5. Finalize alternative designs
    6. Compare alternative designs
    7. Consult contracting agency
    8. Consult company
    9. Clear with local air pollution control agency
    10. Make detailed design and specifications of demonstration pilot plant.

Task 3 - Prepare detailed test plan

a. Develop plan
b. Error analysis
c. Define procedures
d. Finalize measurement and monitoring procedures

Task 4 - Fabricate, install, start up

a. Select vendors and place orders
b. Arrange for site modifications
c. Follow up vendors and assemble components
d. Install pilot plant
e. Start up pilot plant

Task 5 Conduct test

a. At near-optimum conditions

b. At excursions from optimum

c. Configuration variations

Task 6 - Remove pilot system and restore site

Task 7 - Engineering analysis

a. Operating and capital costs

b. Operating and maintenance problems

c. Reliability

d. Performance

1. Scrubber

2. Liquor system and other auxiliaries

Task 8 - Optimum FF/C system

a. For this plant condition

b. For other capacities.

Task 9 - Evaluate FF/C scrubbing system performance to define areas for additional investigation

Task 10- Survey emissions from other sources to determine a group of operations with similar emission problems

Task 11- Recommend full scale test program

A performance schedule for this program is described in Table 8-1. The overall period of performance is 18 months for the demonstration program. It is noted that additional demonstration programs performed on the other industrial sources would require 14 months, if performed by the same contractor.

A detailed cost breakdown for the demonstration program is described in Table 8-2. It is noted that the costs were based on 1974 prices and for the FF/C scrubbing system only. If there are special construction and installation problems at the industrial source, the costs should be adjusted accordingly. It is expected that additional demonstration

TABLE 8-1: ESTIMATED SCHEDULE OF PERFORMANCE

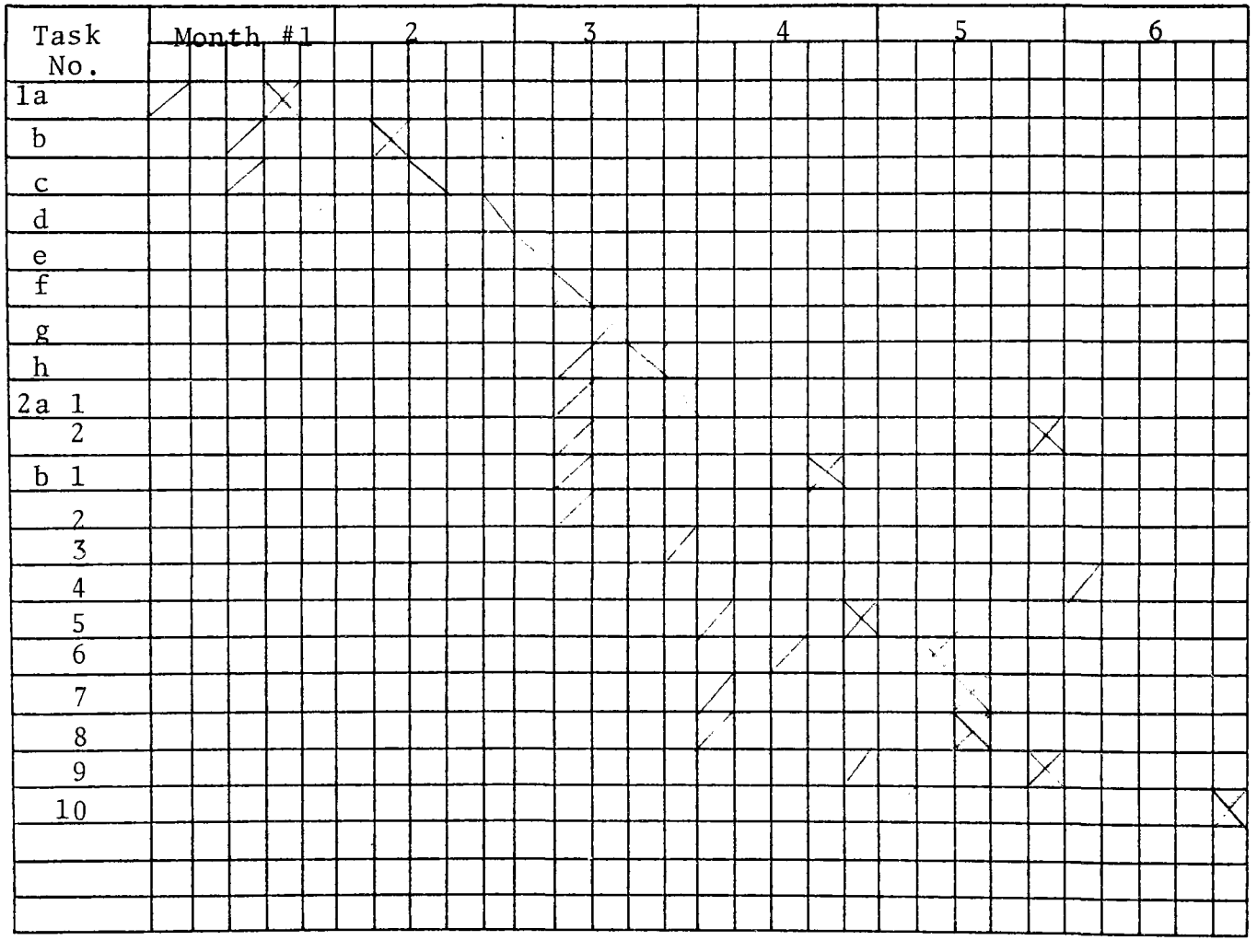

TABLE 8-1: (Cont.)

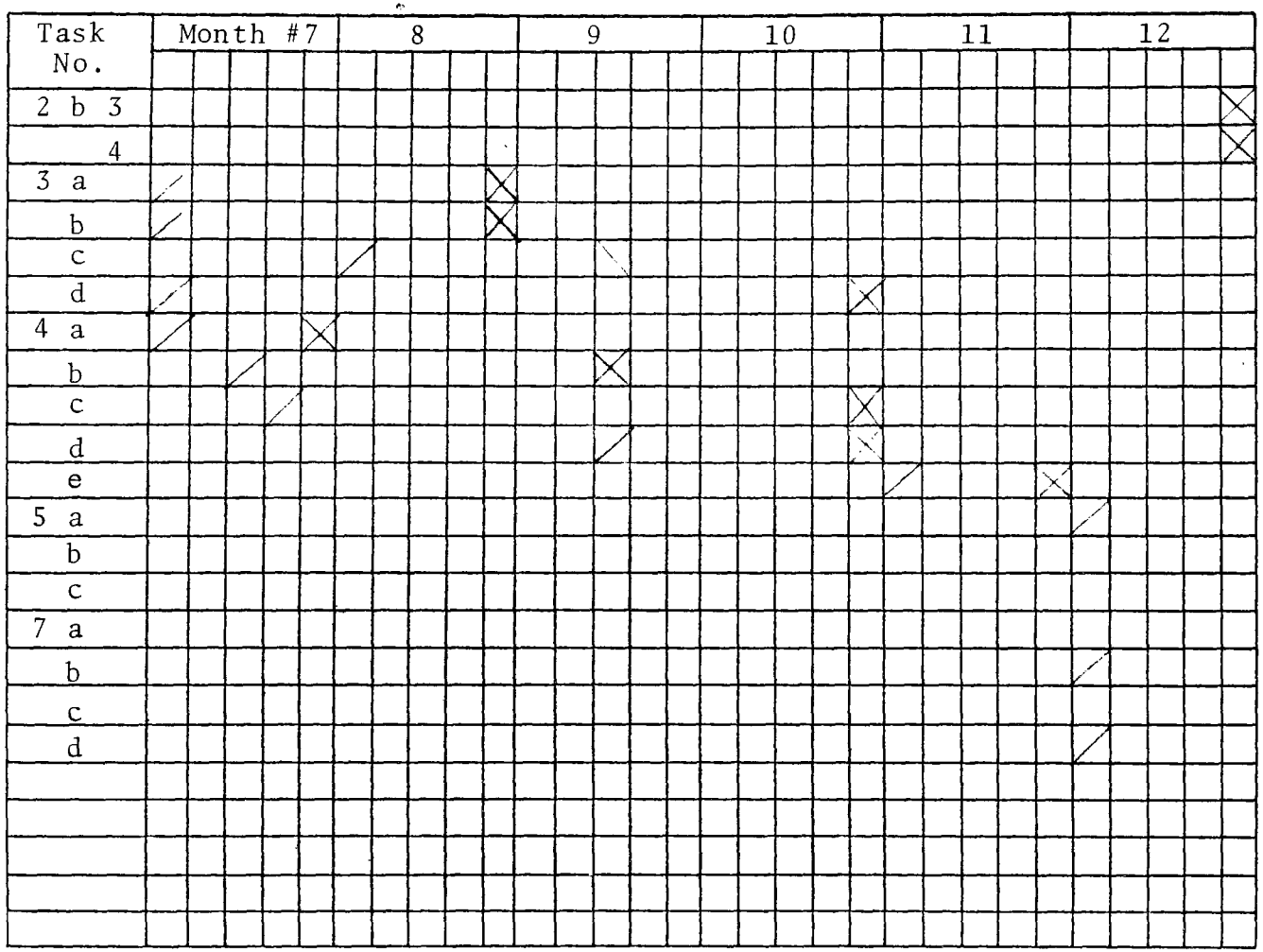

TABLE 8-1: (Cont.)

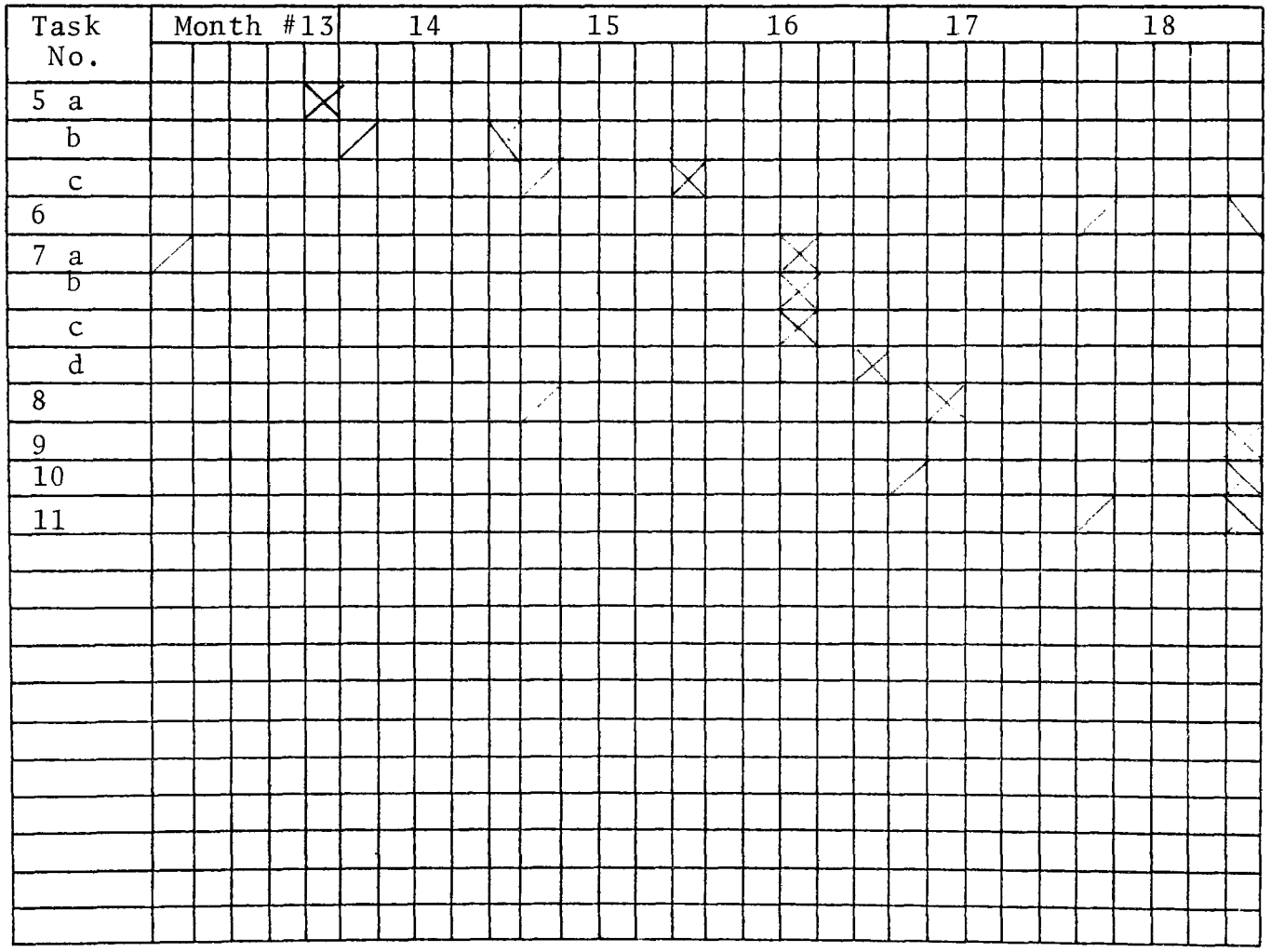

programs at the other industrial sources would cost about 80% overall, if performed by the same organization.

Table 8 -2

DETAILED COST BREAKDOWN

Task No.	Direct Labor ($)	Other Direct Costs ($)
1	16,000	4,000
2	32,000	18,500
3	15,000	5,000
4	19,000	40,000
5	19,500	4,500
6	6,500	---
7	4,500	2,500
8	4,500	---
9	4,000	---
10	5,000	---
11	4,000	---
TOTAL	130,000	74,500

The above estimates were made on the assumption that the performing organization is eminently qualified in the research and development field, with special knowledge, background and interest in the specific field of particulate removal by FF/C scrubbing.

EVALUATION OF OTHER SCRUBBER CONFIGURATIONS

During the performance of this contract, multiple sieve plate and horizontal spray scrubbers were evaluated, when operated in the FF/C scrubbing mode. Several other configurations of conventional and novel designs are presently available for low pressure drop scrubbing, such as the mobile bed scrubber and the packed bed scrubber with conventional and new packings. We recommend that these configurations be evaluated to determine their applicability to FF/C scrubbing. The following approach is recommended:

1. Survey scrubber manufacturers and users to assimilate design and operating information on low energy scrubbers with high gas residence times. The scrubbers should be multi-stage or continuous contact type.
2. Screen and select promising scrubber configurations based on theoretical evaluation of the scrubber performance when operated in the FF/C scrubbing mode, for the collection of fine particles.
3. Conduct a limited bench scale study to obtain information in the critical areas of scrubber operation, so that the FF/C scrubber model could be theoretically derived.
4. Determine the technical and economic feasibilities and the special area of application for these scrubbers by using the models developed above. The feasibilities should be determined by a comparative evaluation of all the FF/C scrubbers considered.
5. Select promising scrubber mechanisms and conduct a detailed experimental study as follows:
   a. Laboratory pilot scale study with scrubber capacity between 14 and 28 m^3/min.

b. Pilot scale demonstration on selected industrial sources with scrubber capacity between 140 to 280 m^3/min.

c. Full scale demonstration on a selected industrial source.

It is noted that performance of each of the above tasks would depend on the results of the preceding tasks. The program objective is to determine FF/C scrubber configurations best suited for specific industrial operations or a group of operations with common particulate control problems.

DEVELOPMENT OF LIQUOR COOLING SYSTEM

Due to the large requirement of cold scrubber liquor and the complications introduced by dissolved and suspended solids, the liquor cooling procedure has a significant effect on the economics of a FF/C scrubber system. The scope of the proposed work is to evaluate the liquor cool ing system alternatives, select the most promising system and make an experimental study to determine its performance, economics and applicability.

The following approach is recommended:

1. Determine all factors affecting the liquor cooling system for a FF/C scrubber. These include such things as economic considerations, effect on scrubber performance and the concentrations of dissolved and suspended impurities in the liquor.
2. Evaluate cooling system alternatives and select the most promising for experimental study.
3. Conduct an experimental study on a suitable scale to determine its performance, economics, applicability and scale-up considerations.

APPENDIX 5.A

MULTIPLE SIEVE PLATE FF/C SCRUBBER OPERATING CONDITIONS AND PERFORMANCE

Table 5.A.1 FIVE PLATE FF/C SCRUBBER; OPERATING CONDITIONS AND PERFORMANCE

Plate configuration Five identical plates with 3.2 mm round perforations
Free area 9%; Plate active area = 9.29×10^{-2} m^2

Dust used Pure black iron oxide, 16 mesh, dry dispersed

Cold water introduced on top plate, flow rate 0.64 liters/sec.

Run No.	Gas Inlet Conditions			q' x10	Liquid Temp. (°C)		Particulate						Scrubber Press. drop (cm W.C.)
	Flow $\left(\frac{DNm^3}{min}\right)$	Temp. (°C)	Moisture (% Vol.)				Load $x10^3$ (g/DNm^3)		d_{pg}		σ_g		
					In	Out	In	Out	In	Out	In	Out	
1	5.17	20	1.2		18		45.1	9.4		Filter	Samples		34.8
2	5.3	25	1.3		22		43.1	7.1	1.27	0.92	1.8	1.4	32.5
3	5.3	23	1.4				46.3	10.5	1.37	1.06	1.8	1.5	32.8
4	5.14	42	8.2	0.4	19.5	28.0	44.0	7.33	0.79	0.68	2.0	1.5	34.8
5	4.73	43	8.5	0.49	13.8	22.9	28.8	1.63	1.21	0.73	1.7	1.6	32.3
6	4.85	55	16.0	1.04	13.5	33	58.9	0.94	1.12	0.74	1.8	1.6	32.5
7	5.06	60	18.2	1.27	11	42.5	15.7	0.35	0.97	0.8	1.6	1.7	33.8
8	3.08	68.2	27.8	2.32	15.3	45.0	28.1	0.42	1.21	0.6	1.8	1.4	34.2
9	2.83	71.2	33.4	2.81	27	57.5	46.0	0.74	1.16	0.55	1.6	1.4	31.9

Table 5.A.2 FOUR PLATE FF/C SCRUBBER; OPERATING CONDITIONS AND PERFORMANCE

Plate configuration Four identical plates with 3.2 mm round perforations
Free area 9%; Plate active area 9.29×10^{-2} m^2

Dust used Pure black iron oxide, -16 mesh, dry dispersed

Cold water introduced on top plate, flow rate 0.64 liters/sec.

Run No.	Gas Inlet Conditions			q' x10	Liquid Temp. (°C)		Particulate							Scrubber Pressure Drop (cm W.C.)
	Flow $\left(\frac{DNm^3}{min}\right)$	Temp. (°C)	Moisture (% Vol.)				Load $x10^2$ (g/DNm^3)		d_{pg}		σ_g		n_i	
					In	Out	In	Out	In	Out	In	Out	$x10^{-4}$	
10	10.05	33.0	2.44		26	31	30.35	12.76	1.15	1.13	2.1	1.9	85	35.6
11	9.88	40.6	2.30		27	36	32.22	12.45	1.07	0.8	1.9	1.7	71	34.0
12	8.86	50.5	11.26	0.51	27	48	30.41	6.97	1.34	0.89	2.0	1.5	40	31.6
13	9.02	49.7	11.52	0.61	22	47	22.58	2.98	1.07	0.71	1.7	2.0	32	31.2
14	8.81	50.3	11.78	0.62	24	50	8.36	0.65	1.0	0.6	1.6	1.6	12	30.8
15	8.59	51.3	12.78	0.70	22	51	11.58	1.06	0.96	0.89	1.6	1.5	20	31.33
16	8.89	51.3	13.21	0.74	20	48	23.41	4.64	1.6	0.92	2.0	1.5	17	30.6
17	7.43	60.0	19.35	1.23	25	60	23.03	1.7	2.7	0.56	2.6	2.6	17	29.6
18	7.6	60.2	19.31	1.24	22	59	10.11	0.83	0.85	0.58	1.6	1.9	26	29.5

Table 5.A.3. FOUR PLATE FF/C SCRUBBER, OPERATING CONDITIONS & PERFORMANCE

Plate configuration: Four identical plates with 3.2 mm round perforations. Free area = 9%; Plate active area = 9.29×10^{-2} m^2

Dust used: Titanium dioxide, -16 mesh
Cold water introduced on the top plate, flow rate = 0.64 liters/sec

Run No.	Gas Inlet Conditions			q' x10	Liquid Temp. (°C)		Scrubber Pressure Drop (cm W.C.)
	Flow ($\frac{dsm^3}{min}$)	Temp. (°C)	Moisture (% Vol.)		In	Out	
19	7.90	56.0	16.2	0.90	27.5	55.4	29.8
20	8.13	63.0	21.4	1.23	31.2	54.7	37.2
21	8.43	60.5	20.8	1.25	27.8	53.0	33.9
22	8.51	61.0	21.0	1.35	24.5	60.0	34.9
23	8.31	60.5	20.8	1.32	25.0	60.0	35.1

Run No.	Particulate							$\overline{Pt}$ (%)
	Load x 10^3 (g/dsm^3)		d_{pg}		σ_g		n_i x10^{-8}	
	In	Out	In	Out	In	Out		
19	244	58.8	0.72	0.60	2.9	2.0	4.5	24.1
20	308	65.1	0.97	0.58	3.0	1.7	3.0	21.1
21	456	59.7	0.89	0.63	3.0	1.8	5.9	13.1
22	271	47.6	0.88	0.87	2.7	2.6	1.1	17.6
23	359	53.8	Filter Run					15.0

Table 5.A.3. FOUR PLATES FF/C SCRUBBER: OPERATING CONDITIONS & PERFORMANCE (continued)

Plate configuration: Four identical plates with 3.2 mm round perforations. Free are = 9%; plate active area = $9.29 \times 10^{-2} m^2$

Dust used: Titanium dioxide, -16 mesh
Cold water introduced on the top plate; flowrate = 0.64 liters/sec

Run No.	Gas Inlet Conditions			q' x10	Liquid Temp. (°C)		Scrubber Press Drop (cm W.C.)
	Flow ($\frac{dsm^3}{min}$)	Temp. (°C)	Moisture (% vol.)		In	Out	
24	8.23	22.8	1.7	—	15.2	18	28.3
25	8.28	28.3	1.5	—	18.5	26.5	28.4
26	8.37	34.5	1.6	—	20.3	23.5	29.5
27	8.14	44.3	9.2	0.40	22.5	43.5	30.7
28	8.25	45.3	9.8	0.53	14.8	39.2	32.1
29	8.33	49.3	9.1	0.55	21	49	32.5
30	8.35	49.8	12.2	0.63	25.3	49	33.5
31	8.28	59	19	1.11	26.2	58.8	34.8
32	8.30	59.8	19.7	1.17	26	59.5	33.8

Run No.	Particulate							$\overline{Pt}$ (%)
	Load x 10^3 (g/dsm^3)		d_{pg}		σ_g		n_i x 10^{-7}	
	In	Out	In	Out	In	Out		
24	203	88.9	filter run				—	43.8
25	166	65.6	1.15	0.89	2.1	2	0.5	39.6
26	267	114	filter run				—	42.8
27	181	46.2	0.91	0.77	2.6	1.9	4.5	25.6
28	74.2	19	0.98	0.72	2.4	1.9	1.4	25.6
29	190	37.4	0.66	0.66	2.7	2.4	23.5	19.7
30	169	38.8	filter run				—	22.9
31	313	70.9	filter run				—	22.6
32	296	52.2	0.91	0.70	3.2	1.9	103.3	17.7

Table 5.A.3. FOUR PLATES FF/C SCRUBBER; OPERATING CONDITIONS & PERFORMANCE (continued)

Run No.	Gas Inlet Conditions			q' x10	Liquid Temp. (°C)		Scrubber Press Drop (cm W.C.)
	Flow ($\frac{dsm^3}{min}$)	Temp. (°C)	Moisture (% vol.)		In	Out	
33	7.90	60.8	20.2	1.22	23	60.5	35.7
34	8.53	60.3	19.82	1.23	23.4	51	35.3
35	8.43	61	20.78	1.26	22.5	52	35.7
36	8.70	69.8	31.1	2.24	21.5	68	36.5
37	6.14	73.8	36.22	2.31	28.9	73	37.2
38	6.11	70.8	31.9	2.36	22.6	70.5	37.1
39	6.76	70.5	32.4	2.60	19	70.5	34
40	7.02	74	36.55	2.99	25.5	74	37.1
41	6.53	76	38.5	3.01	22.3	78	35.1
42	5.78	76	39.6	3.20	25	77.5	38.9
43	4.66	78	42.5	3.30	23.8	77	38.2
44	5.25	77.8	42.9	3.48	27	79	38.4
45	5.51	77	42.2	3.72	22.5	76	34.7

Run No.	Particulate								$\overline{Pt}$ (%)
	Load x 10^3 (g/dsm^3)		d_{pg}			σ_g		n_i x 10^{-7}	
	In	Out	In	Out		In	Out		
33	198	32.7	filter run			—	—	—	16.5
34	236.5	34.9	filter run			—	—	—	14.8
35	156.4	35.1	1.21	0.62	2	1.7		0.31	22.4
36	296	25	1.11	0.81	3	2		1.9	8.5
37	346.4	54.5	1.1	0.62	2.7	1.9		7.3	15.7
38	337	31.7	1.05	0.83	2.8	1.9		9.5	9.4
39	158	16.6	filter run			—	—	—	10.5
40	339.7	40.1	filter run			—	—	—	11.8
41	81.4	3.9	1.25	0.68	3.4	2.1		29.5	4.8
42	330	44.5	0.77	0.55	3.6	1.4		648.3	13.5
43	360	56	0.85	0.76	3.5	2.8		720	15.6
44	548	81.7	filter run			—	—	—	14.9
45	290	31.9	filter run			—	—	—	11

Table 5.A.4 FOUR PLATE FF/C SCRUBBER; OPERATING CONDITIONS AND PERFORMANCE

Plate configuration: Four identical plates with 3.2 mm round perforations. Free area = 9%; plate active area = $9.29 \times 10^{-2} m^2$

Dust used: Titanium dioxide, —16 mesh, dry dispersed.

Cold water introduced on the top plate; flowrate = 0.38 liters/sec

Run No.	Gas Inlet Conditions			q' x10	Liquid Temp. (°C)		Scrubber Press Drop (cm W.C.)
	Flow ($\frac{DNm^3}{min}$)	Temp. (°C)	Moisture (% vol.)		In	Out	
46	9.56	33.0	2.52	—	30.0	22.0	34.2
47	11.15	27.0	1.6	—	16.0	19.3	38.0
48	8.72	36.0	1.72	—	23.0	22.0	34.0
49	10.19	21.5	1.7	—	19.5	20.0	35.6
50	9.64	45.8	9.9	0.43	19.0	46.8	31.8
51	9.72	44.8	9.7	0.43	22.5	43.8	31.4
52	9.68	45.0	9.4	0.40	21.2	45.5	31.8
53	9.58	46.5	10.4	0.52	16.0	43.0	31.9
54	10.06	55.0	15.7	0.68	23.0	54.5	37.6

Run No.	Particulate								$\overline{Pt}$ (%)
	Load x 10^3 (g/DNm^3)		d_{pg}			σ_g		n_i x 10^{-7}	
	In	Out	In	Out		In	Out		
46	151.6	50.7	filter run			—	—	—	33.4
47	271	96.3	filter run			—	—	—	35.5
48	89.4	30.57	1.1	0.95	1.95	1.7		2.42	34.2
49	264	78.7	filter run			—	—	—	29.4
50	224	51.8	filter run			—	—	—	23.2
51	246	63.8	filter run			—	—	—	26.0
52	209	62.2	0.91	0.82	2.0	1.9		11.8	29.7
53	140	30.8	1.15	0.85	2.9	2.3		44.5	22.0
54	217	43.8	filter run			—	—	—	20.2

Table 5.A.4 FOUR PLATE FF/C SCRUBBER; OPERATING CONDITIONS AND PERFORMANCE (continued)

Run No.	Gas Inlet Conditions			q' x10	Liquid Temp. (°C)		Scrubber Press Drop (cm W.C.)
	Flow ($\frac{DNm^3}{min}$)	Temp. (°C)	Moisture (% vol.)		In	Out	
55	9.84	56.8	16.6	0.82	20.5	58.0	37.2
56	10.08	54.5	15.5	0.71	23.3	54.5	36.5
57	12.7	55.0	15.6	0.74	56.0	24.0	37.1
58	8.56	65.0	23.7	0.99	20.7	65.5	37.1
59	7.38	67.5	25.1	1.16	22.0	58.0	35.2
60	8.07	65.3	25.0	1.24	22.0	65.5	34.5
61	8.45	64.5	24.9	1.34	16.5	61.0	37.1
62	7.07	69.5	29.3	1.05	24.0	73.0	37.0
63	6.98	70.3	31.1	1.2	23.0	70.2	39.0
64	6.51	71.5	33.0	1.4	22.3	75.4	37.2
65	6.96	72.5	33.7	1.8	20.0	73.5	37.6
66	6.31	71.0	32.3	1.15	24.5	71.5	35.3
67	4.9	73.5	33.8	1.3	22.0	73.0	38.6

Run No.	Particulate							$\overline{Pt}$ (%)
	Load x 10^3 ((g/DNm^3)		d_{pg}		σ_g		n_i x 10^{-7}	
	In	Out	In	Out	In	Out		
55	156	40.3	filter run		—	—	—	25.8
56	203	49.3	0.81	0.80	2.4	1.9	43.5	24.4
57	122	29.9	0.85	0.74	2.4	2.2	20.0	24.5
58	174	30.2	filter run		—	—	—	17.4
59	304	54.9	filter run		—	—	—	18.0
60	166	33.7	0.97	0.96	2.3	2.1	15.76	20.3
61	204	38.5	0.99	0.72	2.2	1.9	14.71	18.8
62	271	49.6	filter run		—	—	—	19.0
63	358	61.0	filter run		—	—	—	17.0
64	282	53.0	filter run		—	—	—	18.8
65	267	42.8	filter run		—	—	—	16.8
66	215	39.7	1.09	0.79	2.5	2.4	23.9	18.5
67	192	31.4	1.35	1.02	2.5	2.1	10.1	16.1

Table 5.A.4 FOUR PLATE FF/C SCRUBBER; OPERATING CONDITIONS AND PERFORMANCE (continued)

Run No.	Gas Inlet Conditions			q' x10	Liquid Temp. (°C)		Scrubber Press Drop (cm W.C.)
	Flow ($\frac{DNm^3}{min}$)	Temp. (°C)	Moisture (% vol.)		In	Out	
68	7.17	71.8	32.8	1.3	22.5	70.0	38.6
69	7.06	70.8	31.7	1.4	17.5	72.0	36.8
70	7.27	71.5	33.2	2.0	17.5	69.5	37.5
71	5.07	77.0	39.4	1.50	23.0	80.6	38.7
72	5.38	77.3	39.9	1.70	26.0	78.3	38.6
73	5.65	76.2	37.7	1.60	23.3	75.0	38.5
74	4.96	80.2	40.7	1.80	23.3	83.8	36.7
75	5.51	76.8	40.5	2.15	19.8	78.0	36.8

Run No.	Particulate							$\overline{Pt}$ (%)
	Load x 10^3 (g/DNm^3)		d_{pg}		σ_g		n_i x 10^{-7}	
	In	Out	In	Out	In	Out		
68	344	63.6	0.99	0.80	2.8	2.6	13.4	18.5
69	191	45.2	0.85	0.83	2.8	2.5	13.6	23.7
70	129	21.6	1.15	0.84	2.6	2.2	15.2	16.8
71	344	48.2	filter run		—	—	—	14.0
72	325	50.1	filter run		—	—	—	15.4
73	297	52.2	1.08	0.93	2.5	2.4	34.5	17.5
74	344	59.9	1.12	0.95	2.1	2.0	12.5	17.4
75	332	41.9	0.99	0.71	2.7	2.4	88.4	12.6

Table 5.A.5. FIVE PLATE FF/C SCRUBBER; OPERATING CONDITIONS AND PERFORMANCE

Plate configuration: Five identical plates with 3.2 mm round perforations. Free area = 9%; Plate active area = $9.29 \times 10^{-2} m^2$

Dust used: Titanium dioxide, -16 mesh, dry dispersed

Cold water introduced on the top plate, flowrate = 0.38 liters/sec

Note: Scrubber inlet and outlet sampled simultaneously with University of Washington Mark III cascade impactors.

Run No.	Gas Inlet Conditions			q' x10²	Liquid Temp. (°C)		Scrubber Press Drop (cm W.C.)
	Flow ($\frac{DNm^3}{min}$)	Temp (°C)	Moisture (% vol.)		In	Out	
76	8.80	30	1.9	-	26	20	35.4
77	7.38	18.5	1.13	-	17	18	33.4
78	8.66	18.5	1.8	-	21	22	20.8

Run No.	Particulate							$\overline{Pt}$ (%)
	Load x 10^3(g/DNm³)		d_{pg}		σ_g		n_i x10^{-6}	
	In	Out	In	Out	In	Out		
76	68	26	1.35	1.12	1.7	1.4	0.5	38.2
77	82.5	26.6	1.30	1.01	1.7	1.8	0.7	32.25
78	138	28.9	1.35	0.86	1.9	1.8	1.7	20.8

Table 5.A.5 FIVE PLATE FF/C SCRUBBER; OPERATING CONDITIONS AND PERFORMANCE (continued)

Run No.	Gas Inlet Conditions			q' x10²	Liquid Temp. (°C)		Scrubber Press Drop (cm W.C.)
	Flow ($\frac{DNm^3}{min}$)	Temp (°C)	Moisture (% Vol.)		In	Out	
79	6.61	47.8	9.87	4.1	14	46.5	33.3
80	7.72	47.0	9.60	4.6	18	47	47.2
81	7.91	46.0	9.66	4.7	21	47	43.2
82	7.72	46.0	9.22	5.3	15	43	42.5
83	7.68	55	15.35	8.3	22	56	48.3
84	6.78	57	15.63	8.7	20	57	40.4
85	7.07	56	15.62	8.9	23	53	45.7

Run No.	Particulate							$\overline{Pt}$ (%)
	Load x 10^3(g/DNm³)		d_{pg}		σ_g		n_i x10^{-6}	
	In	Out	In	Out	In	Out		
79	65.4	6.5	1.49	0.67	2.0	1.7	0.7	10
80	76.0	11.5	1.51	0.96	1.8	1.8	0.5	15.16
81	165.5	29.0	1.32	0.98	1.9	1.7	1.4	17.5
82	125.7	20.7	1.4	0.84	2.0	1.8	1.2	16.76
83	200	33.8	1.3	0.85	1.6	1.6	1.6	16.9
84	186	34.4	1.19	0.98	2.1	1.8	16.7	16.3
85	233	32.1	1.1	0.92	2.1	1.7	8.0	13.7

Table 5.A.5 FIVE PLATE FF/C SCRUBBER; OPERATING CONDITIONS AND PERFORMANCE (continued)

Run No.	Gas Inlet Conditions			q' x10²	Liquid Temp. (°C)		Scrubber Press Drop (cm W.C.)
	Flow ($\frac{DNm^3}{min}$)	Temp (°C)	Moisture (% Vol.)		In	Out	
86	4.92	67.8	24.51	15.30	19	73.5	42.04
87	5.5	66.8	26.0	15.35	18	69	41.9
88	4.44	76.5	32.9	16.0	19	79	42.54
89	4.39	75.25	35.06	19.0	19	78	40.5
90	3.29	79	40.49	16.6	19		45.6
91	3.25	76.5	40.57	18.5	20		42.96

Run No.	Particulate							$\overline{Pt}$ (%)
	Load x 10^3 (g/DNm^3)		d_{pg}		σ_g		n_i x10^{-6}	
	In	Out	In	Out	In	Out		
86	89.7	5.2	2.2	1.15	2.2	2.1	5.6	5.8
87	131	7.2	1.47	0.81	1.5	1.8	1.4	5.5
88	97.2	11.0	1.50	1.39	2.1	2.2	1.13	11.46
89	76.74	3.9	1.48	1.0	2.1	1.8	10.0	5.14
90	159	17	1.51	1.0	1.9	1.6	1.1	10.6
91	227	22.4	1.8	1.06	1.8	1.8	0.92	9.67

Table 5.A.6 FIVE PLATE FF/C SCRUBBER; OPERATING CONDITIONS AND PERFORMANCE

Note: Scrubber operating mode identical as in Table 5.A.5.
Scrubber inlet and outlet sampled simultaneously with Gelman Type A glass fiber filters.

Run No.	Gas Inlet Conditions			q' x10²	Liquid Temp (°C)		Particulate Load x10^3 (g/DNm^3)		Scrubber Press Drop (cm W.C.)	$\overline{Pt}$ (%)
	Flow ($\frac{DNm^3}{min}$)	Temp (°C)	Moisture (% Vol.)		In	Out	In	Out		
92	7.74	47	10.03	4.8	21	46	204	27.4	43.9	13.4
93	7.97	56	15.4	8.3	20	56	322	38.3	48.1	11.9
94	6.81	57	15.6	8.5	20	56	237	34.5	40.4	14.5
95	4.93	68	24.58	9.4	22		126	5.3	40.9	4.2
96	5.76	66.5	25.8	12.3	18	66	129	7.9	39.9	6.13
97	5.49	69	26.4	13.85	20	70	195	36.9	40.9	18.9
98	4.38	75	31.5	17.6	18		175	16.0	41.2	9.1
99	3.23	79	39.6	16.0	17.5		128	16.8	44.2	13.1
100	3.32	76.5	41.6	19.5	20.4		235	17	43.4	7.3

Table 5.A.7. FIVE PLATE FF/C SCRUBBER; OPERATING CONDITIONS AND PERFORMANCE

Plate configuration: Five identical plates with 3.2 mm round perforations. Free area = 9%; Plate active area = 9.29 x $10^{-2} m^2$
Dust used: Titanium dioxide, -16 mesh, dry dispersed
Cold water introduced on the top plate, flowrate = 0.38 liters/sec
Dry steam introduced in the scrubbed gas at scrubber inlet and under plate no. 4 (second from the top)

Run No.	Gas Inlet Conditions			q' x10^2	Liquid Temp. (°C)		Scrubber Press Drop (cm W.C.)
	Flow ($\frac{DNm^3}{min}$)	Temp (°C)	Moisture (% vol.)		In	Out	
101	7.7	42	7.35	6.65	15	43.5	36.9
102	7.65	42	7.43	7.53	16	43.5	45.7
103	6.70	48.5	10.49	9.98	15	54	34.9
104	7.24	48	9.82	11.73	15	52	41
105	7.0	48	9.46	11.8	15.5	50.0	42.3
106	7.48	48	9.15	11.45	16.5	52.5	41.6

Run No.	Particulate							$\overline{Pt}$ (%)
	Load x 10^3 (g/DNm^3)		d_{pg}		σ_g		n_i x10^{-6}	
	In	Out	In	Out	In	Out		
101	81.37	6.08	1.39	0.82	1.8	1.6	0.6	7.5
102	95.20	4.20	1.48	0.83	2.0	1.9	0.9	4.4
103	102.22	4.36	1.48	1.01	2.0	2.1	1.2	4.27
104	69.03	1.96	1.70	1.17	1.7	1.8	0.3	2.84
105	71.3	2.6	1.6	0.84	1.7	1.6	3.36	3.65
106	68.7	1.27						1.8

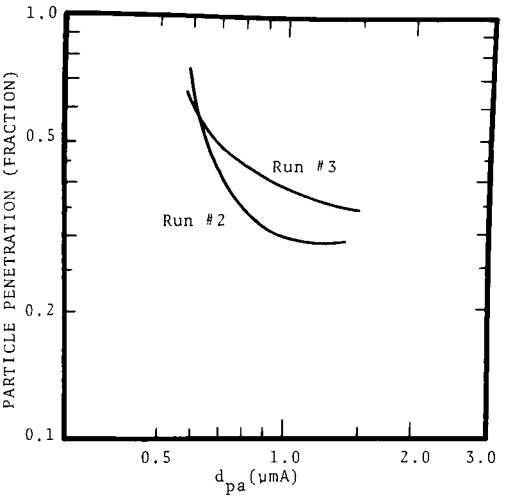

Figure 5.A.1 Particle penetration versus aerodynamic diameter, five plates.

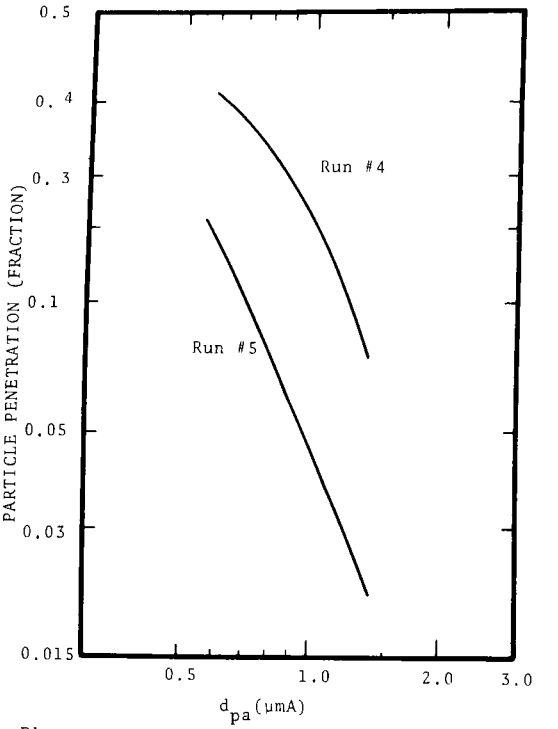

Figure 5.A.2 Particle penetration versus aerodynamic diameter, five plates.

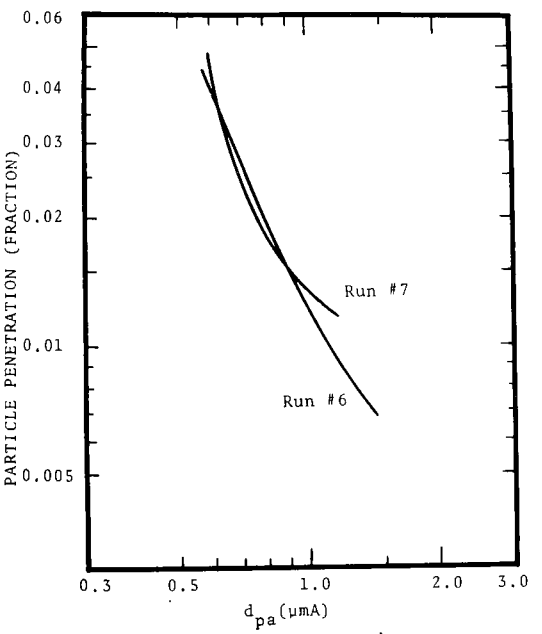

Figure 5.A.3 Particle penetration versus aerodynamic diameter, five plates.

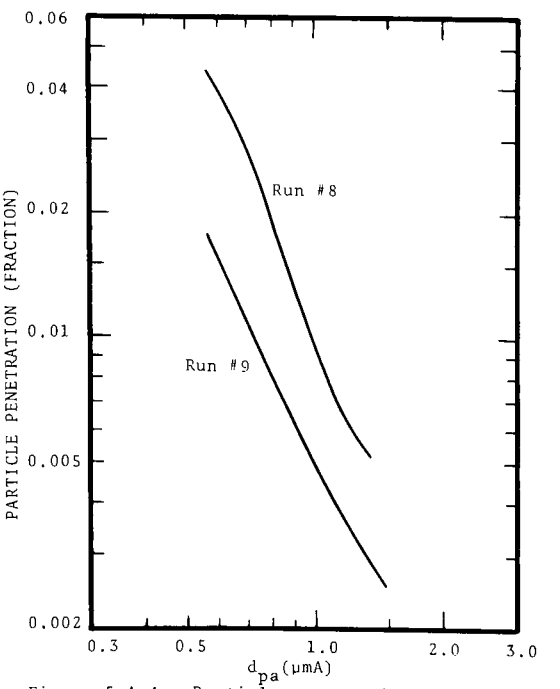

Figure 5.A.4 Particle penetration versus aerodynamic diameter, five plates.

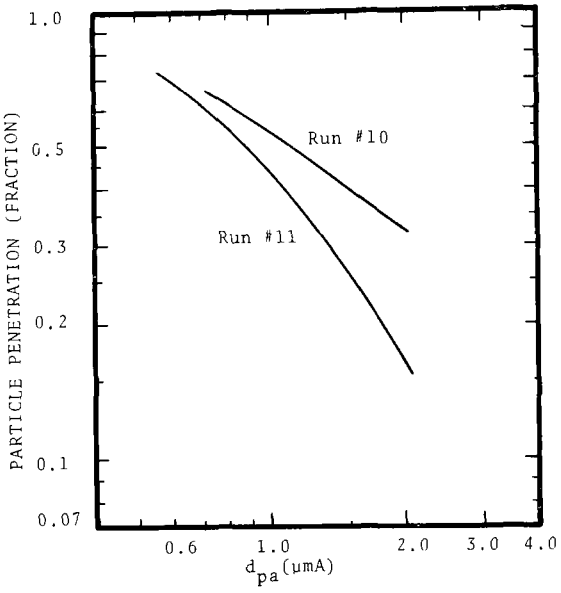

Figure 5.A.5 Particle penetration versus aerodynamic diameter, four plates.

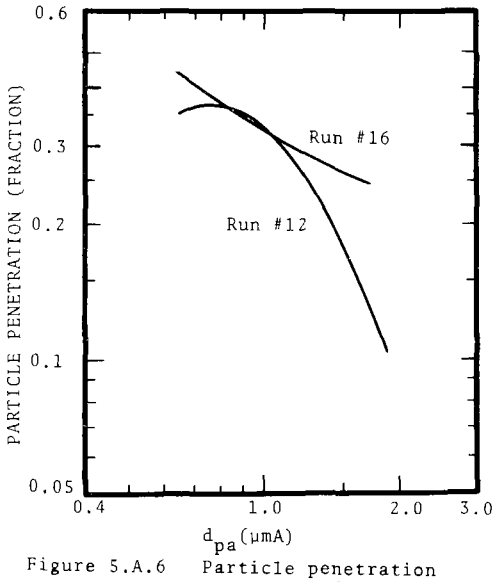

Figure 5.A.6 Particle penetration versus aerodynamic diameter, four plates.

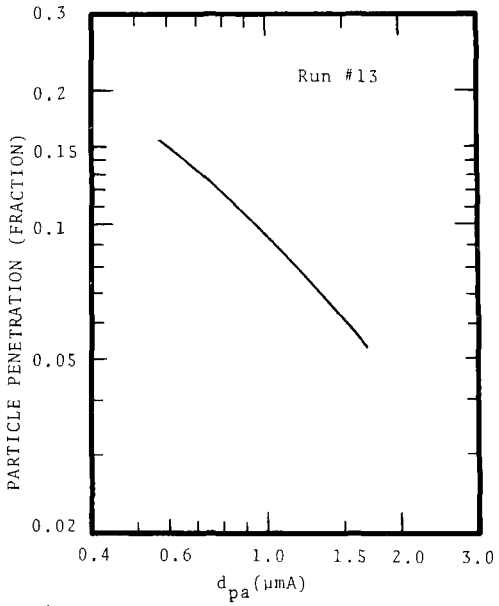

Figure 5.A.7 Particle penetration versus aerodynamic diameter, four plates.

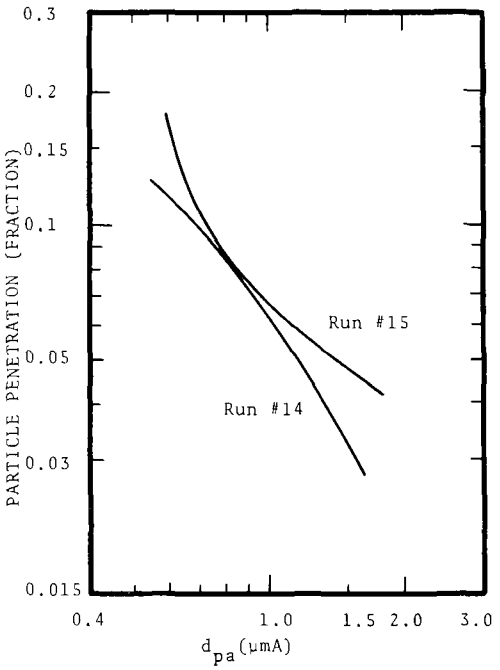

Figure 5.A.8 Particle penetration versus aerodynamic diameter, four plates.

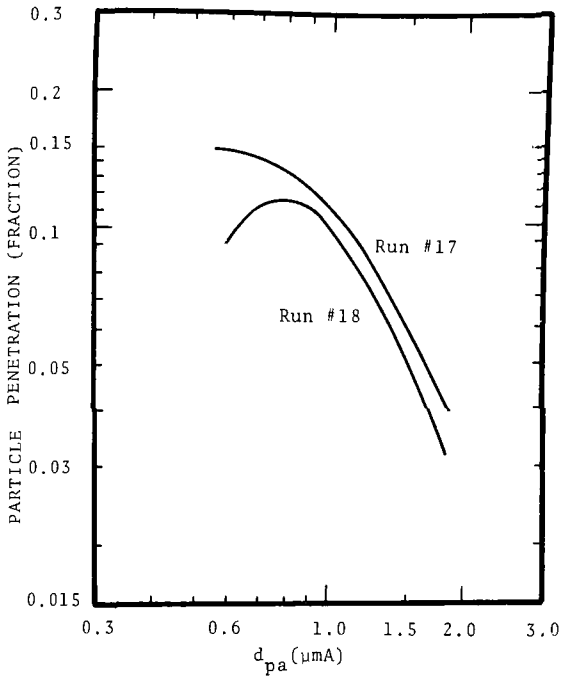

Figure 5.A.9 Particle penetration versus aerodynamic diameter, four plates.

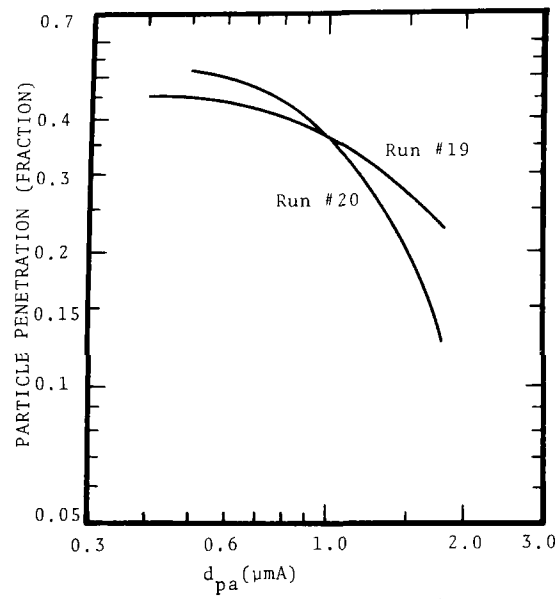

Figure 5.A.10 Particle penetration versus aerodynamic diameter, four plates.

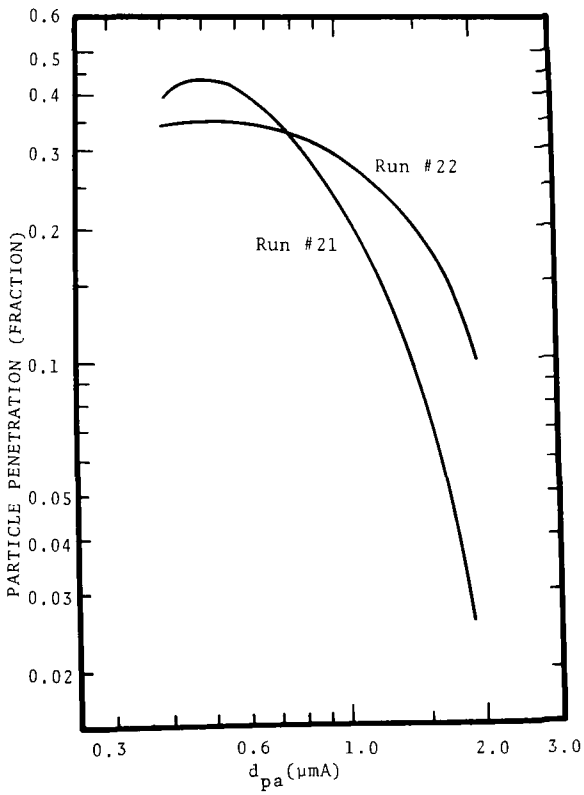

Figure 5.A.11 Particle penetration versus aerodynamic diameter, four plates.

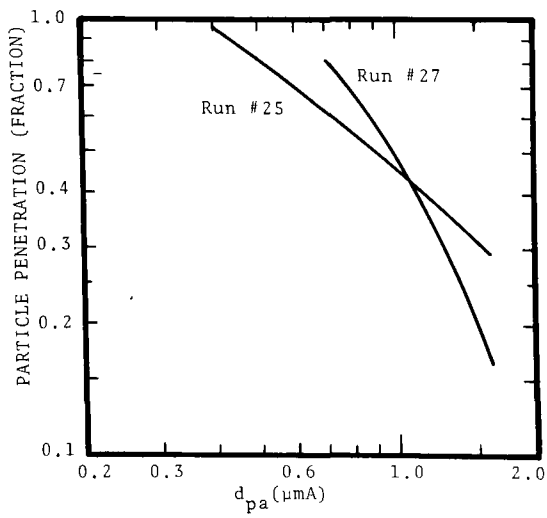

Figure 5.A.12 Particle penetration versus aerodynamic diameter, four plates.

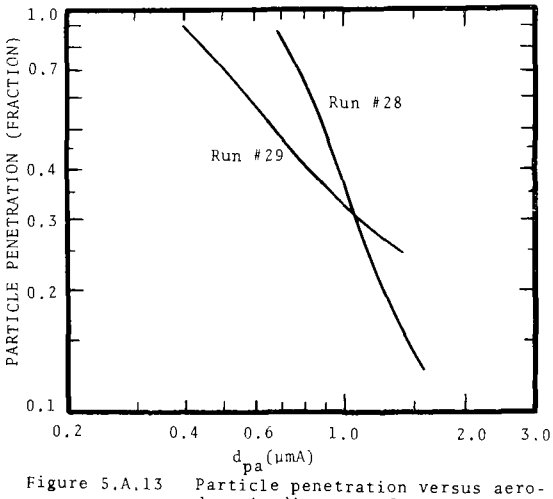

Figure 5.A.13 Particle penetration versus aerodynamic diameter, four plates.

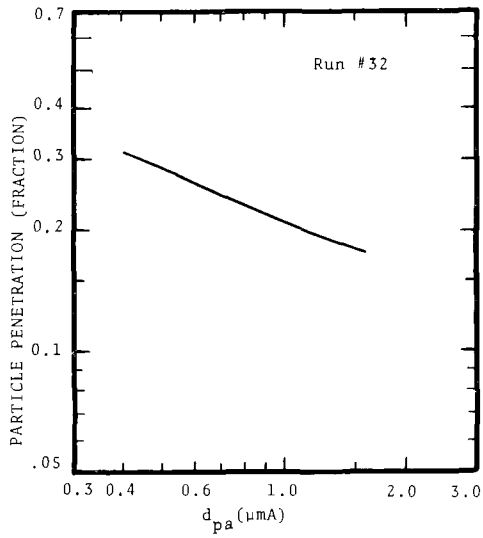

Figure 5.A.14 Particle penetration versus aerodynamic diameter, four plates.

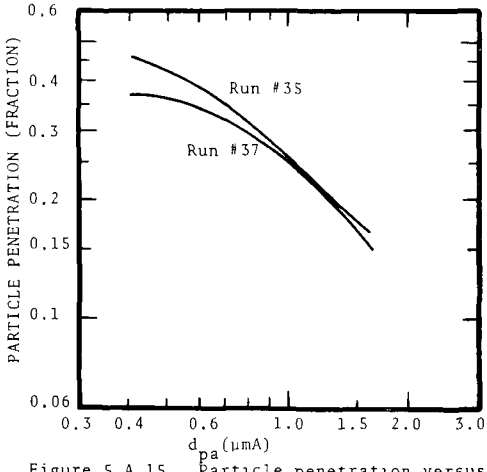

Figure 5.A.15 Particle penetration versus aerodynamic diameter, four plates.

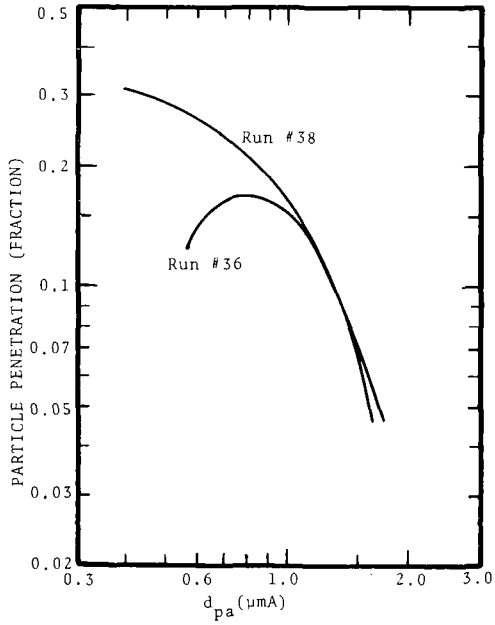

Figure 5.A.16 Particle penetration versus aerodynamic diameter, four plates.

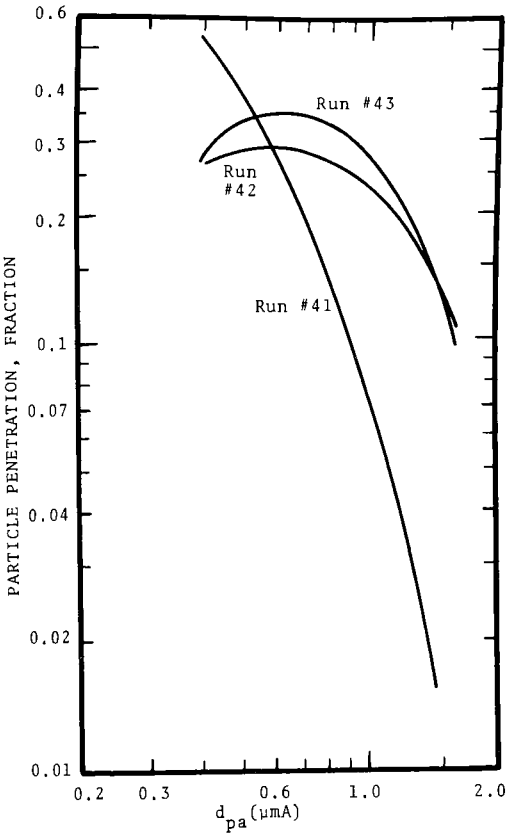

Figure 5.A.17 Particle penetration versus aerodynamic diameter, four plates.

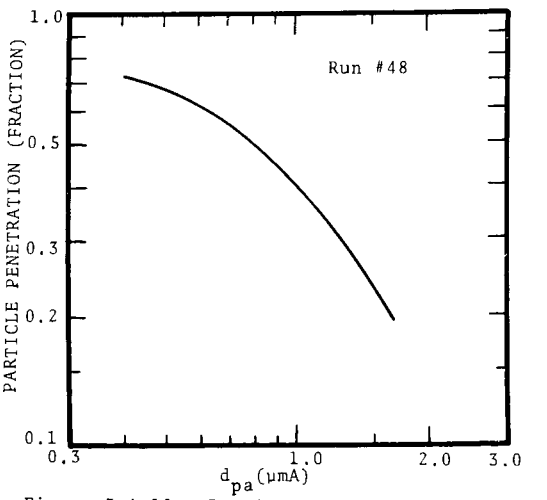

Figure 5.A.18 Particle penetration versus aerodynamic diameter, four plates.

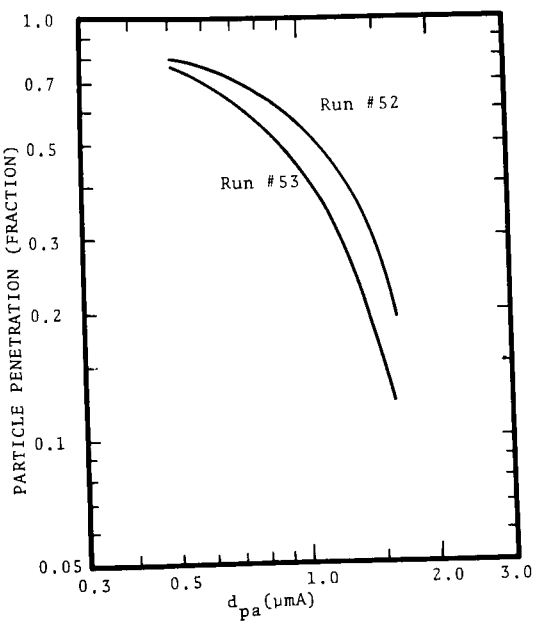

Figure 5.A.19 Particle penetration versus aerodynamic diameter, four plates.

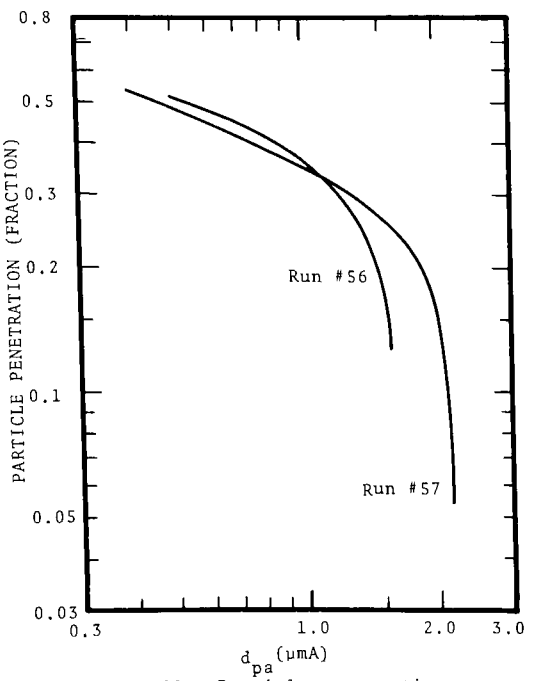

Figure 5.A.20 Particle penetration versus aerodynamic diameter, four plates.

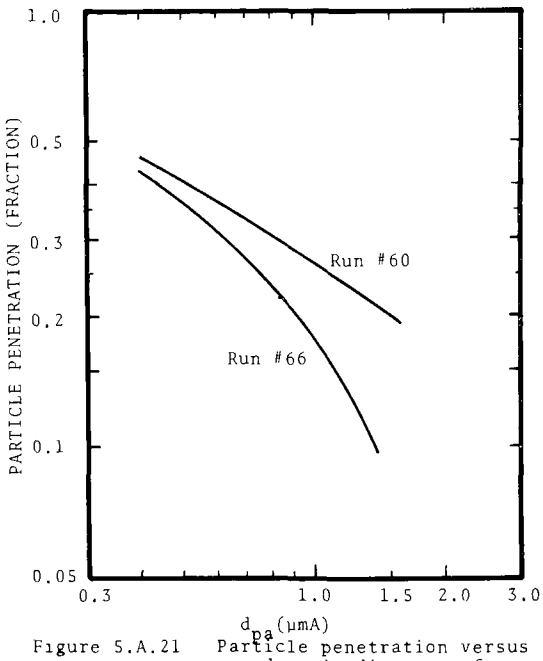

Figure 5.A.21 Particle penetration versus aerodynamic diameter, four plates.

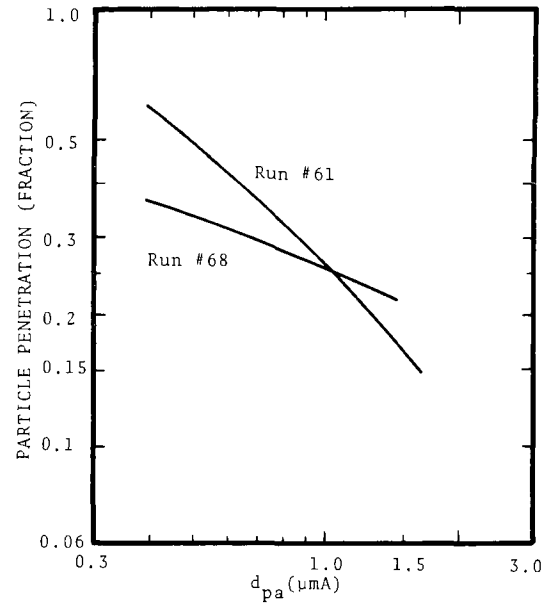

Figure 5.A.22 Particle penetration versus aerodynamic diameter, four plates.

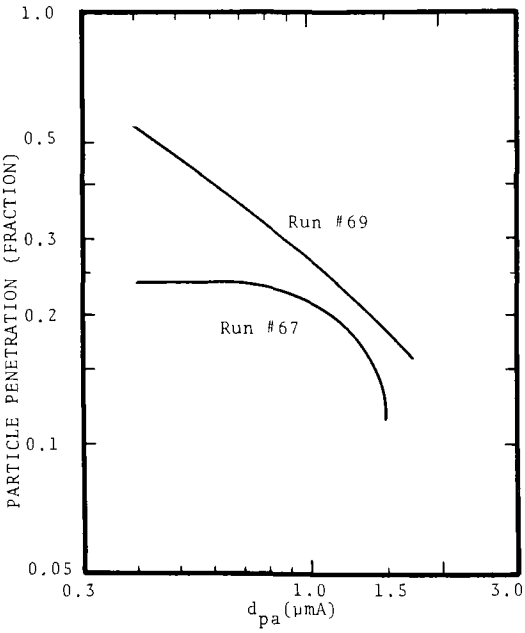

Figure 5.A.23 - Particle penetration versus aerodynamic diameter, four plates.

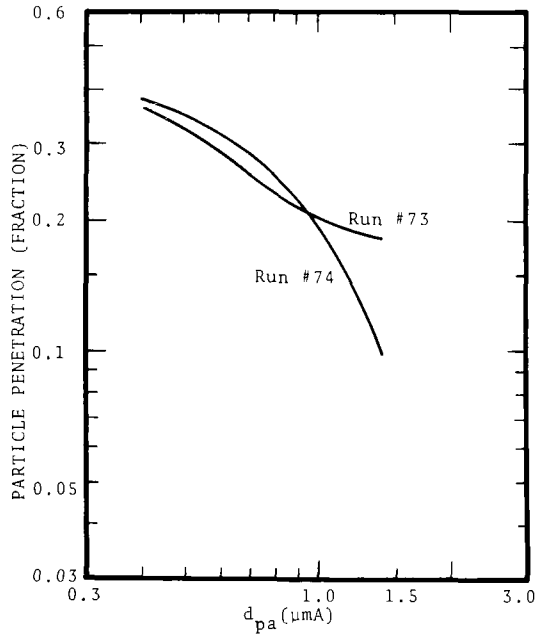

Figure 5.A.24 Particle penetration versus aerodynamic diameter, four plates.

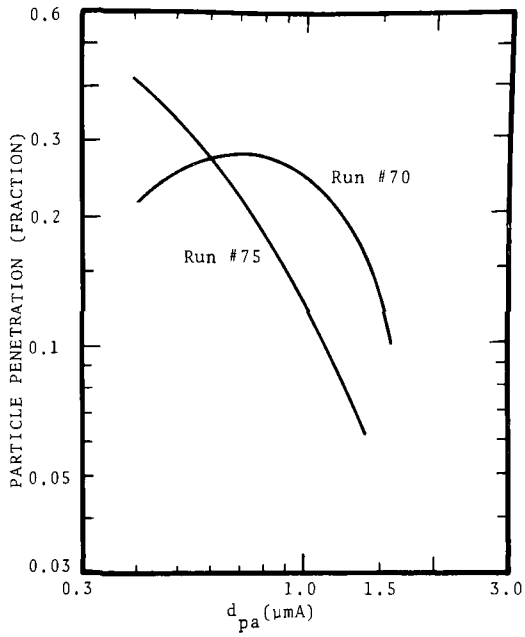

Figure 5.A.25 Particle penetration versus aerodynamic diameter, four plates.

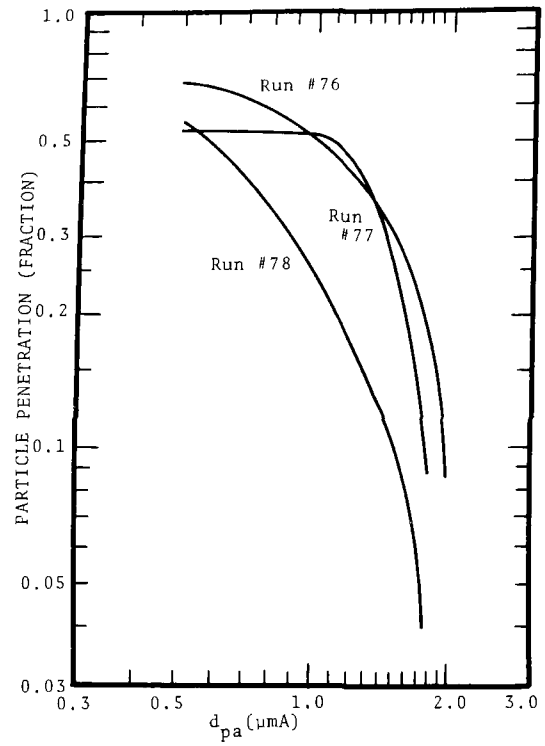

Figure 5.A.26 Particle penetration versus aerodynamic diameter, five plates.

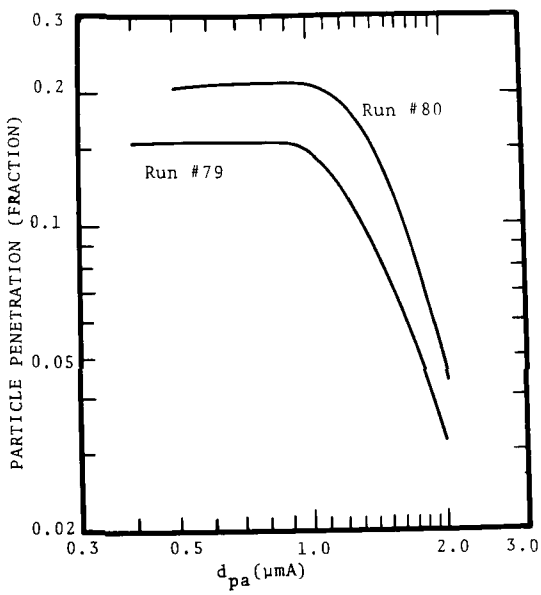

Figure 5.A.27 Particle penetration versus aerodynamic diameter, five plates.

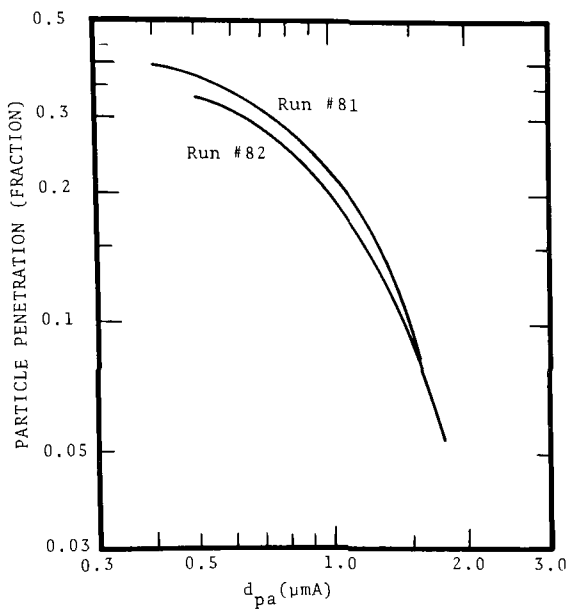

Figure 5.A.28 Particle penetration versus aerodynamic diameter, five plates.

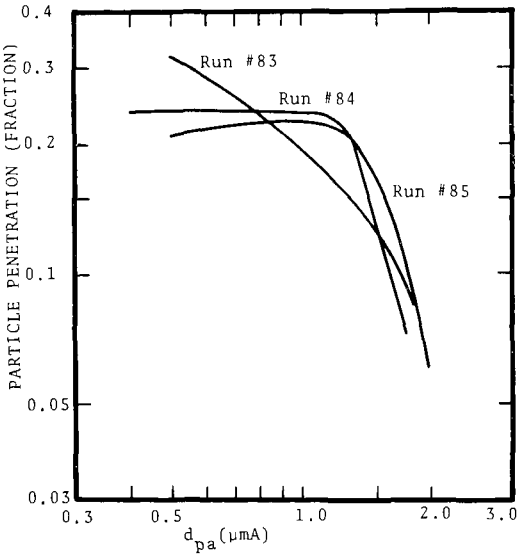

Figure 5.A.29 Particle penetration versus aerodynamic diameter, five plates.

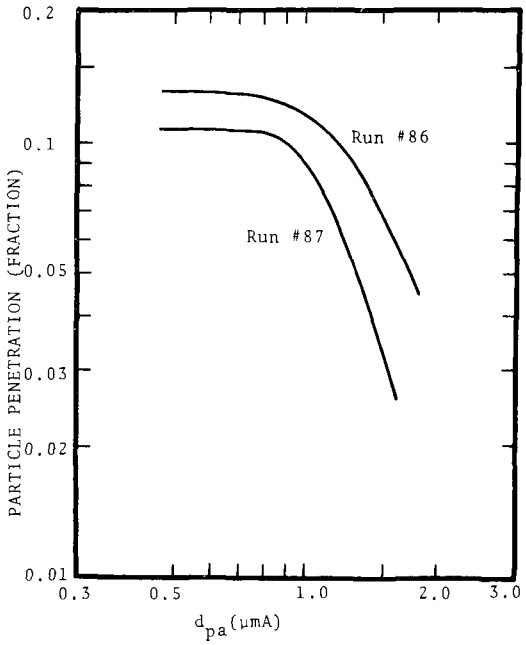

Figure 5.A.30 Particle penetration versus aerodynamic diameter, five plates

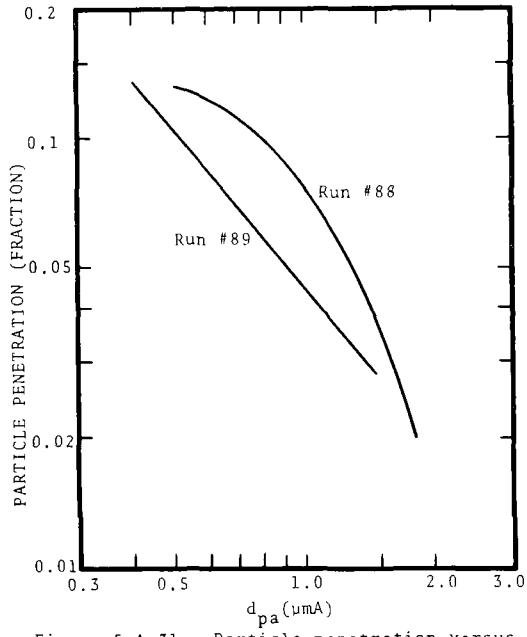

Figure 5.A.31 Particle penetration versus aerodynamic diameter, five plates.

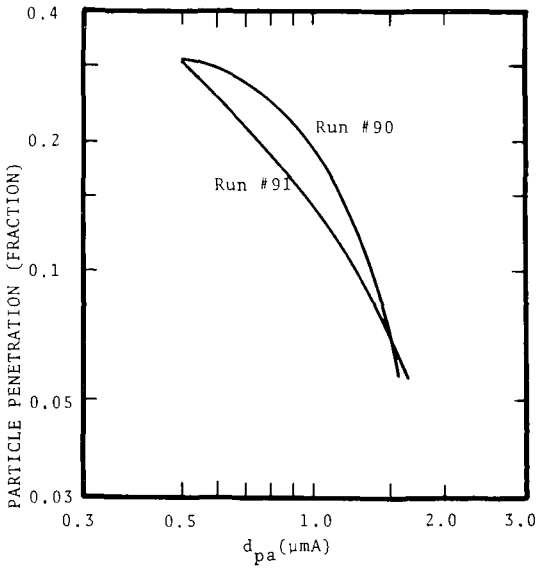

Figure 5.A.32 Particle penetration versus aerodynamic diameter, five plates.

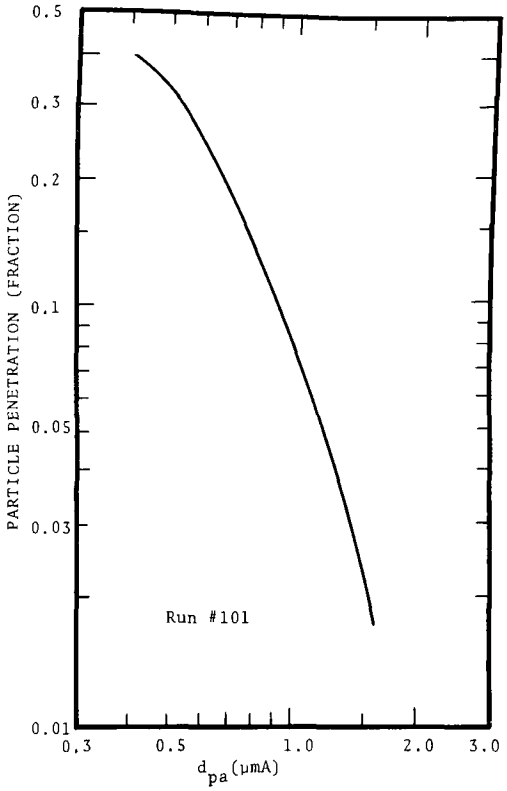

Figure 5.A.33 Particle penetration versus aerodynamic diameter, five plates, steam under #4.

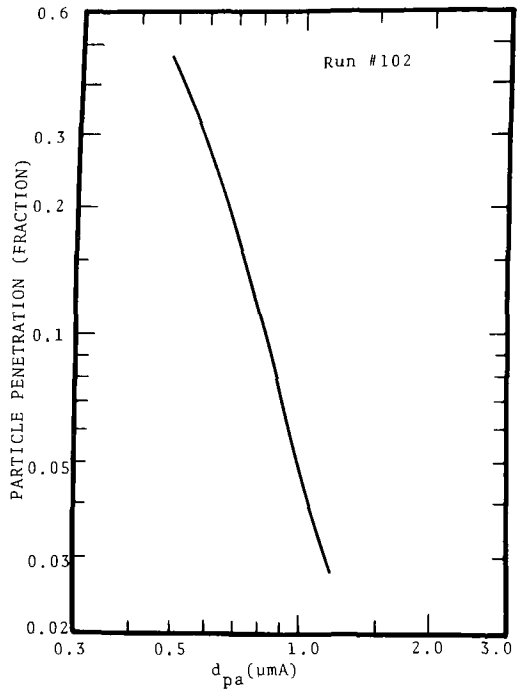

Figure 5.A.34 Particle penetration versus aerodynamic diameter, five plates, steam under #4.

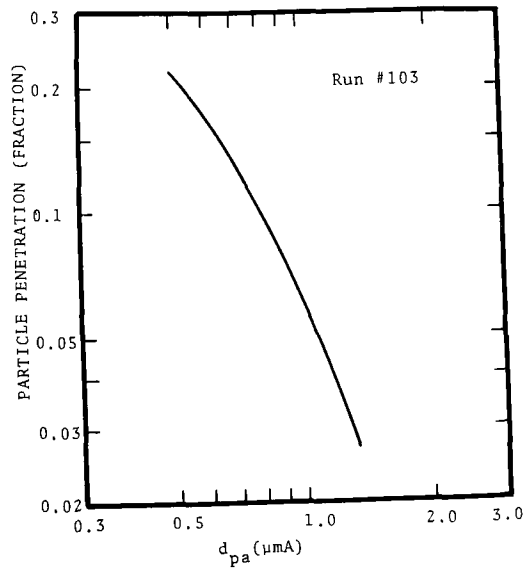

Figure 5.A.35 Particle penetration versus aerodynamic diameter, five plates, steam under #4.

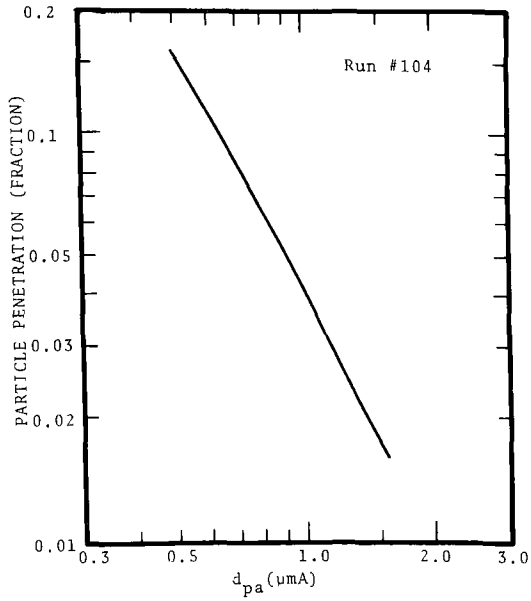

Figure 5.A.36 Particle penetration versus aerodynamic diameter, five plates, steam under #4.

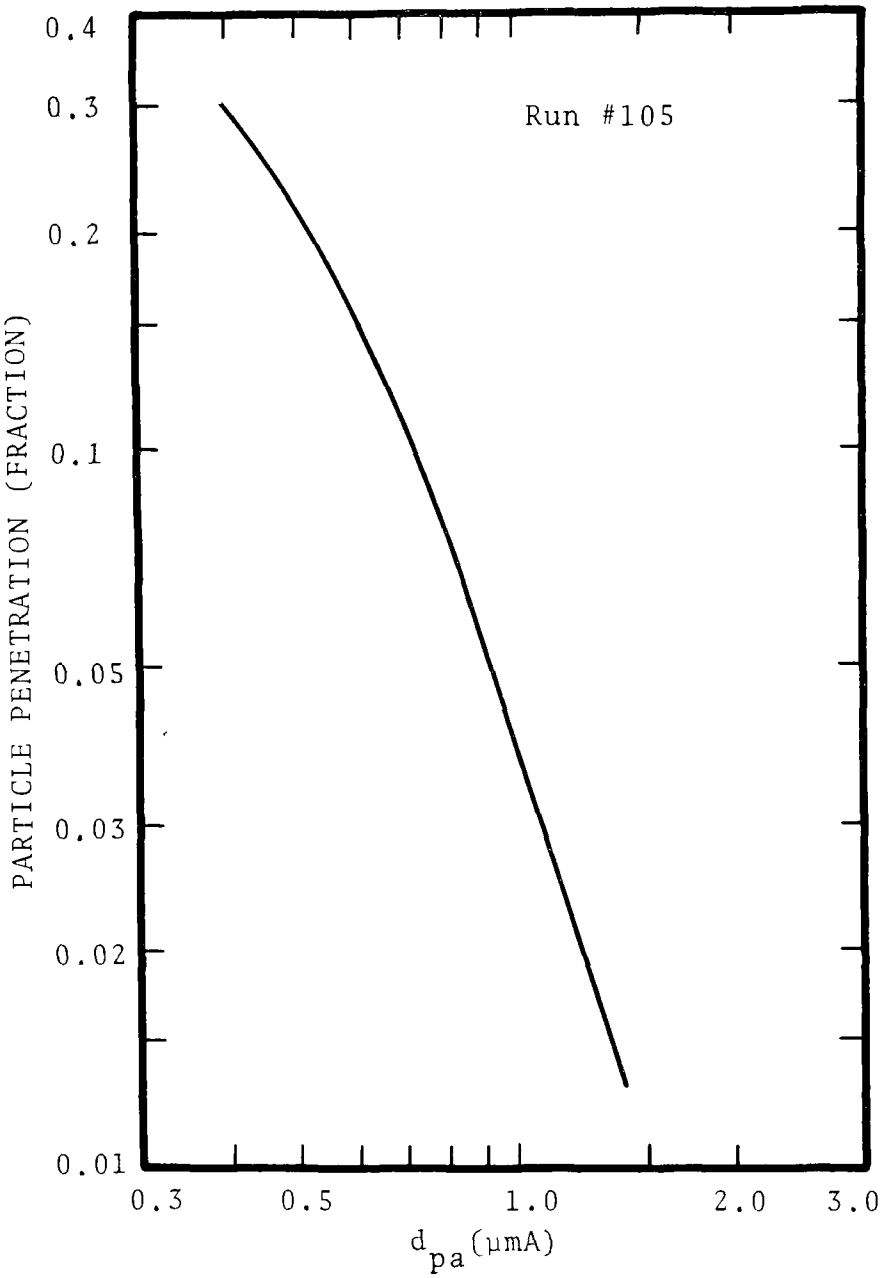

Figure 5.A.37 Particle penetration versus aerodynamic diameter, five plates, steam under #4.

APPENDIX 5.B

HORIZONTAL SPRAY FF/C SCRUBBER OPERATING CONDITIONS AND PERFORMANCE

Table 5.B.1 HORIZONTAL SPRAY SCRUBBER; OPERATING CONDITIONS AND PERFORMANCE

Dust used: Titanium dioxide, -16 mesh
Spray configuration: Cold water sprayed in all of the three sections and drained out through a common outlet. Thus, scrubber operated in the single stage mode.
Inlet water flowrates: First Section: 1.05 liters/sec @ 2.67 kg/cm^2
Second Section: 1.09 liters/sec @ 2.67 kg/cm^2
Third Section: 1.0 liters/sec @ 2.85 kg/cm^2

Run No.	Gas Inlet Conditions				Liquid Temp. (°C)		Scrubber Pressure Differences (cm W.C.)		
	Flow ($\frac{DNm^3}{min}$)	Temp (°C)	Moisture (% vol.)	Relative Humidity (%)	In	Out	ΔP_S	ΔP_E	ΔP_O
1	26.2	14.8	0.6	29	11	9	+0.9	-0.7	+0.2
2	25.9	12.8	0.6	35	11	9	+0.9	-0.6	+0.2
3	25.3	44.5	9.5	92	18	20	+0.9	-1.1	-0.2
4	24.6	45.5	10.0	97	19	24	+0.9	-1.0	-0.1
5	24.8	44.5	9.9	100	19	24	+0.9	-1.0	-0.1
6	20.8	46.3	9.9	92	17	21	+0.9	-1.1	-0.2
7	22.0	49.3	9.6	78	16	21	+0.8	-0.7	+0.1

Run No.	Particulate							q' x10	$\overline{Pt}$
	Load x 10^3 (g/DNm^3)		d_{pg}		σ_g		n_i x10^{-6}		
	In	Out	In	Out	In	Out			
1	192.0	84.0	1.00	1.00	2.0	1.8	6.8	---	43.8
2	180.0	84.0	1.13	1.10	1.9	1.6	4.4	---	46.7
3	106.2	8.3	1.09	0.96	2.0	1.4	3.2	0.5	7.8
4	91.1	11.9	0.99	0.95	1.7	1.6	1.0	0.5	13.1
5	107.6	11.1		Filter run				0.5	10.3
6	138.1	13.3		Filter run				0.5	9.6
7	53.3	3.5		Filter run				0.5	6.6

Note: ΔP_S : pressure difference across the scrubber

ΔP_E : pressure difference across the entrainment separator

ΔP_O : overall pressure difference, ΔP_S ΔP_E ,
positive sign denotes pressure gain while pressure loss is denoted by a negative sign.

Table 5.B.1 (continued)

Run No.	Gas Inlet Conditions				Liquid Temp. (°C)		Scrubber Pressure Differences (cm W.C.)		
	Flow ($\frac{DNm^3}{min}$)	Temp (°C)	Moisture (% vol.)	Relative Humidity (%)	In	Out	ΔP_S	ΔP_E	ΔP_O
8	22.9	57.3	15.6	86	20	25	+0.9	-0.9	---
9	22.8	57.0	15.7	86	21	27	+0.8	-0.9	-0.1
10	23.7	58.0	16.6	86	21	26	+1.0	-1.1	-0.1
11	23.0	57.5	16.8	90	20.5	25.5	+0.9	-0.9	---
12	22.3	64.5	23.3	90	22	40	+1.0	-1.0	---
13	21.9	66.5	25.7	90	22	43	+1.0	-1.0	---
14	22.3	67.0	25.5	89	23	45	+1.0	-1.0	---
15	23.3	67.8	25.5	85	23.5	44.5	+1.1	-1.0	+0.1

Run No.	Particulate							q' x10	$\overline{Pt}$
	Load x 10^3 (g/DNm^3)		d_{pg}		σ_g		n_i x10^{-6}		
	In	Out	In	Out	In	Out			
8	72.8	5.4	1.13	0.96	1.7	1.6	2.0	0.9	7.5
9	110.6	5.1		Filter run				0.9	4.6
10	113.4	5.2	1.31	0.92	1.9	1.6	1.5	1.0	4.5
11	97.3	3.7		Filter run				1.0	3.8
12	58.7	2.3		Filter run				1.5	3.9
13	46.6	2.6	1.36	1.00	2.0	1.6	0.7	1.6	5.6
14	136.0	7.6	1.29	0.90	1.9	1.6	1.9	1.6	5.6
15	154.7	7.5		Filter run				1.7	4.8

Table 5.B.1 (continued)

Run No.	Gas Inlet Conditions				Liquid Temp. (°C)		Scrubber Pressure Differences (cm W.C.)		
	Flow ($\frac{DNm^3}{min}$)	Temp (°C)	Moisture (% vol.)	Relative Humidity (%)	In	Out	ΔP_S	ΔP_E	ΔP_O
16	21.1	68.5	27.7	90	22	46	+0.9	-0.9	---
17	17.2	73.5	34.1	91	25	50	+0.8	-0.7	+0.1
18	17.7	73.0	35.0	95	27	55	+1.0	-0.7	+0.3
19	17.7	74.0	34.0	89	27	52	+0.9	-0.6	+0.3
20	21.3	75.5	28.8	70	22	44	+1.0	-0.9	+0.1
21	19.8	81.5	32.7	62	27	53	+1.0	-0.7	+0.3
22	19.2	79.5	33.6	70	25.5	48	+1.0	-0.8	+0.2
23	22.2	78.0	42.5	95	24	49	+1.0	-0.6	+0.4

Run No.	Particulate							q' x10	$\overline{Pt}$
	Load x 10^3 (g/DNm^3)		d_{pg}		σ_g		n_i x10^{-6}		
	In	Out	In	Out	In	Out			
16	147.0	5.8	1.30	0.94	1.9	1.7	2.0	1.8	3.9
17	77.1	4.3	1.32	1.09	2.4	1.5	3.4	2.5	5.6
18	102.6	3.5		Filter run				2.5	3.4
19	75.8	3.5	1.40	1.05	1.9	1.5	0.8	2.8	4.6
20	105.1	24.7		Filter run				2.0	23.5
21	73.6	17.0	1.21	0.98	2.0	1.7	1.6	2.5	23.1
22	79.8	17.2	1.11	0.97	2.2	1.7	3.7	2.9	21.6
23	68.9	6.13	1.45	0.98	2.2	1.6	1.3	3.6	8.9

Table 5.B.2 HORIZONTAL SPRAY SCRUBBER; OPERATING CONDITIONS AND PERFORMANCE

Dust used: Titanium dioxide, -16 mesh
Spray configuration: Cold water sprayed in all of the three sections and drained out through a common outlet. Thus, scrubber operated in the single stage mode.
Inlet water flow rates: First section - 1.05 ℓ/sec @ 2.67 Kg/cm²
Second section - 1.09 ℓ/sec @ 2.67 Kg/cm²
Third section - 1.0 ℓ/sec @ 2.85 Kg/cm²

Run No.	Gas Inlet Conditions				Liquid Temp. (°C)		Scrubber Pressure Differences (cm W.C.)		
	Flow ($\frac{DNm^3}{min}$)	Temp (°C)	Moisture (% vol.)	Relative Humidity (%)	In	Out	ΔP_S	ΔP_L	ΔP_O
24	23.7	10	0.76	71	8	9.5	0.8	1.0	-0.2
25	23.0	12	1.0	68	8	9.5	0.8	1.0	-0.2
26	23.9	11.5	1.1	96	8	9.5	0.8	1.0	-0.2
27	24.2	11	1.4	77	8	9.5	0.8	1.0	-0.2
28	24	11	1.1	77	9	10.5	0.8	1.0	-0.2
29	23	46	10.1	95	16	23.5	0.8	0.9	-0.1
30	22.8	45.5	10.3	97	15.5	21.5	0.8	0.9	-0.1
31	23	45	10	100	14.5	22.5	0.8	1.0	-0.2

Run No.	Particulate								
	Load x 10^3 (g/DNm^3)		d_{pg}		σ_g		n_i x10^{-6}	q' x10	$\overline{Pt}$
	In	Out	In	Out	In	Out			
24	122.4	47.43						--	0.39
25	52.3	21.7	1.2	1.02	1.7	1.6	0.6	--	0.42
26	97.4	37.8						--	0.38
27	98.4	41.6	1.07	1.04	1.8	1.7	1.9	--	0.42
28	106	46.6	1.05	0.96	1.8	1.7	2.3	--	0.44
29	90.2	9.41	1.2	1.06	1.9	1.6	1.5	0.48	0.10
30	104.0	9.47						0.50	0.92
31	100	11.9	1.06	1.0	1.8	1.7	1.9	0.50	0.12

Table 5.B.2 (continued)

Run No.	Gas Inlet Conditions				Liquid Temp. (°C)		Scrubber Pressure Differences (cum W.C.)		
	Flow ($\frac{DNm^3}{min}$)	Temp (°C)	Moisture (% vol.)	Relative Humidity (%)	In	Out	ΔP_S	ΔP_L	ΔP_O
32	22.1	56	17.3	97	16	28	0.8	0.8	0
33	21.9	57	17.4	90	18	31.5	0.8	0.8	0
34	21.7	56	16.4	95	22	34	0.9	0.9	0
35	20.7	66	26.04	95	23	38	0.8	0.8	0
36	20.3	65.5	26.9	100	19	38	0.8	0.8	0
37	19.5	82.5	36.3	66	23	49	0.9	0.8	0.1
38	18.8	73.5	1.2	90	24	48.8	0.8	0.8	0
39	19.6	84.5	35.1	60	22	47.5	0.9	0.7	0.2
40	19.6	84.5	36	57	22	47.5	0.9	0.7	0.2

Run No.	Particulate								
	Load x 10^3 (g/DNm^3)		d_{pg}		σ_g		n_i x10^{-6}	q' x10	$\overline{Pt}$
	In	Out	In	Out	In	Out			
32	133	6.02	1.23	0.9	1.9	1.9	2.0	1.01	0.045
33	128	5.98	----	Filter	Run	---	------	0.97	0.047
34	101	9.29	1.04	0.84	1.5	1.5	1.3	1.01	0.092
35	121.0	8.59	1.01	0.79	1.6	1.7	1.9	1.9	0.071
36	158.0	6.37	----	Filter	Run	---	------	1.75	0.040
37	131.0	22.4	1.06	0.88	1.8	1.7	3.1	2.20	0.17
38	128.4	10.0	1.21	0.77	1.9	1.62	2.1	2.45	0.078
39	146.0	22.1	1.16	0.96	1.8	1.5	2.3	2.65	0.15
40	144.0	22.1	----	Filter	Run	---	------	2.27	0.15

Table 5.B.3. HORIZONTAL SPRAY SCRUBBER; OPERATING CONDITIONS AND PERFORMANCE

Dust used: Titanium dioxide, -16 mesh
Spray configuration: Scrubber operated in single stage mode. The number of nozzles was decreased to obtain the lower water flowrates, maintaining the small spray drop diameter
Inlet water flowrates: 0.76 ℓ/sec in each section

Run No.	Gas Inlet Conditions				Liquid Temp. (°C)		Scrubber Pressure Differences (cm W.C.)		
	Flow ($\frac{DNm^3}{min}$)	Temp (°C)	Moisture (% vol.)	Relative Humidity (%)	In	Out	ΔP_S	ΔP_E	ΔP_O
41	23.37	11	.77	56	10.5	10.1	0.8	-1.0	-0.2
42	22.32	45	10.0	100	18.4	26.4	0.7	-0.9	-0.2
43	22.2	45	9.8	97	14.8	12.5	0.7	-0.9	-0.2
44	22.4	46	10.1	94	13.9	22.7	0.7	-0.8	-0.2
45	21.7	56	16.5	95	18.8	31.3	0.8	-0.8	---
46	22.0	57	16.9	95	18.5	31.3	0.8	-0.8	---
47	22.1	56	16.9	98	18.1	30.8	0.8	-0.8	---
48	20.8	66	25.6	95	20.6	40.0	0.8	-0.8	---
49	20.4	68	26.7	91	22.0	42.5	0.8	-0.8	---
50	20.5	66	26.8	98	21.8	41.3	0.8	-0.8	---

Run No.	Particulate							q' x10	$\overline{Pt}$
	Load x 10^3 (g/DNm^3)		d_{pg}		σ_g		n_i x10^{-6}		
	In	Out	In	Out	In	Out			
41	72.3	20.2	1.5	.82	2.9	1.5	1.0	---	27.9
42	77.1	9.7	.78	.64	2.0	1.7	7.7	.48	12.6
43	99.8	11.5	.94	.85	1.8	1.6	2.9	.49	11.5
44	121.5	10.1	----	Filter Run	----	------		.52	8.3
45	72.4	4.1	1.05	1.05	1.6	1.6	1.11	.94	5.7
46	84.2	2.6	1.1	.9	1.8	1.7	1.73	.98	3.0
47	97.8	5.2	----	Filter Run	----	------		.99	5.3
48	66.4	2.8	.92	1.1	1.6	2.2	1.5	1.66	4.25
49	161.9	4.8	----	Filter Run	----	------		1.77	2.95
50	77.2	3.3	.96	.96	1.7	1.7	1.7	1.78	4.27

Table 5.B.4. HORIZONTAL SPRAY SCRUBBER; OPERATING CONDITIONS AND PERFORMANCE

Dust used: Titanium dioxide, -16 mesh
Spray configuration: Scrubber operated in the single stage mode. The lower water flowrates were sprayed through same number of nozzles, thus the spray drops were of larger size.
Inlet water flowrates: 0.76 ℓ/sec in each section

Run No.	Gas Inlet Conditions				Liquid Temp. (°C)		Scrubber Pressure Differences (cm W.C.)		
	Flow ($\frac{DNm^3}{min}$)	Temp (°C)	Moisture (% vol.)	Relative Humidity (%)	In	Out	ΔP_S	ΔP_E	ΔP_O
51	23.7	17	1.4	64	9.6	11.5	0.4	-0.9	-0.5
52	23.7	15	1.2	66	10.4	11.5	0.4	-0.9	-0.5
53	23.8	10	1.1	82	9.6	10.4	0.4	-0.8	-0.4
54	23.7	12	1.1	73	10.4	11.2	0.4	-0.9	-0.5
55	24.6	14	1.0	65	10.4	11.3	0.9	-1.0	-0.1
56	24.3	10	0.9	79	10.4	10.8	0.9	-1.0	-0.1
57	21.9	46	1.4	94	17.2	26.7	0.4	-0.8	-0.4
58	22.1	47	1.3	92	16.9	26.7	0.5	-0.8	-0.3

Run No.	Particulate							q' x10	$\overline{Pt}$
	Load x 10^3 (g/DNm^3)		d_{pg}		σ_g		n_i x10^{-6}		
	In	Out	In	Out	In	Out			
51	91.3	56.2	1.06	1.04	1.8	1.6	2.0	---	61.6
52	60.0	45.1	----	Filter Run	----	------		---	75.2
53	81.3	49.4	----	Filter Run	----	------		---	60.8
54	57.2	39.9	.98	1.03	1.7	1.6	1.3	---	69.7
55	72.8	31.4	1.01	.96	1.8	1.6	1.4	---	43.2
56	77.3	33.8	1.03	.94	1.7	1.6	1.5	---	43.7
57	75.8	16.1	----	Filter Run	----	------		.47	21.2
58	102.9	24	----	Filter Run	----	------		.47	23.3

Table 5.B.4 (continued)

Run No.	Gas Inlet Conditions				Liquid Temp. (°C)		Scrubber Pressure Differences (cm W.C.)		
	Flow ($\frac{DNm^3}{min}$)	Temp (°C)	Moisture (% vol.)	Relative Humidity (%)	In	Out	ΔP_S	ΔP_E	ΔP_O
59	22	47	1.3	92	17.2	25.5	0.5	-0.8	-0.3
60	21.9	47	1.4	95	16.6	21.9	0.4	-0.7	-0.3
61	21.7	57	.56	90	15.6	28.8	0.5	-0.7	-0.2
62	21.4	58	.59	88	16.7	30	0.5	-0.7	-0.2
63	21.5	57	.61	93	16.9	30	0.5	-0.8	-0.3
64	21.3	58	.57	90	16	28.8	0.5	-0.8	-0.3
65	21.5	57	.60	95	14.1	28.1	0.5	-0.8	-0.3
66	20.8	66	.83	91	19.6	41.9	0.5	-0.8	-0.3

Run No.	Particulate								
	Load x 10^3 (g/DNm^3)		d_{pg}		σ_g		n_1 x10^{-6}	q' x10	$\overline{Pt}$
	In	Out	In	Out	In	Out			
59	83.2	25.7	1.07	.91	1.7	1.5	.98	.49	30.9
60	66.6	14.6	1.1	.95	1.8	1.6	1.6	.49	21.9
61	86.7	21.3	1.14	.92	1.6	1.7	1.0	.92	24.5
62	86.6	14.9	----	Filter	Run	----	------	.97	17.2
63	108.6	21.9	1.15	.94	1.7	1.6	1.4	.99	20.2
64	93.8	10.1	1.11	.92	1.7	1.5	1.5	1.0	10.8
65	64.3	7.9	----	Filter	Run	----	------	1.1	12.3
66	94.4	9.3	1.15	.89	1.7	1.5	1.4	1.5	9.8

Table 5.B.4 (continued)

Run No.	Gas Inlet Conditions				Liquid Temp. (°C)		Scrubber Pressure Differences (cm W.C.)		
	Flow ($\frac{DNm^3}{min}$)	Temp (°C)	Moisture (% vol.)	Relative Humidity (%)	In	Out	ΔP_S	ΔP_E	ΔP_O
67	19.9	68	.68	86	18.9	44.4	0.5	-0.8	-0.3
68	20.9	66	.84	95	18.9	42.5	0.5	-0.8	-0.3
69	20.8	67	.62	92	18	40.6	0.5	-0.7	-0.2
70	20.5	67	.62	96	18.3	39.4	0.5	-0.7	-0.2
71	19.4	73	1.2	94	22	49.4	0.6	-0.7	-0.1
72	19.8	73	.8	96	20.8	49.4	0.5	-0.7	-0.2
73	19.3	74	1.2	92	22.3	50.5	0.6	-0.7	-0.1
74	19.1	73	1.1	96	22.2	49.3	0.6	-0.8	-0.2

Run No.	Particulate								
	Load x 10^3 (g/DNm^3)		d_{pg}		σ_g		n_1 x10^{-6}	q' x10	$\overline{Pt}$
	In	Out	In	Out	In	Out			
67	82.7	10.5	1.25	.91	1.7	1.5	.78	1.5	12.7
68	111.2	21.8	----	Filter	Run	----	------	1.7	19.6
69	109.1	10.7	----	Filter	Run	----	------	1.8	9.8
70	115.5	13.8	1.2	.95	1.8	1.6	1.4	1.9	12
71	99.3	13	1.18	.92	1.8	1.6	1.4	2.4	13.1
72	122.6	10.3	1.13	.95	1.8	1.5	2.0	2.5	8.4
73	129.2	12.7	----	Filter	Run	----	------	2.6	9.8
74	117.9	9.7	----	Filter	Run	----	------	2.7	8.2

Table 5.B.5 HORIZONTAL SPRAY SCRUBBER; OPERATING CONDITIONS AND PERFORMANCE

Dust used: Titanium dioxide, -16 mesh
Spray configuration: Scrubber operated in three stage mode. Cold water sprayed into the first section. The drained water of section 1 resprayed into section 2 and the drain of section 2 sprayed into section 3. Thus, the scrubber is operated in co-current scheme.
Spray water flow rates: First Section: 1.05 liters/sec @ 2.67 Kg/cm^2
Second Section: 1.09 liters/sec @ 2.67 Kg/cm^2
Third Section: 1.0 liters/sec @ 2.85 Kg/cm^2

Run No.	Gas Inlet Condition				Liquid Temperature						Scrubber Pressure Differences (cm W.C.)		
	Flow ($\frac{DNm^3}{min}$)	Temp °C	Moisture % vol.	Rel. %Hum.	1st Section		2nd Section		3rd Section				
					In	Out	In	Out	In	Out	ΔP_S	ΔP_E	ΔP_O
75	24.1	17	0.13	42	12.5	12.5	12.5	11.5	13	11.5	0.8	1.0	-0.2
76	24.4	21	0.88	60	13	13	13	12	13.5	11.8	0.9	1.0	-0.1
77	24.4	23	2.7	92	13.5	13.5	13.5	12	14.5	12	0.8	1.0	-0.2
78	24.4	25	2.7	95	14.5	14.5	12	12.5	15.3	12.5	0.8	1.0	-0.2
79	24.7	18.5	0.5	22	10	10	10.5	9	10.5	8	0.9	1.0	-0.1

Run No.	Particulate								
	Loadx10^3 (g/DNm^3)		d_{pg}, µmA		σ_g		$n_i \times 10^{-6}$	$q' \times 10$	$\overline{Pt}$
	In	Out	In	Out	In	Out			
75	223.1	84.1	0.95	1.0	2	1.6	5.1	0	0.38
76	251.2	100.3	---------- Filter -- Run ----------					0	0.40
77	245.2	85.6	1.0	2.1	2.1	1.6	3.9	0	0.35
78	242.1	82.19	---------- Filter -- Run ----------					0	0.34
79	189.9	82.1	1.1	1.2	2	1.8	4.7	0	0.43

Note: ΔP_S: Pressure difference across the scrubber
ΔP_E: Pressure difference across the entrainment separator
ΔP_O: Overall pressure difference, $\Delta P_S - \Delta P_E$, positive sign denotes pressure gain while pressure loss is denoted by a negative sign.

Table 5.B.5 (continued)

Run No.	Gas Inlet Condition				Liquid Temperature						Scrubber Pressure Differences (cm W.C.)		
	Flow ($\frac{DNm^3}{min}$)	Temp °C	Moisture % vol.	Rel. %Hum.	1st Section		2nd Section		3rd Section				
					In	Out	In	Out	In	Out	ΔP_S	ΔP_E	ΔP_O
80	23.3	46	10	95	15.5	24.5	20.5	25.5	25.5	25.5	0.9	0.9	0
81	23.2	45	9.7	97	12.5	22.5	18.5	23.5	23.5	23.5	0.8	0.9	-0.1
82	23.0	46.5	9.5	97	14	23.5	21.5	25.0	25.0	25.0	0.8	0.9	-0.1
83	22.8	46	9.7	95	18.5	26.5	24	28	28.5	28	0.9	0.9	0
84	22.3	56.5	17.1	92	18	34.2	28.5	35.5	34.5	35.5	0.8	0.8	0
85	22.3	55.5	16.1	96	18	33	22.5	33.5	32	33.5	0.8	0.8	0
86	22.2	55.5	16.1	96	17	35	27	35.5	32.5	35.5	0.8	0.8	0
87	22.2	55.8	16	92	17	32	28.5	33	33	33	0.9	0.9	0
88	22.5	56.5	16.3	92	17	33	19.5	34	31.5	33.5	0.9	0.9	0

Run No.	Particulate								
	Loadx10^3 (g/DNm^3)		d_{pg}, µmA		σ_g		$n_i \times 10^{-6}$	$q' \times 10$	$\overline{Pt}$
	In	Out	In	Out	In	Out			
80	152.0	22.3	1.3	0.87	2.0	1.5	2.4	0.46	0.147
81	196	19.6	0.87	0.97	2.2	1.6	22.0	0.45	0.10
82	199.5	22.8	---------- Filter --- Run ----------					0.46	0.114
83	163	20.2	---------- Filter --- Run ----------					0.41	0.124
84	162.2	9.7	---------- Filter --- Run ----------					0.84	0.061
85	207	16.9	1.3	0.94	1.8	1.5	2.1	0.87	0.082
86	161	13	1.2	0.94	1.8	1.5	2.1	0.87	0.081
87	152	13.8	---------- Filter --- Run ----------					0.9	0.091
88	186	15.0	1.2	0.92	1.7	1.6	2.3	0.9	0.081

Table 5.B.5 (continued)

Run No.	Gas Inlet Condition				Liquid Temperature						Scrubber Pressure Differences (cm W.C.)		
	Flow ($\frac{DNm^3}{min}$)	Temp °C	Moisture % vol.	Rel. Hum.	1st Section		2nd Section		3rd Section				
					In	Out	In	Out	In	Out	ΔP_S	ΔP_E	ΔP_O
89	20.1	66	25.6	94	17.5	42.5	34	45.5	41	45.5	0.8	0.7	0.1
90	20.1	65.5	24.2	94	17.5	42	34.5	43	40.5	42.5	0.8	0.8	0
91	19.6	67	27.2	95	17.5	43.5	33	46	40.5	46	0.8	0.7	0.1
92	20.7	67	26.4	92	16.5	41	34.5	40	40	40	0.8	0.8	0
93	18.2	72.5	35.7	100	16.5	53.5	44.5	51.5	51.5	55	0.8	0.7	0.1
94	19	72.5	35.7	95	17	50.5	40.5	48.5	48.5	53	0.8	0.7	0.1
95	18.8	72.5	36.4	100	17	50.5	41	50	50	54.5	0.9	0.9	0
96	18.7	73	33.8	91	17	54	42.5	51	51	55.5	0.9	0.8	0.1

Run No.	Particulate						$n_i \times 10^{-6}$	$q' \times 10$	$\overline{Pt}$
	Loadx10^3 (g/DNm^3)		d_{pg}, µmA		σ_g				
	In	Out	In	Out	In	Out			
89	173	14.7	1.2	0.97	1.8	1.5	2.2	1.35	0.085
90	162	15.1	----------	Filter	--- Run	----------	---------	1.35	0.094
91	158	12.7	1.1	1.05	1.8	1.5	2.6	1.55	0.08
92	120	6.48	1.3	0.95	1.7	1.6	4.1	1.53	0.054
93	154	11.4	----------	Filter	--- Run	----------	---------	2.1	0.074
94	165	9.6	----------	Filter	--- Run	----------	---------	2.26	0.058
95	186	12.4	1.1	0.94	2	1.5	5.4	2.32	0.067
96	168	15	1.2	0.9	1.8	1.6	2.8	2.07	0.089

Table 5.B.6 HORIZONTAL SPRAY SCRUBBER; OPERATING CONDITIONS AND PERFORMANCE

Dust used: Titanium dioxide, -16 mesh
Spray configuration: Scrubber operated in three stage mode. Cold water sprayed into the third section and the scrubber operated in counter-current scheme.
Spray water flow rates: First section: 1.05 ℓ/sec @ 2.67 kg/cm²
Second section: 1.09 ℓ/sec @ 2.67 kg/cm²
Third section: 1.0 ℓ/sec @ 2.85 kg/cm²

Run No.	Gas Inlet Condition				Liquid Temperature						Scrubber Pressure Differences (cm W.C.)		
	Flow ($\frac{DNm^3}{min}$)	Temp °C	Moisture % vol.	Rel. %Hum.	1st Section		2nd Section		3rd Section				
					In	Out	In	Out	In	Out	ΔP_S	ΔP_E	ΔP_O
97	23.4	17.3	10.9	50	7.7	12.0	7.2	11.2	10.1	11.3	0.9	-1.0	-0.2
98	24.0	10.5	10.5	77	10.7	10.4	9.9	10.1	12.5	10.4	0.4	-1.0	-0.6
99	23.4	20	20	41	9.9	11.2	9.9	9.9	11.7	10.9	0.9	-1.0	-0.1
100	23.2	21	21	39	9.2	12.0	9.1	11.7	12.3	12.8	0.8	-1.0	-0.2
101	22.8	23	23	34	9.1	10.7	9.9	9.7	13.2	11.5	0.8	-1.0	-0.2
102	23.2	13	13	54	8.5	9.3	8.9	9.3	12.3	9.6	0.8	-1.0	-0.2

Run No.	Particulate						$n_i \times 10^{-6}$	$q' \times 10$	$\overline{Pt}$
	Loadx10^3 (g/DNm^3)		d_{pg}, µmA		σ_g				
	In	Out	In	Out	In	Out			
97	64.3	28.7	----------	Filter	Run ------	----------	---------	---	44.6
98	60.3	37.1	----------	Filter	Run ------	----------	---------	---	61.5
99	100.6	44.5	0.98	0.92	1.8	1.5	2.6	---	44.2
100	122.8	51.3	----------	Filter	Run ------	----------	---------	---	41.7
101	95.3	41.4	0.96	0.9	1.7	1.5	2.0	---	43.4
102	79.4	36.0	0.96	0.88	1.7	1.5	1.7	---	45.3

Table 5.B.6 (continued)

Run No.	Gas Inlet Condition				Liquid Temperature						Scrubber Pressure Differences (cm W.C.)		
	Flow ($\frac{DNm^3}{min}$)	Temp °C	Moisture % vol.	Rel. Hum.	1st Section		2nd Section		3rd Section				
					In	Out	In	Out	In	Out	ΔP_S	ΔP_E	ΔP_O
103	23.8	11	1.1	77	18.1	12.8	17.3	12.8	19.7	12.5	0.4	-0.9	-0.5
104	22.3	46	10.0	94	24.5	31.5	22.9	29.0	18.7	26.7	0.8	-1.0	-0.2
105	22.8	46	10.0	94	25.1	29.8	23.5	26.0	17.1	24.3	0.9	-1.1	-0.2
106	22.9	46.5	10.0	92	23.5	31.5	20.8	26.7	14.4	24.0	0.9	-1.0	-0.1
107	22.7	46.5	10.3	95	24.5	30.0	21.9	26.5	18.1	24.3	0.9	-1.0	-0.1
108	22.5	47.5	10.2	89	25.9	30.5	20.8	26.5	13.3	22.9	0.9	-1.0	-0.1
109	21.7	56.5	16.0	90	30.5	43.8	26.3	37.5	14.4	30	0.8	-0.9	-0.1
110	21.5	56	16.4	95	31.3	44.4	27.5	38.8	16.7	31.3	0.9	-0.9	0.0
111	21.4	56.5	16.8	95	30.6	43.8	27.5	40.0	17.3	32.5	0.9	-1.0	-0.1

Run No.	Particulate								
	Loadx10^3 (g/DNm^3)		d_{pg}, µmA		σ_g		$n_i \times 10^{-6}$	$q' \times 10$	$\overline{Pt}$
	In	Out	In	Out	In	Out			
103	76.4	49.8	0.96	1.0	1.8	1.6	2.1	---	65.2
104	106.3	29.8	0.94	0.84	1.6	1.5	2.4	0.47	28.0
105	68.4	16.0	1.0	0.82	1.6	1.5	1.2	0.47	23.4
106	107.8	17.9	----------	--- Filter	Run	----------	----------	0.48	16.6
107	110.6	31.0	----------	--- Filter	Run	----------	----------	0.50	28.0
108	68.3	11.5	0.94	0.92	1.7	1.6	1.7	0.52	16.8
109	96.6	13.6	1.1	0.82	1.6	1.6	1.2	0.87	14.1
110	127.5	22.4	----------	--- Filter	Run	----------	----------	0.9	17.5
111	133.4	19.1	----------	--- Filter	Run	----------	----------	0.9	14.3

Table 5.B.6 (continued)

Run No.	Gas Inlet Condition				Liquid Temperature						Scrubber Pressure Differences (cm W.C.)		
	Flow ($\frac{DNm^3}{min}$)	Temp °C	Moisture % vol.	Rel. Hum.	1st Section		2nd Section		3rd Section				
					In	Out	In	Out	In	Out	ΔP_S	ΔP_E	ΔP_O
112	21.1	56.5	16.9	95	31.9	41.3	30.0	38.3	20.0	35.6	0.9	-0.9	-0.1
113	21.5	57.5	17.2	93	33.1	42.5	30.0	38.8	18.7	30.6	0.9	-1.0	0.0
114	20.4	66	26.2	96	43.8	57.2	38.8	53.6	18.7	42.5	0.9	-0.9	-0.1
115	20.8	66	25.5	93	43.8	56.0	38.8	51.1	19.3	41.3	0.9	-0.9	0.0
116	20.1	66	25.6	93	47.0	54.8	40.0	51.1	19.7	40.0	0.9	-0.9	0.0
117	19.9	68	27.3	91	45.6	58.4	42.5	54.8	20.0	43.8	0.9	-0.9	0.0
118	20.2	67.5	26.7	91	45.0	55.4	40.0	51.1	18.7	41.3	0.9	-0.9	0.0
119	19.3	74	34.7	90	52.3	67.0	48.8	62.1	20.7	52.3	0.9	-0.9	0.0
120	19.6	73	36.3	100	50.5	65.7	48.8	63.3	24.0	52.3	0.9	-0.9	0.0

Run No.	Particulate								
	Loadx10^3 (g/DNm^3)		d_{pg}, µmA		σ_g		$n_i \times 10^{-6}$	$q' \times 10$	$\overline{Pt}$
	In	Out	In	Out	In	Out			
112	109.6	19.9	1.03	0.85	1.5	1.5	1.3	0.9	18.2
113	86.8	13.2	1.2	0.82	1.6	1.5	0.7	0.95	15.2
114	154.1	32.6	1.03	0.82	1.7	1.6	2.5	1.5	21.2
115	150.5	23.5	1.1	0.88	1.6	1.5	2.1	1.5	15.6
116	167.6	42.0	----------	--- Filter	Run	----------	----------	1.5	25.1
117	131.0	24.1	1.0	0.86	1.6	1.5	2.6	1.5	18.4
118	140.5	29.8	----------	--- Filter	Run	----------	----------	1.6	21.2
119	129.4	24.3	----------	--- Filter	Run	----------	----------	2.1	18.8
120	169.6	20.0	----------	--- Filter	Run	----------	----------	2.3	11.8

Table 5.B.6 (continued)

Run No.	Gas Inlet Condition				Liquid Temperature						Scrubber Pressure Differences (cm W.C.)		
	Flow ($\frac{DNm^3}{min}$)	Temp °C	Moisture % vol.	Rel. Hum.	1st Section		2nd Section		3rd Section				
					In	Out	In	Out	In	Out	ΔP_S	ΔP_E	ΔP_O
121	18.1	74	36.3	94	47.5	64.5	43.8	60.9	21.3	50.0	0.9	-0.8	0.1
122	19.4	73.5	36.3	96	48.1	64.5	43.8	60.9	21.3	49.9	0.9	-0.9	0.0
123	19.1	71	33.2	98	49.9	63.3	45.6	59.7	16.0	48.8	0.8	-0.8	0.0

Run No.	Particulate								
	Loadx10^3 (g/DNm^3)		d_{pg}, μmA		σ_g		$\mu_i \times 10^{-6}$	$q' \times 10$	$\overline{Pt}$
	In	Out	In	Out	In	Out			
121	135.4	9.0	1.23	0.88	1.8	1.6	1.7	2.5	6.7
122	98.3	12.4	1.12	0.82	1.7	1.5	1.4	2.5	12.6
123	76.8	10.0	1.05	0.8	1.7	1.4	1.2	3.0	13.0

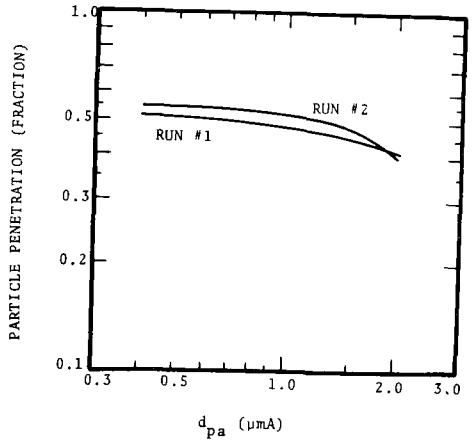

Figure 5.B.1 Particle penetration versus aerodynamic diameter, single stage spray scrubber.

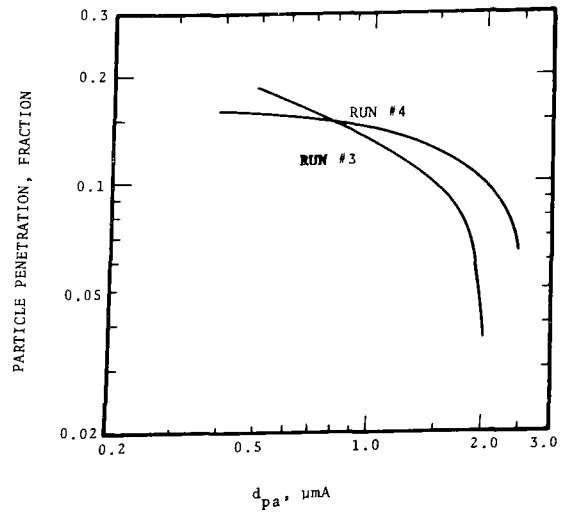

Figure 5.B.2 Particle penetration versus aerodynamic diameter, single stage spray scrubber.

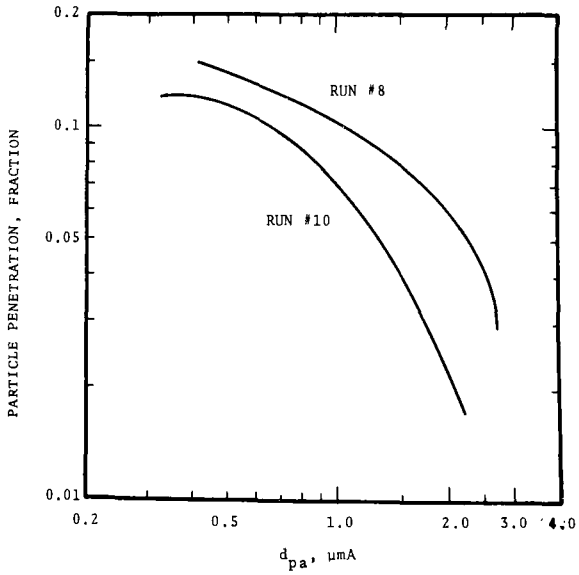

Figure 5.B.3 Particle penetration versus aerodynamic diameter, single stage spray scrubber.

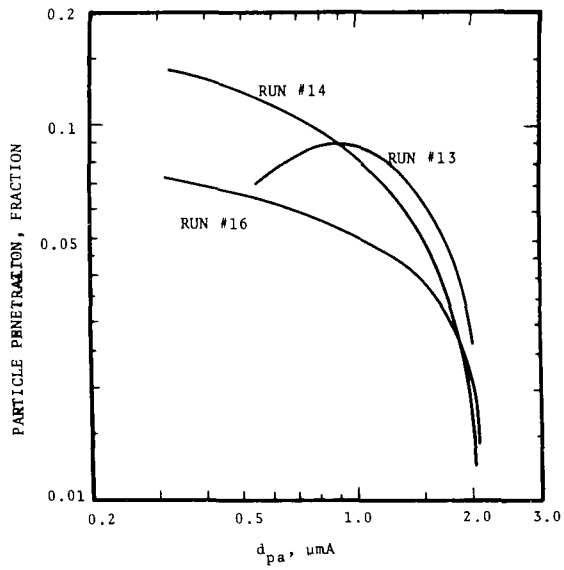

Figure 5.B.4. Particle penetration versus aerodynamic diameter, single stage spray scrubber.

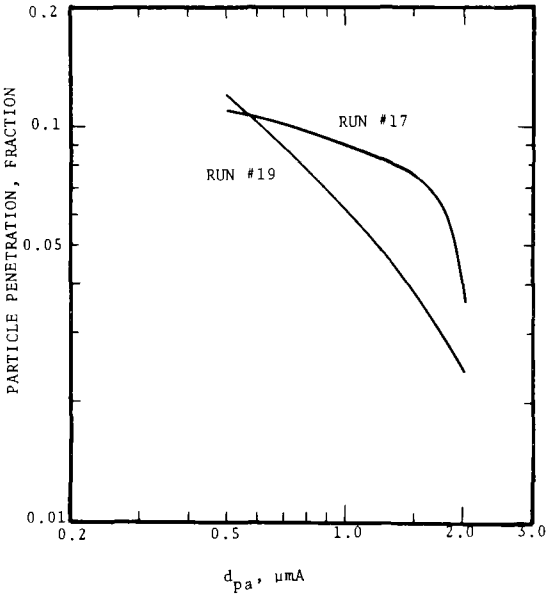

Figure 5.B.5. Particle penetration versus aerodynamic diameter, single stage spray scrubber.

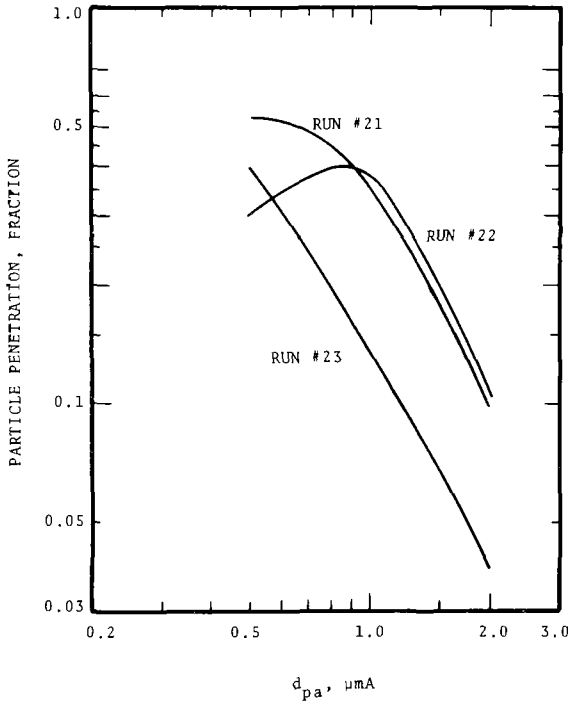

Figure 5.B.6. Particle penetration versus aerodynamic diameter, single stage spray scrubber

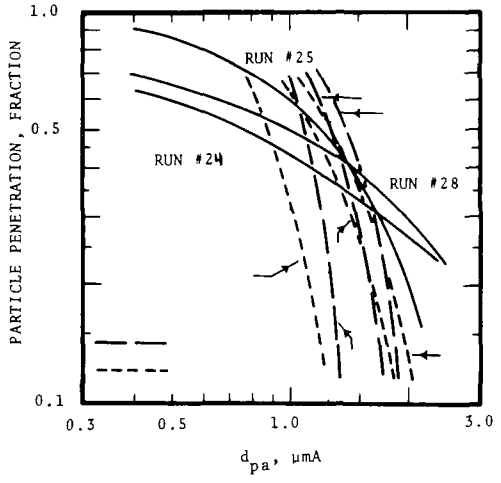

Figure 5.B.7. Particle penetration versus aerodynami diameter, single stage spray scrubber.

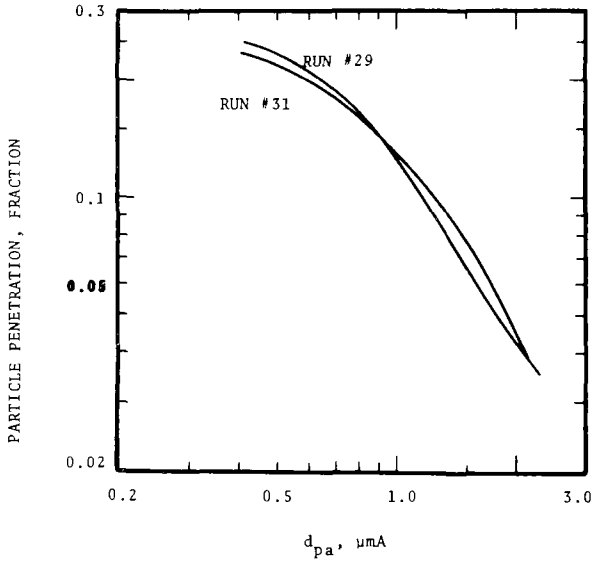

Figure 5.B.8. Particle penetration versus aerodynamic diameter, single stage spray scrubber.

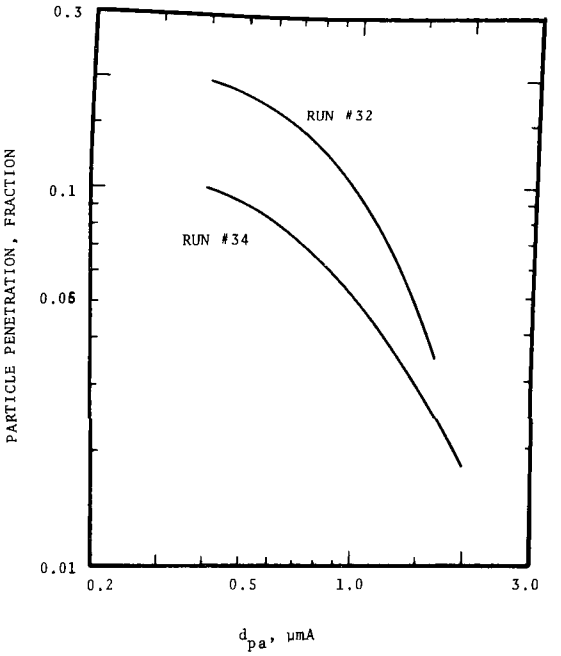

Figure 5.B.9. Particle penetration versus aerodynamic diameter, single stage spray scrubber.

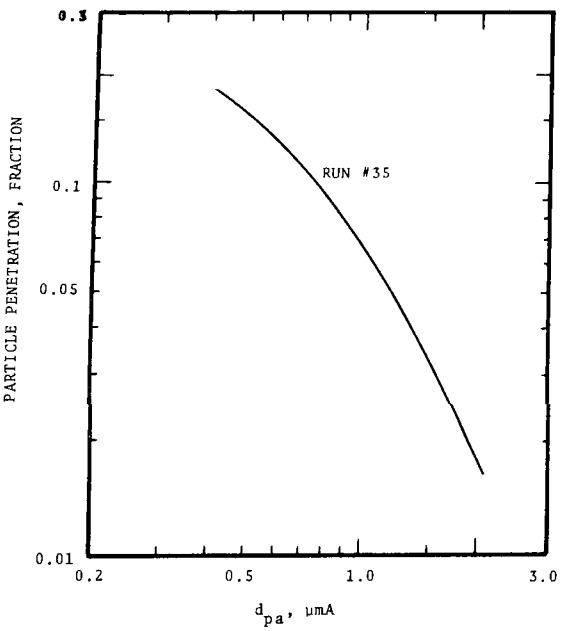

Figure 5.B.10. Particle penetration versus aerodynamic diameter, single stage spray scrubber.

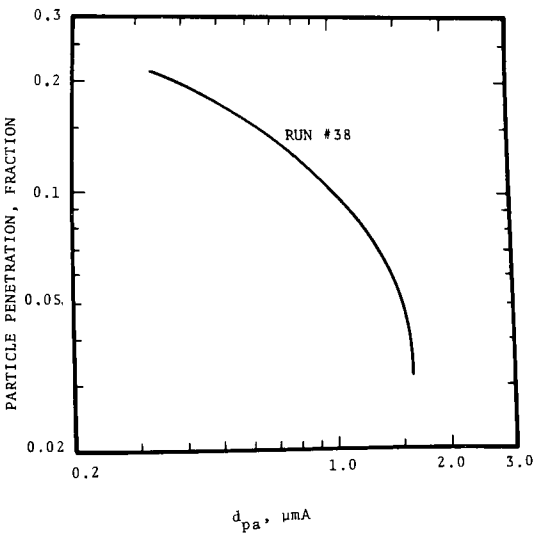

Figure 5.B.11. Particle penetration versus aerodynamic diameter, single stage spray scrubber.

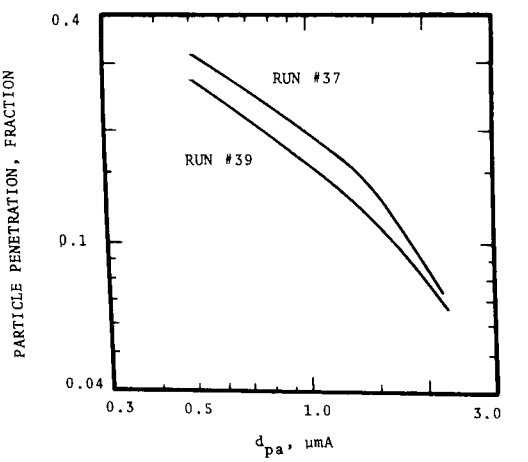

Figure 5.B.12. Particle penetration versus aerodynamic diameter, single stage spray scrubber.

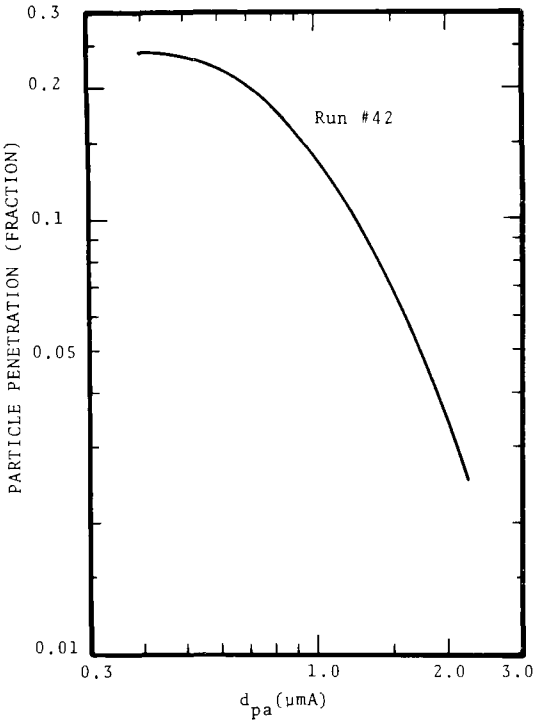

Figure 5.B.13 Particle penetration versus aerodynamic diameter, one stage.

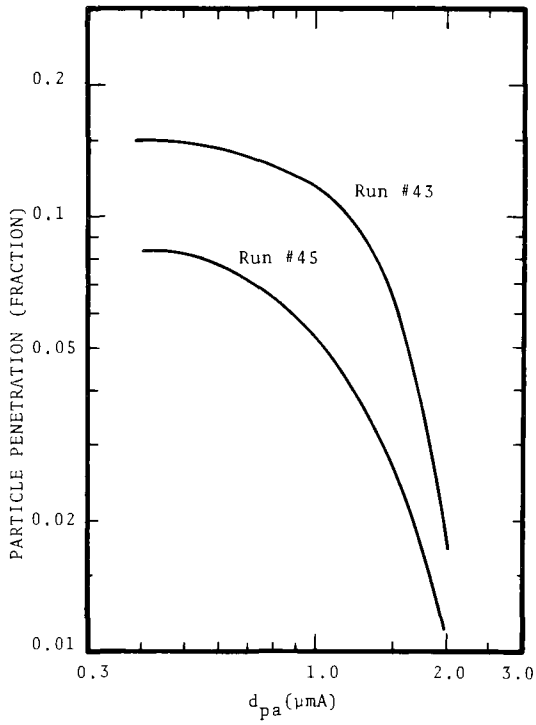

Figure 5.B.14 Particle penetration versus aerodynamic diameter, one stage.

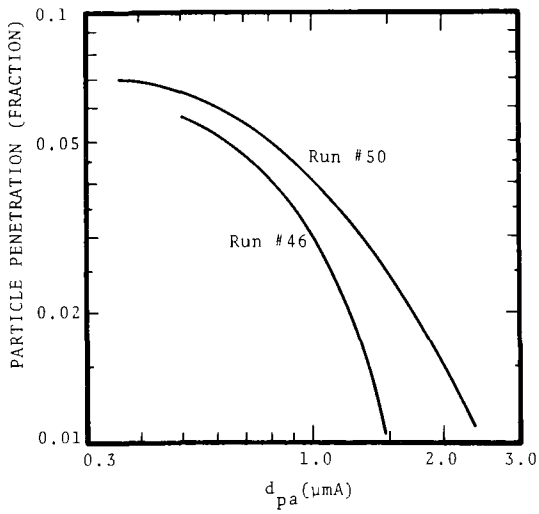

Figure 5.B.15 Particle penetration versus aerodynamic diameter, one stage.

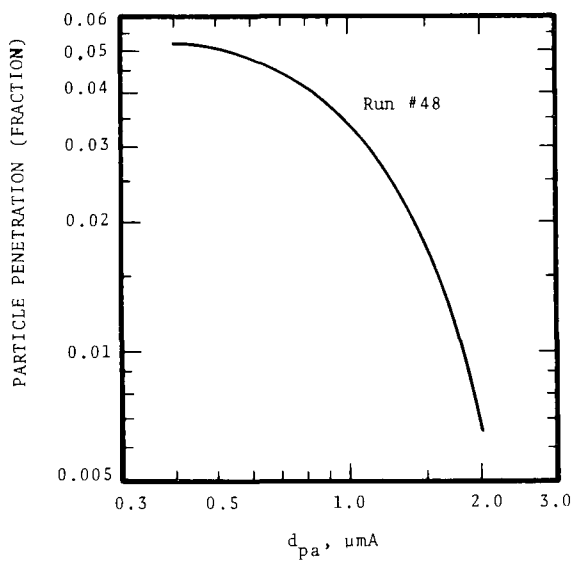

Figure 5.B.16 Particle penetration versus aerodynamic diameter, single stage.

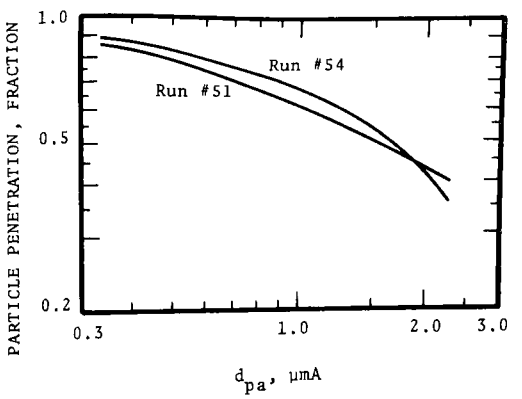

Figure 5.B.17 Particle penetration versus aerodynamic diameter, one stage.

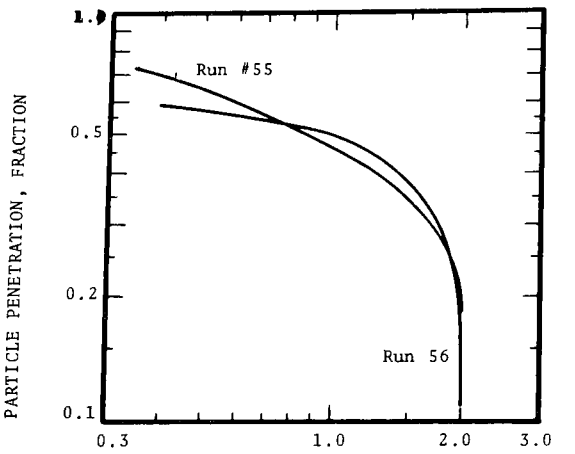

Figure 5.B.18 Particle penetration versus aerodynamic diameter, one stage.

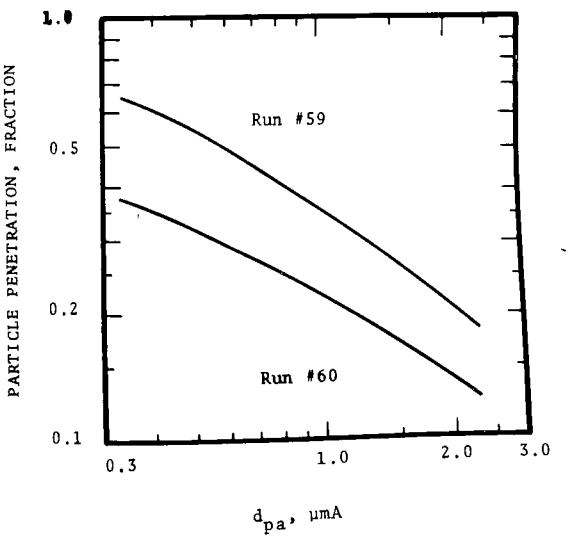

Figure 5.B.19 Particle penetration versus aerodynamic diameter, one stage.

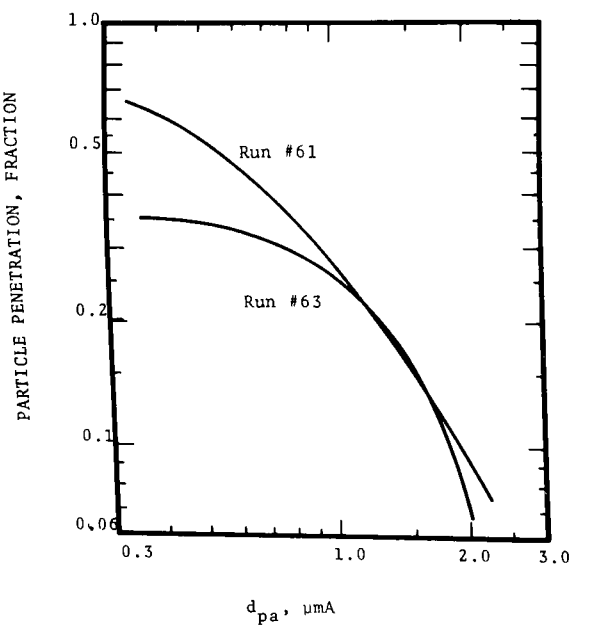

Figure 5.B.20 Particle penetration versus aerodynamic diameter, one stage

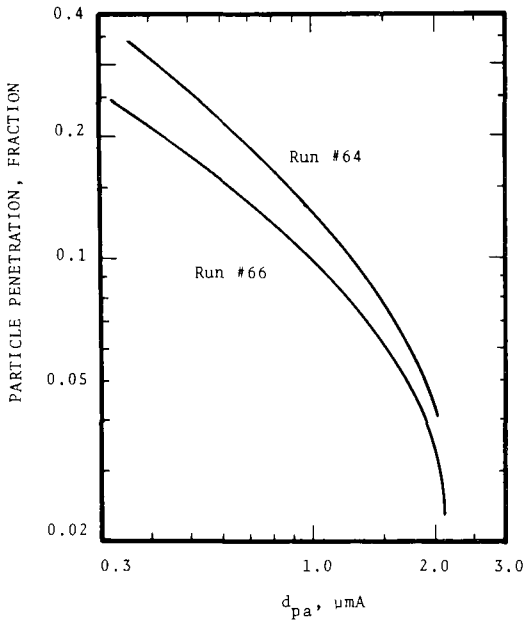

Figure 5.B.21 Particle penetration versus aerodynamic diameter, one stage.

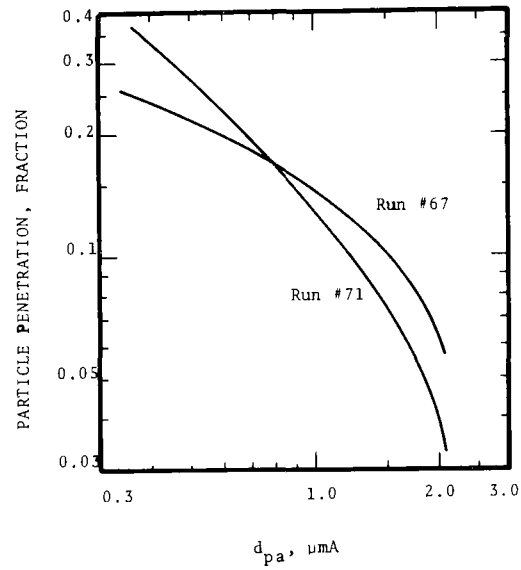

Figure 5.B.22- Particle penetration versus aerodynamic diameter, one stage.

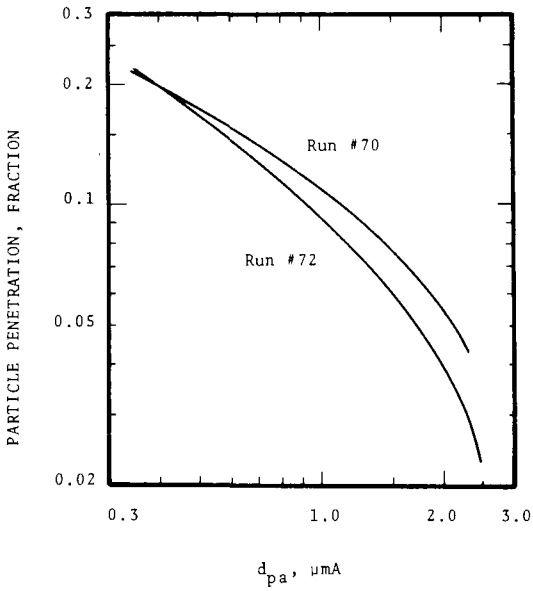

Figure 5.B.23 Particle penetration versus aerodynamic diameter, one stage.

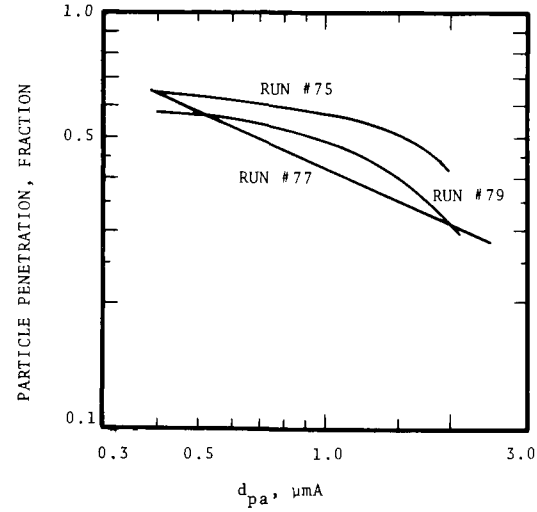

Figure 5.B.24 Particle penetration versus aerodynamic diameter, 3 stage co-current spray scrubber.

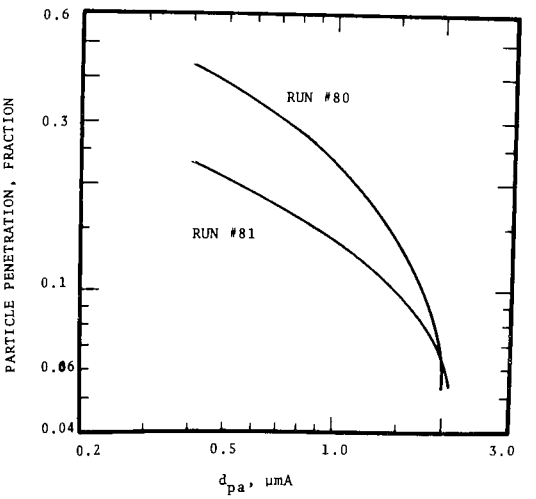

Figure 5.B.25 Particle penetration versus aerodynamic diameter, 3 stage co-current spray scrubber.

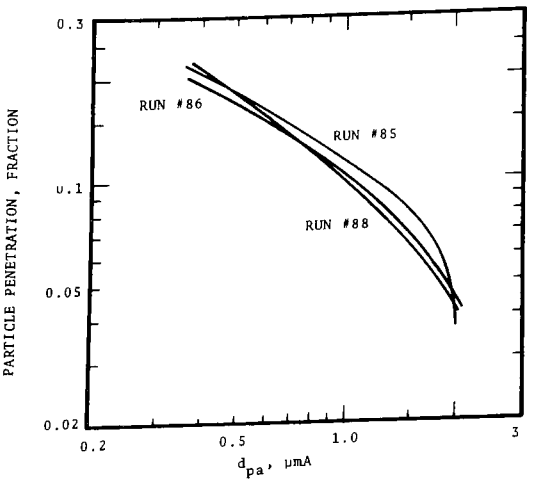

Figure 5.B.26 Particle penetration versus aerodynamic diameter, three stage co-current spray scrubber.

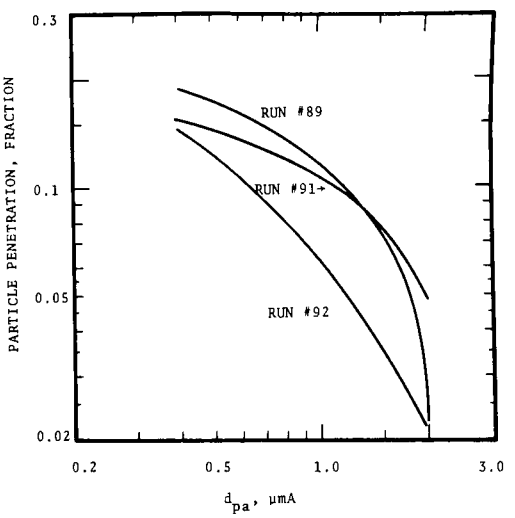

Figure 5.B.27 Particle penetration versus aerodynamic diameter, three stage co-current spray scrubber.

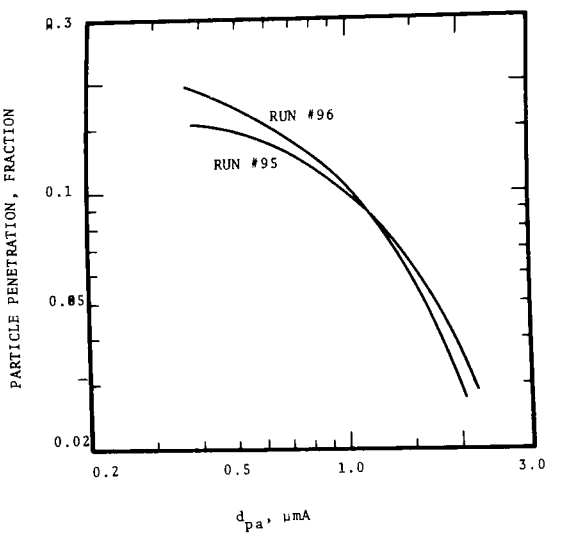

Figure 5.B.28 Particle penetration versus aerodynamic diameter, three stage co-current spray scrubber.

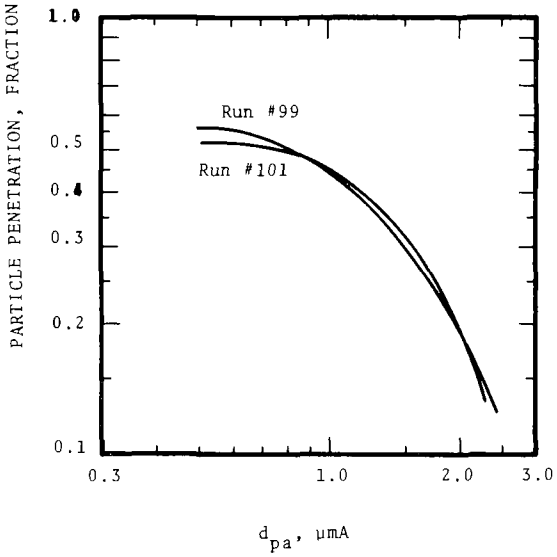

Figure 5.B.29 Particle penetration versus aerodynamic diameter, three stage counter-current.

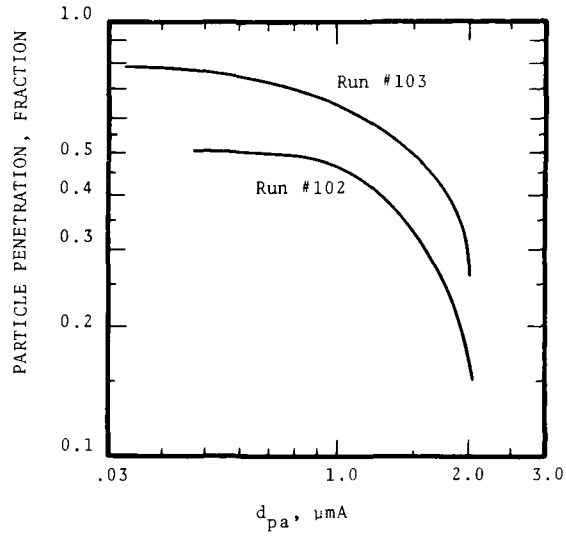

Figure 5.B.30 Particle penetration versus aerodynamic diameter, three stage counter-current.

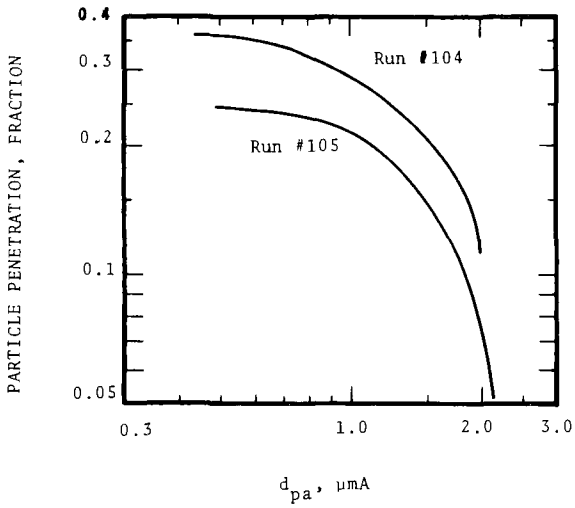

Figure 5.B.31 Particle penetration versus aerodynamic diameter, three stage counter-current.

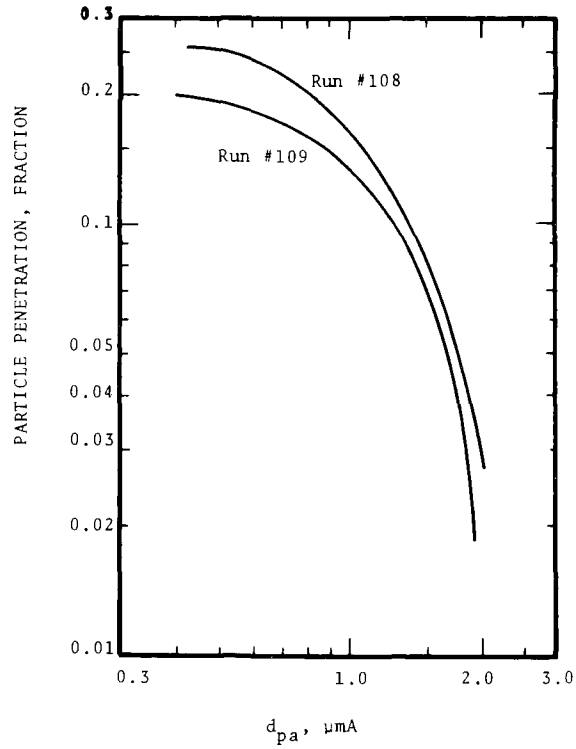

Figure 5.B.32 Particle penetration versus aerodynamic diameter, three stage counter current.

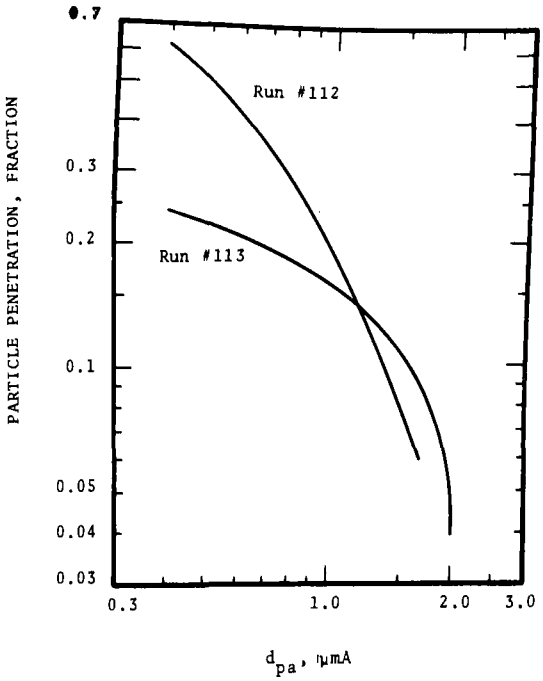

Figure 5.B.33 Particle penetration versus aerodynamic diameter, three stage counter-current.

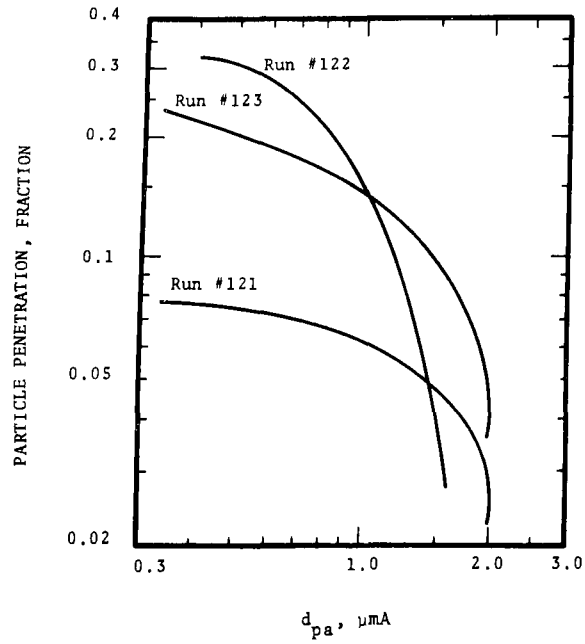

Figure 5.B.34 Particle penetration versus aerodynamic diameter, three stage counter-current.

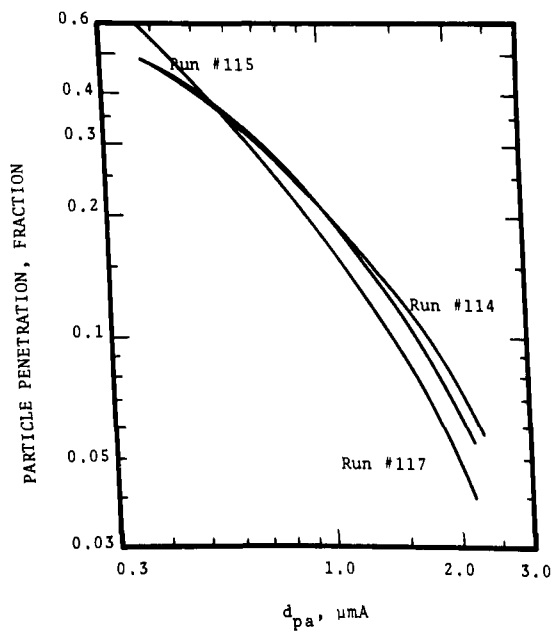

Figure 5.B.35- Particle penetration versus aerodynamic diameter, three stage counter-current

APPENDIX 6.A

PROGRAM FOR CORRECTING PARTICLE COLLECTION ON A SIEVE PLATE

APPENDIX 6.A.

Program for Correcting Particle Collection on a Sieve Plate

```
C  THIS IS A FØRTRAN IV PRØGRAM FØR CALCULATING PARTICLE REMØVAL
C  ØN A SIEVE PLATE DUE TØ FLUX FØRCES AND PARTICLE GRØWTH
C  RESULTING IN ENHANCED INERTIAL IMPACTIØN. PLEASE REFER TØ
C  TEXT FØR EXPLANATIØNS ØF INPUT AND ØUTPUT DATA,CØMPUTATIØNAL
C  PRØCEDURES AND PRØGRAM APPLICATIØNS.
DIMENSIØN Y(4)
REAL MP,NMP
PRINT,"INPUT?TIN,PIN,TLB,RP,CNP"
INPUT,TIN,PIN,TLB,RP,CNP
GM=7.17E-3
RKL=4.18E+2
RHL=2.4775
RK=4.18E-4
RH=2.4775E-2
GMØ=GM
DB=0.4
VELB=20.0
VB=0.6
NJ=5
NI=13
THT=0.02
THT=THT/NJ
DZ=0.4
DZ=DZ/NJ
GLDT=TIN-TLB
RØ=RP
ØCNP=CNP
N=4
YMAX=1.0
YMIN=0.0
DX=0.1
CALL PLØT(X,Y,YMAX,YMIN,N,1,NI)
C THIS SUBRØUTINE, FRØM THE GENERAL ELECTRIC MARK II TIME-SHARING
C SYSTEM SUBRØUTINE LIBRARY, PLØTS 4 CURVES SIMULTANEØUSLY
C AGAINST ØNE INDEPENDENT VARIABLE.
TPS=TIN
DTP=0.0
TLS=TLB
```

```
      DØ 100 I=1,NI
      DØ 80 J=1,NJ
      DØ 30 II=1,400
      TLS=TLB+0.5*(II-1.0)
      PS=EXP(13.64-(5.1E+3/TLS))
      DTL=RKL*(PIN-PS)/(2.0-PIN)-TLS+TLB
     &-RHL*(TLS-TIN)/SQRT(TIN)
      IF (DTL.LE.0.0)GØ TØ 40
   30 CØNTINUE
   40 DØ 60 IJ=1,10
      TLS=TLS-0.1*(IJ-1.0)
      PS=EXP(13.64-(5.1E+3/TLS))
      DTL=RKL*(PIN-PS)/(2.0-PIN)-TLS+TLB
     &-RHL*(TLS-TIN)/SQRT(TIN)
      IF (DTL.GE.0.0)GØ TØ 70
   60 CØNTINUE
   70 DMP=0.0
      DMT=0.0
      QP=0.0
      AB=VB*(6.0/DB)
      ØPIN=PIN
      ØTIN=TIN
      AKBG=RK/(2.0-PIN)
      DMB=AKBG*AB*(PIN-PS)*THT*DZ
      DMA=DMT+DMP+DMB
      HB=RH/SQRT(TIN)
      QT=QP+HB*AB*(TLS-TIN)*DZ*THT
      CPH=7.0*(1.0-PIN)+8.1*PIN
      ATIN=TIN+QT/(GM*CPH*THT)
      APIN=PIN-DMA*(1.0-PIN)/(GM*THT)
      PA=(ØPIN+APIN)/2.0
      AKBG=RK/(2.0-PA)
      DMB=AKBG*AB*(PA-PS)*THT*DZ
      DMT=DMT+DMP+DMB
      TA=(ØTIN+ATIN)/2.0
      TPS=TA
      PPS=EXP(13.64-(5.1E+3/TPS))
      IF(PA-PPS.LT.0.0)GØ TØ 50
```

```
AKPG=(2.85E-7*(TA**0.75))/RP*(2.0-PPS-PA)
HP=7.25E-5/RP
TEP=5.1E+3/(13.64-ALØG(PA))
EM=(0.042*PA)+5.0E-4
AC=HP/(AKPG*1.0E+4)
TPS=((1.0/(1.0+AC/EM))*(TEP-TA))+TA
PPS=EXP(13.64-(5.1E+3/TPS))
MP=4.2*RP*RP*RP*CNP*VB*DZ
RPD=5.2E-6*(TA**0.75)*(PA-PPS)*THT
RP=SQRT(RPD+(RP*RP))
NMP=4.2*RP*RP*RP*CNP*VB*DZ
DMP=(NMP-MP)/18.0
QP=1.0E+4*DMP
50 CØNTINUE
DMT=DMP+DMB
HB=RH/SQRT(TA)
QT=QP+HB*AB*(TLS-TA)*DZ*THT
UD=34.38*RK*(PA-PS)*TA/(1.0-PA)
CC=1.0+(0.8E-5/RP)
UT=6.14E-3*RH*CC*(TA-TLS)*(SQRT(TA))
UC=(RP*RP*CC*7.4E+8)/TA
US=(UD+UT+UC)*0.3
PT=EXP(-(6.0/DB)*US*THT)
CNP=PT*CNP*GM/(GM-(DMP+DMB)/THT)
CPH=7.0*(1.0-PA)+8.1*PA
TIN=TIN+QT/(GM*CPH*THT)
PIN=PIN-DMT*(1.0-PA)/(GM*THT)
GM=GM-(DMP+DMB)/THT
80 CØNTINUE
X=0.02*I
Y(1)=(TIN-TLB)/GLDT
Y(2)=RØ/RP
Y(3)=CNP*GM/(ØCNP*GMØ)
Y(4)=PIN/(2.0*EXP(13.64-(5.1E+3/TIN)))
CALL PLØT(X,Y,YMAX,YMIN,N,0,NI)
100 CØNTINUE
PRINT,PIN,TIN,RP,CNP*GM/(ØCNP*GMØ)
STØP
END
```

REFERENCES

Barnes, T. M., and H. W. Lownie, Jr. A Cost Analysis of Air Pollution Controls in the Integrated Iron and Steel Industry. Battelle Memorial Institute. NAPCA Contract No. PH-22-68-65. P. 259. May 1969.

Calvert, S., J. Goldshmid, D. Leith, and D. Mehta. Scrubber Handbook. A.P.T., Inc. EPA Contract No. CPA-70-95. NTIS #PB 213 016. August 1972.

Calvert, S., J. Goldshmid, D. Leith, and N. Jhaveri. Feasibility of Flux Force/Condensation Scrubbing for Fine Particulate Collection. A.P.T., Inc. EPA Contract No. 68-02-0256. NTIS #PB 227 307. October 1973.

Calvert, S. Engineering Design of Fine Particle Scrubbers. J. Air Pollution Control Association. 24 (10):929-933. October 1974.

Calvert, S., and N. C. Jhaveri. Flux Force/Condensation Scrubbing. J. Air Pollution Control Association. 24 (10): 947-951. October 1974.

Calvert, S., and S. Yung. Evaluation of Venturi-Rod Scrubber. A.P.T. Inc. EPA Contract No. 68-02-1328, Task No. 5. August 1974.

Chilton, C. H. Cost Engineering in the Process Industries. New York, McGraw-Hill. P. 475. 1960.

Goldsmith, P., and F. G. May. Diffusiophoresis and Thermophoresis in Water Vapor Systems. Aerosol Science. New York, Academic Press. P. 163-194. 1966.

Handbook of Emissions, Effluents and Control Practices for Stationary Particulate Pollution Source. Midwest Research Institute. Report to NAPCA, Contract No. CPA-22-69-104. 1970.

Hardison, L. C., and C. A. Greathouse. Air Pollution Control Technology and Costs in Nine Selected Areas. Industrial Gas Cleaning Institute, Inc. EPA Contract No. 68-02-031. P. 587. September 1972.

Henschen, H. C. Wet vs. Dry Gas Cleaning in the Steel Industry. J. Air Poll Control Assoc. 18;338-342. 1968.

Hidy, G. M., and J. R. Brock. The Dynamics of Aerocolloidal Systems. New York, Pergamon Press. P. 379. 1970.

Klauss, P. R., P. L. Sieffert, and J. F. Skelly. Costs and Performance of Control Systems and Control Equipment. Swindell-Dressler Company. In Appendix C: A Cost Analysis of Air Pollution Controls in the Integrated Iron and Steel Industry. Battelle Memorial Institute. NAPCA Contract No. PH-22-68-65. P. 122. May 1969.

Kotrappa, P., and C. J. Wilkinson. Densities in Relation to Size of Spherical Aerosols Produced by Nebulization and Heat Degradation. A.I.H.A. Journal. 33(7):449-453. July 1972.

Lancaster, B. W., and W. Strauss. A Study of Steam Injection Into Wet Scrubbers. Ind Eng Chem Fundamentals. 10(3):362-369. March 1971.

Lapple, C. W., and H. J. Kamack. Performance of Wet Dust Scrubbers. Chem Eng Prog. 51(3):110-121. March 1955.

McAllister, R. A., P. H. McGinnis, and C. A. Plank. Perforated Plate Performance. Chemical Engineering Science. 9:25-35. 1958.

Oglesby, Jr., S., and G. B. Nichols. A Manual of Electrostatic Precipitator Technology. Part II. Southern Research Institute. 1970.

Popper, H. Modern Cost Engineering Techniques. New York, McGraw-Hill. 1970.

Rozen, A. M., and V. M. Kostin. Collection of Finely Dispersed Aerosols in Plate Columns by Condensation Enlargement. Inter Chem Eng. 7:464-467. July 1967.

Schauer, P. J. Removal of Submicron Aerosol Particles from Moving Gas Stream. Ind Eng Chem. 43(7): 1532-1538. July 1951.

Semran, K., and C. L. Witham. Wet Scrubber Liquid Utilization. Stanford Research Institute. EPA Contract No. 68-02-1079. P. 115. October 1974.

Taheri, M., and S. Calvert. Removal of Small Particles from Air by Foam in a Sieve-Plate Column. J. Air Poll Control Assoc. 18:240-245. 1968.

Waldmann, L., and K. H. Schmitt. Thermophoresis and Diffusiophoresis of Aerosols. Aerosol Science. New York, Academic Press. P. 137-161. 1966.

Walton, W. M., and A. Woolcock. The Suppression of Airborne Dust by Water Spray. Inter J Air Poll. 3:129-153. October 1960.

Wheeler, D. M. Fume Control in L. D. Plants. J. Air Poll Control Assoc. 18(2):98-101. January 1968.

TECHNICAL REPORT DATA
(Please read Instructions on the reverse before completing)

1. REPORT NO.	2.	3. RECIPIENT'S ACCESSION NO.
EPA-600/2-75-018		

4. TITLE AND SUBTITLE	5. REPORT DATE
Study of Flux Force/Condensation Scrubbing of Fine Particles	August 1975
	6. PERFORMING ORGANIZATION CODE

7. AUTHOR(S)	8. PERFORMING ORGANIZATION REPORT NO.
Seymour Calvert, Nikhil C. Jhaveri, and Timothy Huisking	

9. PERFORMING ORGANIZATION NAME AND ADDRESS	10. PROGRAM ELEMENT NO.
A. P. T., Inc. 4901 Morena Boulevard, Suite 402 San Diego, CA 92117	1AB012; ROAP 21ADL-005
	11. CONTRACT/GRANT NO. 68-02-1082

12. SPONSORING AGENCY NAME AND ADDRESS	13. TYPE OF REPORT AND PERIOD COVERED
EPA, Office of Research and Development Industrial Environmental Research Laboratory Research Triangle Park, NC 27711	Final; 10/73 - 6/75
	14. SPONSORING AGENCY CODE

15. SUPPLEMENTARY NOTES

16. ABSTRACT The report gives results of a laboratory pilot scale evaluation of a multiple plate, horizontal spray, flux force/condensation (FF/C) scrubber for the removal of fine particulates. Effects of the significant operational parameters on the scrubber performance were experimentally studied. Scrubber performance data are presented in terms of particle penetration as a function of particle size. The experimental results are compared with predictions from mathematical models. Optimum operational regions and technical and economic feasibility of FF/C scrubbing are determined and demonstrated for a single fine particle pollution source. The promising experimental results clearly indicate that further development of FF/C scrubbing is warranted.

17. KEY WORDS AND DOCUMENT ANALYSIS

a. DESCRIPTORS	b. IDENTIFIERS/OPEN ENDED TERMS	c. COSATI Field/Group
Air Pollution	Air Pollution Control	13B
Condensing	Stationary Sources	07D
Scrubbers	Flux Force/Condensation Scrubber	07A
Dust	Fine Particulate	11G
Mathematical Models	Particle Growth	12A
	Stephan Flow	

18. DISTRIBUTION STATEMENT	19. SECURITY CLASS *(This Report)*	21. NO. OF PAGES
Unlimited	Unclassified	190
	20. SECURITY CLASS *(This page)*	22. PRICE
	Unclassified	

EPA Form 2220-1 (9-73)